NCHRP 24-9

STATIC AND DYNAMIC LATERAL LOADING OF PILE GROUPS

FINAL REPORT

D.A. Brown   (Auburn University)
M.W. O'Neill   (University of Houston)
M. Hoit   (University of Florida)
M. McVay   (University of Florida)
M.H. El Nagger   (University of Western Ontario)
S. Chakraborty   (Auburn University)

Highway Research Center
Harbert Engineering Center
Auburn University, Alabama 36849-5337

JANUARY, 2001

STATIC AND DYNAMIC LATERAL LOADING OF PILE GROUPS

FINAL REPORT

Prepared for
National Cooperative Highway Research Program
Transportation Research Board
National Research Council

D.A. Brown   (Auburn University)
M.W. O'Neill   (Auburn University)
M. Hoit   (University of Florida)
M. McVay   (University of Florida)
M.H. El Nagger   (University of Western Ontario)
S. Chakraborty   (Auburn University)

Highway Research Center
Auburn University, Alabama

January, 2001

Information on NCHRP Goes Here

(To be supplied by NCHRP Staff)

FOREWORD

To be written by TRB Staff and inserted here

CONTENTS

SUMMARY   Groups of piles, commonly used to support bridge structures, are frequently subjected to lateral loadings during extreme events, such as vessel impacts and earthquakes. There is evidence that during past extreme-event loadings pile-group foundations have undergone lateral translations severe enough to cause loss of bearing support for superstructure elements and, on rare occasions, structural failure in the piles themselves. Current design methods for deep foundations for highway structures most often involve making an estimate of the ratio of shear load to lateral deflection for the group as a whole and using this constant stiffness ratio as an input to model the foundation in linear modal analysis computer codes to analyze the structural response, especially for seismic loading. The code also outputs the dynamic loads on the foundations. For critical structures, nonlinear pushover analyses are then conducted on the substructure and foundation to ensure that there is adequate ductile reserve at these loads to preclude complete collapse.

However, lateral pile foundation response to static or dynamic loading is nonlinear, often considerably so. It is therefore more desirable to analyze the foundation and substructure considering this nonlinearity and either to couple such a nonlinear analysis method with a nonlinear superstructure analysis code or to use a nonlinear foundation analysis code independently, iterating with the superstructure analysis code until the loads assumed to act on the foundation for determining equivalent linear foundation stiffnesses equal the loads exerted on the foundation from the superstructure analysis.

In this project, several full-scale field tests were conducted on pile groups of six to 12 piles, both bored and driven, in relatively soft cohesive and cohesionless soils. All of the groups were loaded laterally statically to relatively large deflections, and groups of instrumented pipe piles were also loaded dynamically to large deflections, equivalent to deflections that might be suffered in major ship impact and seismic events. Dynamic loading was provided by a series of impulses of increasing magnitude using a horizontally mounted Statnamic device. While such loading did not capture the aspects of lateral loading and ground shaking that may generate high pore water pressures, it did capture the damping that occurs at very large pile deflections and the inertial effects of the problem.

A dynamic version of the computer code FLPIER [FLPIER(D)] was developed in parallel with the field tests. This program has the capability of modeling complete hysteresis in the soil surrounding the piles via p-y curves, as well as cracking and hysteresis in the structural components of the pile group, inertia in the structural components, viscous damping in the soil, lateral group action by the application of adjustment factors for the p-y curves (termed p-multipliers), loading of the piles directly through vibrating soil and simple superstructure feedback (inertia) loads. FLPIER(D) was used mainly to interpret the results of the field

tests. The results of this interpretation can be used in similar codes that simulate the dynamic behavior of systems of piles and coupled pile-structure systems.

Simultaneously with the development of FLPIER(D), separate analytical solutions were also developed for dynamic p-y curves and simplified dynamic p-multipliers for piles in cohesionless soils, as well as for frequency dependent damping in the soil. These solutions were programmed into FLPIER(D). The p-y curves, however, were non-hysteretic. While the option to use them is available in FLPIER(D), they were not used in the interpretation of the dynamic field load tests. Through analysis of the full-scale field load tests with FLPIER(D), it was found that use of p-y curves that are prescribed in standard programs for static (non-cyclic) loading, modified to simulate unloading, reloading and gap development, and default values of static p-multipliers that were derived from a review of many historical static lateral group loading tests and given in the help files of FLPIER, were reasonably accurate in simulating the initial load-deformation response and subsequent free vibration of groups of piles loaded with the Statnamic impulse device to large lateral deflections. In general, the computed group response was in reasonable agreement with the measured response.

FLPIER(D), or any other program that uses p-multipliers that are defined row-by-row, outputs shear and moment diagrams that are constant from pile to pile in each row. That is, the shear and moment diagrams are averages for piles in a given row. However, measurements of shear and moment, while indicating average row-wise values that were near those predicted by FLPIER(D), were quite variable. This variability was apparently caused by point-to-point variations in lateral stiffness of the soil within the pile groups and other random factors such as inadvertent minor batter of plumb piles. In order to account for these random effects, a load factor of approximately 1.2 should be applied to the computed maximum bending moments in the piles when the piles are designed structurally.

It is also suggested that, for assessing pile group stiffness, it is quite acceptable to use an average p-multiplier for all piles in the group, rather than defining p-multipliers row-by-row, as is the standard practice. Use of a single average group effect parameter (p-multiplier) is justified for seismic loading on the basis that the direction of loading changes, constantly and often unpredictably, during the loading event and load reversals occur, converting "leading" rows of piles (high p-multipliers) instantaneously into "trailing rows" (low p-multipliers).

Regarding the testing method and load test components, impulse loading by the Statnamic device was found to be a feasible way to test the pile groups economically by applying dynamic loads that produced large defections and induce vibrations in the pile groups at natural periods of 2 to 4 Hz. It is recommended that in future tests the piles be tied together at their heads by cast-in-place reinforced concrete caps rather than by the steel frame first envisioned by the research team. The Statnamic device and the instrumented test piles used on this research project are available for future use to assist state DOT's in the design of laterally loaded pile groups on production-level projects.

Chapter 1: INTRODUCTION AND RESEARCH APPROACH

INTRODUCTION

A key concern of bridge engineers is the design and performance of pile group foundations under lateral loading events, such as ship or ice impacts and earthquakes. This report documents a research program in which the following were developed: (a) a numerical model to simulate static and dynamic lateral loading of pile groups, including structural and soil hysteresis and energy dissipation through radiation, (b) an analytical soil model for nonlinear unit soil response against piles (p-y curves) for dynamic loading and simple factors (p-multipliers) to permit their use in modeling groups of piles, (c) experimental data obtained through static and dynamic testing of large-scale pile groups in various soil profiles, and (d) preliminary recommendations for expressions for p-y curves, damping factors and p-multipliers for analysis of laterally loaded pile groups for design purposes. The report also describes experimental equipment for performing site-specific, static and dynamic lateral load tests on pile groups.

Background

Observations made during two recent earthquakes in California, the 1989 Loma Prieta and the 1994 Northridge events, as well as the 1995 Hanshin-Awaji earthquake near Kobe, Japan, and the Chi-Chi earthquake in central Taiwan in 1999, provide clear evidence of the types of damage that occur in pile foundations and the structures that they support.

Bridge Performance — Loma Prieta Earthquake

During the Loma Prieta earthquake of October 17, 1989, significant damage occurred to bridges located in the five-county area near the earthquake epicenter south of

3

San Francisco. Of the approximately 1,500 bridges located in the five-county area, more that 80 suffered minor damage, 10 needed temporary supports, and 10 were closed due to major structural damage [1]. The cost to restore these structures to their pre-earthquake operational capacity was estimated at between $1.8 and $2.0 billion.

The greatest bridge damage occurred to older structures on soft ground. Collapses of the Cypress Street Viaduct and a link span for the San Francisco-Oakland Bay Bridge are the most well-known examples of this damage. The death toll from the Cypress Street Viaduct collapse was 42. It is also reported that other bridges of similar design would have collapsed if the ground shaking had lasted longer.

Ground motions for the bridges damaged in Loma Prieta were often surprisingly low, for example, less than 0.2 g. Typically, the bridges were supported on pile foundations [e.g., cast-in-drill-hole (CIDH) and timber piles]. It was inferred from discussions with Caltrans' engineers that many of the bridge foundations were supported by groups of piles located at spacing ratios of three to five pile diameters.

Structural damage to the pile foundation systems for bridges themselves during the Loma Prieta event was apparently limited. Shear failure occurred near the heads of some piles in the Struve Slough bridges near Watsonville. This failure was attributed to large ground deformation resulting from liquefaction. In most cases, however, amplification of the bedrock acceleration and relative displacement of the ground and bridge structure were generally the principal causes of damage. Some pile group foundations, particularly at the Port of Oakland, experienced evidence of structural distress when a few batter piles were used in that the bents, evidently because the batter

piles, which were stiff with respect to lateral loading compared to the vertical piles in the group, attracted lateral load.

Bridge Performance – Northridge Earthquake

During the Northridge earthquake (Los Angeles metropolitan area) of January 17, 1994, seven highway bridges suffered partial collapses and another 170 bridges suffered damage ranging from minor cracking to the slumping of abutment fills. One life was lost, and several injuries were the direct consequence of these failures [2, 3]. The total repair cost for the damaged bridges was estimated to be about $150,000,000 [4]. Most of the damaged bridges had been designed with pre-1971 design standards.

Peak ground accelerations were much higher than those for the Loma Prieta event, exceeding 1g close to the epicentral area. Soils were, however, typically stronger than those associated with damage during the Loma Prieta event. The damaged bridges were supported on piles [e. g., primarily 406-mm- to 610-mm- (16- to 24-in.-) diameter CIDH piles, but including H-piles and drilled shafts up to 3.66 m (12 ft) in diameter] or combinations of piles and spread footings.

The only bridge where pile damage was possibly noted was the Los Virgenes Bridge on U. S. Route 101. Most of the damage seemed to result from span displacements that exceeded girder seat widths or excessive forces in columns that supported the bridge deck. At one bridge location, the S. R. 14 / I-5 Separation and Overhead Structure, spatial variation in ground motion from support to support was suspected of being a contributor to bridge damage.

Bridge Performance – Hanshin-Awaji Earthquake

The Hanshin-Awaji earthquake occurred on January 17, 1995, near the city of Kobe, Japan. This earthquake caused over 5,000 deaths and extensive property damage in a highly urbanized area of Japan [5]. On the order of 27 highway bridges sustained major damage, and many more suffered moderate to minor damage. One estimate of the cost of the damage to one of the agencies operating freeways in the Hanshin area was $5 billion (U. S.). Most of the damage was confined to structures built more than 30 years ago and before the introduction of modern seismic codes.

Typical damage sustained by the bridge structures included shear and flexural failures in non-ductile concrete columns, flexural and buckling failures in steel columns, steel bearing failures under lateral load, and foundation failures due to liquefaction. Costantino [6] reports that geotechnical observations suggested pile-supported facilities faired well during the event, although some damage was noted, and that significant damage occurred to dock facilities, as well, as at connections to pile-supported structures. The caisson-supported seawall on Port Island showed lateral movement at some locations and extensive collapse of pavements immediately in front of the wall. Most of the observations of pile foundation damage were associated with lateral ground displacement (soil flow).

According to Buckle [5], many of the bridges were founded (on piles) installed in sand-gravel terraces (alluvial deposits) which overlie gravel-sand-mud deposits at depths of less than 10 m. Liquefiable soils were present along the shoreline and in most ports and channels above those founding deposits.

Ishihara [7] concluded that some serious damage occurred where bridges were supported on groups of large-diameter (typically 1 m or greater) bored piles (drilled shafts) during the Hanshin-Awaji event, which had a Richter Magnitude of 7.2 and whose epicenter was less than 10 km from the sites of heavily damaged bridges. The most damaging condition by far was a combination of liquefaction and lateral spreading of the ground surface. Permanent lateral movement of the soil surrounding grouped bored pile foundations in the order of 0.5 to 2.0 m occurred where the groups were located within about 100 m of quay walls that yielded during the earthquake. The permanent lateral movements of the pile heads, which were nominally fixed to the pile caps, were about one-half of the reported permanent ground movements, some as high as 0.5 m. After the earthquake, the damaged piles were cored, subjected to pulse-echo testing and excavated partially for examination by remote television cameras. The most severe structural damage in the piles, as evidenced by severe cracking, was found at three locations: (a) at the bottom of the liquefied zone, (b) at the depth at which the reinforcement schedule or cross-section changed, and (c) at the pile heads, where the bending moments were theoretically the highest, since the piles were fixed into their caps. Although the piles suffered damage, the structures themselves experienced little damage when the piles were more than 12 m long. Presumably, such piles penetrated well below the zone of liquefaction and lateral soil movement.

Matsui et al. [8], who investigated these and other pile group foundations after the Hanshin-Awaji earthquake, stated that pile groups located away from areas where liquefaction and lateral spreading occurred behaved well structurally, with the exception of the development of tension cracks, reflecting high bending moments, in some concrete

piles below the ground surface, especially near the contact between soil zones of high soil stiffness contrast.

Bridge Performance – Chi-Chi Earthquake

An earthquake of Richter Magnitude 7.3 struck the central mountain region of Taiwan, near the town of Chi-Chi, on September 21, 1999, causing widespread damage and over 2,400 deaths. 121 buildings of five stories or higher were damaged so severely that they had to be torn down. Of 457 buildings with damaged foundations that were surveyed (bridges and buildings), 27 percent were discerned to have been damaged by direct movement of one of two causative faults immediately next to or beneath the structure, 15 percent were the result of ground liquefaction and 58 percent were due to "superstructure interface" failure, for example, shear failure of plinths and columns or rotation of substructures to the extent that beams and joists fell from their seats or were buckled [9]. Most of the damaged bridges were near or across the fault breaks and appeared to be due to superstructure interface problems [10].

In the four counties nearest the epicenter, approximately 20 percent of the bridge inventory suffered minor-to-major damage. Damage modes that could possibly be associated with foundation performance included displaced bearings; unseated girders; shear failure in columns, abutment walls and caissons (drilled shafts); foundation failures due to slope movements; joint failures in column-to-girder connections; and liquefaction [11]. Of 183 distinct damage patterns noted in highway bridges damaged in the Chi-Chi event, 14 (8 percent) were identified as structural failures of foundations [11], although many of the superstructure failures may have been caused at least partially by excessive movements of foundations. Most of the bridges with major damage were very close to

8

the epicenter, and many even crossed the Chelungpu fault, one of the two causative faults for this earthquake. In such a case, permanent displacement and/or rotation of the bent or abutment was frequently noted. Only two bridges, both at river crossings, were reported clearly to have been damaged because of liquefaction (although the foundations for others may have suffered excessive movement because of elevated pore water pressures in the fine sand and silt alluvium typical in the four-county area). For severely damaged bridges that were not close to a causative fault, failure most often occurred because of loss of seating for girders in simple-span bridges.

Significance of Damage Observations

Bardet et at. [12] state that the structural performance of the pile foundations, by themselves, during the Loma Prieta, Northridge, and Hanshin-Awaji (Kobe) earthquakes appeared to be quite good, with few if any examples of damage being mentioned, except in places in the Kobe area where there was significant liquefaction and lateral ground spreading. In fact, where there was liquefaction but no lateral spreading of the ground, piles suffered little or no structural damage.

However, while the piles themselves may have survived the earthquakes with little or no damage, many bridge structures in all four of the cited earthquakes did not. Forces in and displacements of the damaged structures exceeded allowable values, in some cases leading to collapse of the structures. Since the forces and displacements are directly related to the stiffness of the foundation systems, it is likely that at least some of the observed damage to the structures could have been prevented or minimized by improved modeling of the deformability of the pile foundations during the design

9

process. Many of the pile foundations in all four earthquakes consisted of groups of piles with center-to-center spacing ratios of three to five diameters.

A significant cause of bridge failures in the Chi-Chi event was a lack of horizontal restraints at the girder seats, which allowed the girders to slide off their supports. This factor may have also reduced inertial loads on the foundations, which, in turn, may have prevented some structural failures of foundations.

A significant factor contributing to the apparent lack of structural damage in the pile foundations in the California events is Caltrans' design philosophy of limiting maximum design loads applied to the foundation so as to preclude severe inelastic behavior (without development of plastic hinges within the foundation, for example). This is often achieved by limiting the maximum moment at the connection of the column to the bent cap or the piled footing (forcing the plastic hinge to occur there), thereby providing a limiting maximum load to the pile system. While this approach "protects" the pile system, it does not limit the inertial forces or the displacement that can develop in the structure, and therein is an apparent cause of past superstructure damage. Recognizing that foundation systems have, in general, performed well in earthquakes, suggestions have been made that the next generation of AASHTO seismic design guidelines allow the foundation system to carry more load. If this approach is adopted, it is quite possible that following future earthquakes, evidence of at least some structural damage in the pile system will become more prevalent unless design methods are improved.

In order to minimize future damage to bridges during seismic events, a two-step approach to design will likely be included in the AASHTO guidelines. This two-step

approach will involve linear dynamic response analyses of the structure at a lower level of earthquake loading, say ground response corresponding to return periods of 150 to 200 years (Step 1), and a quasi-static "pushover" or collapse analysis at a higher level of loading, which is currently identified as an event with a return period of approximately 2,500 years (Step 2). For both analyses the modeling of the foundation system will have a direct effect on the capacity demands within the structural system. The accuracy of the foundation model will, therefore, have direct relevance to the improvement or optimization of bridge performance during seismic loading.

Bardet et al. [12], after considering the first three seismic events summarized above, identified several productive areas for research concerning pile foundations in seismic events. At the top of their list were the following:

1. Develop a better understanding of the way the soil is modeled, including the effects of pile-soil-pile interaction in soft ground, including

   - "p-y" and "t-z" response of soil (defined later) or liquefied ground under extreme event loading conditions,

   - relations between lateral ground pressures, p-y curves and free-field ground displacements,

   - lateral loads imposed on pile foundations by lateral ground spreading, including the effects of non-liquefied crustal soil sliding laterally upon layers of liquefied ground, and

   - the influence of site stratigraphy.

11

2. Evaluate systematically methods of analysis against case histories and refine design/analysis methods.

3. Evaluate design philosophy; specifically, should inelastic behavior of the piles be permitted to occur?

Current Design Practice

1997 Survey of Practice

The interim report for this project [13] provided a general overview of current design practice for laterally loaded pile groups, primarily for seismic loading. A brief review of current practice is presented here. First, seismic loads are viewed as being primarily horizontal. Budek et al. [14] indicate that common current DOT practice for the quasi-elastic lateral-load design of pile foundations and bridge columns for seismic loading is to: (a) estimate the lateral stiffness of the foundation (i. e., pile group) under a selected load so that deflections under that load can be computed, (b) replace the foundation with an extension of the bridge column and select a depth to fixity for that column, assuming linearity, that will give the same lateral displacement at the top of the foundation as that of the foundation, (c) determine the expected deflections and rotations at the top of the column through appropriate analysis. In order to analyze for stresses in the superstructure, a dynamic, linear modal analysis of the extended column and the structure it supports may be performed. The piles that support the column are then analyzed under the computed loads at the foundation level to ensure that they do not yield structurally, which is usually the desired situation. This may be viewed as "Step 1" in the analysis of a foundation for seismic loading. A second step, "Step 2," is then sometimes

12

performed to determine the capacity of the foundation at the time plastic failure fully develops. This plastic capacity should exceed the loadings computed from Step 1 by some prescribed amount, to assure that adequate ductility is available to prevent total collapse.

At one level of practice, lateral pile group stiffness for a Step 1 analysis is estimated by performing static, elastic subgrade reaction analyses [e. g., 15] on typical piles within the group using factors that reduce the lateral stiffnesses of the individual piles in the group below the stiffnesses estimated for single, isolated piles in order to account for overlapping strains in the mass of soil in which all of the piles are embedded. The group stiffness is then the sum of the individual pile stiffnesses, and these are inserted as boundary constraints in a linear superstructure modal analysis program without formally computing a depth of fixity for an equivalent column.

Pile stiffness reduction for group action for this approach to design is accomplished in a variety of ways. Many DOT designers use the recommendations given in the Navy's *Foundation and Earth Structure Design Manual* [16] and the 1985 edition of the *Canadian Foundation Engineering Manual* [17]. These documents recommend a factor, R, to reduce the lateral subgrade modulus acting against group piles (not pile stiffness). AASHTO [18] recommends the same reduction factors for drilled shafts but not explicitly for driven piles. The DM-7/CFEM factors, which are summarized in Table 1, along with factors recommended by ASCE and the Corps of Engineers [19], are not specific to the installation method; they are also strictly valid only for static loading conditions, and their origins can be traced to traditions of practice and to small-scale model tests. The most recent (1992) edition of the CFEM refers to

13

procedures to estimate group-pile stiffness, based on theory of elasticity, that are suggested by Poulos and Davis [20] and others.

On the other hand, PoLam and Martin [21] suggested neglecting group effects during seismic loading for sandy soils and introducing as much as a 50 percent reduction in lateral pile stiffness for piles spaced at three diameters on centers or less in soft clays. That recommendation is somewhat inconsistent with Section C4.5.5 of a recent Applied Technology Council report [22], which states "in view of the uncertainties, it is recommended that group effects be neglected for earthquake loading at three-diameter center-to-center spacing or higher."

A listing of specific methods for analyzing pile groups statically as linear systems, with and without batter piles, in which the reduced soil or pile stiffness values are used, is given in the interim report [13].

Commentary on Current Practice

The conventional design procedure discussed above, although relatively easy to apply, is based on the assumption of linearly elasticity in both the superstructure and the foundation; hence, modal analyses are possible. It ignores the fact that both piles and soil can behave in a nonlinear manner during an extreme event. Williams et al. [23] indicate that linear, modal analyses can result in significant errors in the moments and shears in bridge pier columns for certain configurations of piles and certain types of soil. Sometimes, these errors are unconservative. It can be inferred from that paper that linear, model analyses for both the structure and the foundation should be replaced with nonlinear, time-domain analyses. This philosophy, however, has not yet been

14

incorporated in design practice, except on occasion for major structures when designers have redefined iteratively the stiffness of pile foundations based on either the load or displacement computed in the structural analysis at the level of the foundation. The computational model that will be described in this report has the capability of modeling both soil and structural nonlinearities.

While present design practice presumes to keep group piles from experiencing the development of plastic hinges in order to force structural failures to occur and ductility to develop in the superstructure, design philosophy is turning more toward allowing plastic hinge development in grouped piles during seismic events, specifically at the points at which the pile heads are fixed into the pile footing or bent cap, with secondary hinges at the depth of maximum subsurface bending moment [14]. Plastic hinge development in piles profoundly affects their stiffness and energy dissipation capacities. It also affects the natural frequencies of the superstructure-foundation system and thus the way the structure responds to seismic loading. Budek et al. [14] describe the phenomenon of migration of the secondary (below pile-head) plastic hinges in fixed-headed pile groups from the depth at which they initially develop toward the surface, which can materially affect structural response during a seismic event. This observation again suggests that analyses that consider both the nonlinear behavior of the structural elements (piles, substructure and superstructure) and the nonlinear behavior of the supporting soils should be performed if accurate predictions of both pile and structure performance are to be obtained.

Considering the nonlinear nature of soils during extreme events, PoLam et al. [24] recommend "p-y" methods for defining the stiffnesses of laterally loaded piles and pile

groups for seismic loading. The lateral secant stiffnesses of pile heads (single piles or groups) can be developed as functions of head deformations using the p-y method. In an iterative Step 1 analysis, the deformations computed from the linear modal analysis of the structure at the top of the foundation (pile heads) can be matched to a specific linear (secant) stiffness for the piles that was developed through a nonlinear p-y analysis. If that value of stiffness differs from the one assumed in the linear structural analysis, the stiffness is changed and the linear model analysis for the structure is repeated, several times if necessary until closure is achieved. The p-y method models the bending behavior of the pile by either finite difference or finite element techniques and models the soil reaction using nonlinear reaction "springs" (nonlinear Winkler subgrade springs), which have been derived for static loading in many types of soil and rock semi-empirically [e. g., 25].

Detailed ways of handling the effects of cyclic soil degradation and the velocity of the pile relative to that of the soil for extreme event loading using a p-y soil model are described by PMB Engineering [26]. For example, consider the "backbone" (static) p-y curve, Figure 1. A set of such p-y curves for a given pile may be obtained from published criteria or can be measured at a specific site. Values of p can then be tentatively adjusted for cyclic degradation using Equation 1.

$$p_c = 10^{\left(\frac{\log 2}{1 - N_{50}}\right)} \left(p_p - p_d\right) + p_d \quad \text{,}$$ (1)

where p_c = degraded value of p,

N_{50} = number of cycles required to degrade the shear strength by 50 percent, which could be estimated from cyclic triaxial tests or similar soil tests,

p_p = p on the degraded p-y curve for the previous cycle of loading, and

p_d = fully degraded shear strength of the soil, which can also be estimated from triaxial or similar soil tests.

Hysteretic damping can be considered in the p-y model by allowing the unloading path to differ from the loading path and to discount soil resistance whenever the pile displacement relative to that of the soil is less than the displacement that occurred during the last unloading cycle. This model is also illustrated in Figure 1. Radiation damping can be simulated using a viscous damper (dashpot) that may be frequency and/or displacement dependent.

In the mathematical model of the pile-soil system, the instantaneous velocity of the pile relative to that of the soil is multiplied by c (Figure 1) to obtain a resisting force per unit length of the pile that is added to the displacement-dependent value of p (degraded p-y curve). One simple way of estimating c in Figure 1 is to use Equation 2.

$$c = 2D\frac{\gamma}{g}(v_s + v) \ ,$$
(2)

where   D   = pile diameter,

γ = total unit weight of the soil,

g   = acceleration of gravity,

v_s = shear wave velocity of the soil, and

17

v   = average of shear wave and compression wave velocity of the soil.

The p-y method, with consideration of both soil degradation and visco-elastic strength gain has long been used successfully in the design of piles for offshore structures.

WashDOT Method. A more advanced level of design, not yet customary in the United States DOT's, is illustrated by the WashDOT procedure [27] This procedure incorporates the p-y method of analysis in a rational way that involves a linear-iterative superstructure analysis. A detailed summary of the development of that procedure, developed for WashDOT by Geospectra, Inc., is given below to serve as a definition of current high-level state of the practice. The WashDOT procedure recognizes implicitly that the piles in a pile group are loaded along their lengths by the lateral translation of the soil via upward-propagating shear waves produced by seismic motion of the earth at a large depth and at their heads by inertial effects from the vibrating structure that is supported by the piles. These two modes of loading are sometimes referred to as "kinematic" loading and "inertial" loading. The WashDOT method is intended primarily for use in Step 1 of the two-step design approach mentioned earlier.

The WashDOT method includes only stiffness and does not explicitly address foundation damping. The method simplifies and standardizes the procedures for designers by assuming standard earthquake spectra, site conditions, pile types and layouts. Whether in standardizing the design process important effects of differences in these factors at actual construction sites may tend to be overlooked in the interest of simplicity of design remains to be seen.

The WashDOT method recognizes that soil reactions against the piles and the pile cap in the lateral direction occur only when there is relative movement between the piles

and the soil in the free field. The free-field motion, as well as the equivalent, strain-based elastic stiffness of the soil, is controlled by base motion in bedrock and details of the the soil profile.

The procedure used to develop the stiffness terms for pile groups in this method was as follows:

- Select seven standard soil profiles common to the state of Washington.

- Develop 500-year-return-period rock spectra corresponding to peak horizontal ground accelerations of 0.2, 0.3 and 0.4 g and match appropriate recorded acceleration time histories to these spectra.

- Select six typical foundation types used for typical bridges in the state of Washington and combine these with the seven typical soil profiles to arrive at specific analysis cases. Some of these foundations were single-pile foundations and some were grouped-pile foundations.

- Use computer program SHAKE [28] to determine the one-dimensional free-field site response above the elevation of the vibrating rock for all seven soil profiles and for the acceleration time histories determined above that corresponded to the various rock spectra.

- From the SHAKE analysis, which yields shear strain profiles, determine strain-compatible soil properties (e. g., shear and Young's moduli, shear strength) and establish average soil properties for each of the seven standard soil profiles and for each seismic spectrum.

- Compute the horizontal stiffnesses (load / deformation) for a typical single pile as a function of pile-head translation in each foundation group in each typical soil profile

for a pinned- or fixed-head condition. The "p-y" method, referenced above, was used to develop these stiffness values. The pile-head stiffness was defined as shear load / lateral displacement for each of several magnitudes of of displacement (secant stiffness) and is deflection-dependent.

- Compute the vertical stiffness for the typical single pile as a function of pile-head settlement in each foundation group in each typical soil profile. The "t-z" method, similar to the p-y method, but for axial loading, was used to develop the pile-head stiffness values. This stiffness was defined as thrust load / axial displacement for each magnitude of axial displacement (secant stiffness) and is also deflection-dependent.

- Model the lateral and vertical dynamic response of the typical piles and groups using a finite-element program (SASSI) in order to determine how loading of one pile affected the stiffness of other piles in a group. These analyses were elastic, but they were also dynamic and so included inertia and stress-wave propagation effects. The software allowed for the consideration of pile-soil-pile interaction during dynamic loading. Individual pile stiffness reduction factors for static loading were then obtained using elastic methods [e. g., 20] for horizontal and vertical loading for every pile in each typical group in each typical soil profile. The dynamic single-pile stiffness terms (shear / lateral displacement and thrust / axial movement) computed from the finite element analysis were then modified by these stiffness reduction factors. It was found that the group pile stiffnesses obtained by using the simple static stiffness reduction factors were similar to the pile stiffnesses computed form the finite element program for a period of motion, T, exceeding 0.5 sec (frequency < 2

Hz). For shorter periods or higher frequencies the stiffnesses determined for group piles from the linear dynamic finite element analyses differed somewhat from the single-pile dynamic stiffnesses that were modified by the static stiffness reduction factors. A complete set of the dynamic stiffness reduction factors obtained in this step is documented in the referenced report.

- Compute the horizontal stiffnesses of the pile group by summing the reduced stiffnesses of the individual piles in the group determined in the above step. Similarly, compute the vertical stiffness of the group by summing the reduced stiffnesses axial stiffnesses for the individual piles determined in the above step.

- Compute the rocking stiffnesses and torsional stiffness of the group from the stiffness values for the individual piles and their geometric coordinates. [No description is given of how coupling between lateral and rotational modes were; however, cross-coupling values are given in the completed design charts for groups. Norris [29] suggests that relatively accurate analyses can be made by neglecting such cross-coupling if the group is small and the piles are slender.]

- Compute the stiffness of the pile cap versus lateral deflection of the cap by assuming a passive condition against the pile cap (limit equilibrium method).

- Sum the cap and pile stiffnesses to obtain the overall lateral translational group stiffness.

- Tabulate the stiffnesses at zero (very small) displacement and graph the ratios of the stiffnesses of the various groups to the zero-deflection stiffness as a function of pile cap displacement. These stiffness tables become the design aids, and they are given in the reference in detail for all of the typical foundations for all of the typical soil

profiles for each of the typical free-field ground deformations. (This approach allows the designer to vary the stiffness of the pile foundation based on pile-cap deflections computed in the modal analysis of the superstructure, so that displacement-compatible stiffness is achieved in the foundation, even though the analysis is linear.)

- Use the "strain wedge method" [30, 31] to estimate the ground deflections around the group piles that are produced by the lateral translations of the piles. These are compared to the free-field deformation patterns in each soil profile for each base acceleration time. Then the group stiffness values for lateral translation are truncated at lateral pile group deflections corresponding to the free-field ground deflections. That is, the horizontal stiffnesses are taken in design as the values corresponding to the target deflection for the pile cap if that target deflection is equal to or greater than the free-field deflection computed by SHAKE (Case a). If the computed free-field deflection exceeds the deflection targeted for design, the stiffness is evaluated based on the assumption that the pile-cap (and therefore pile-head) displacement is equal to the estimated free-field displacement (Case b). This decision process in essence allows for approximate consideration of inertial loading (a) and kinematic loading (b).

The linear superstructure analysis is then performed using the resulting stiffnesses at the connection between the column and the pile cap, and the connection deformations are compared with the target deformations from which the pile stiffnesses were developed. If they are approximately equal, the computed pile group stiffnesses are satisfactory. If not, they are modified according to the computed values of deflection, using the design tables, and a revised superstructure analysis is made.

Norris [29] questions the use of standard p-y criteria for developing lateral stiffness terms for the individual piles, citing the fact that pile shape and the presence of the pile cap may affect the p-y curves. However, he states that the effects of soil degradation and pile-soil-pile interaction may have a greater effect than the pile shape and surface conditions, so that it was considered reasonable from a design perspective to use the p-y approach in the research described here.

The Washington State DOT method also provides normalized bending moment and shear diagrams for typical piles for each of the cases considered. If analysis beyond this step is not required, these diagrams can provide the basis for checking the adequacy of structural capacity of the piles.

For major structures, however, AASHTO requires that the ductility of the structure be shown to be adequate under extreme event loading. This includes the ductility of the foundation system. Methods for performing a ductility evaluation are documented in the interim report [13]. The computer code FLPIER, developed during the current research project, has the capability of performing a ductility analysis of the substructure.

The p-multiplier Method. In lieu of using dynamic or static soil stiffness reduction factors based on elastic solutions, as was done in the development of the WashDOT procedure, PoLam et al. [24] now recommends that pile groups be modeled by applying p-multipliers, ρ, defined in Figure 2, of 0.5 to static p-y curves for piles or drilled shafts in cohesionless or cohesive soils to reflect both group action (stress overlaps) and cyclic degradation of soil around the piles for seismic loading in deposits that do not liquefy. This can be a simple alternate to the explicit PMB method described

previously. In addition, this factor takes account of the effects of stress overlaps that occur among the piles in a group due to loading of neighboring piles. Table 2 summarizes typical p-multipliers that are used for static analyses of pile groups at present [32, 33]. On the average, these values are quite close to the value of 0.5 recommended by PoLam et al., indicating that for dynamic, cyclic loading, the combined effects of soil degradation and temporary strength and stiffness gain due to radiation damping approximately offset one another.

PoLam et al. [24] also conclude that the effects of pile-head fixity, variations in bending stiffness in the piles during lateral loading, scour, soil liquefaction and the formation of gaps between piles and soil during cyclic loading are major issues that need to be considered in pile-group design. That is, the use of p-multipliers is only one detail that is significant in the design of laterally loaded pile groups.

Alternate Analysis Methods. Alternate methods for the analysis of laterally loaded pile groups are used by some consultants to state DOT's [13]. Some of these methods, like the WashDOT Method, take account of the effects of stress waves that are generated in the soil by laterally vibrating piles on the stiffness of their neighboring piles. These waves in theory can affect both the stiffness and damping in the soil supporting a given pile in the group. Current practice, however, generally concedes that these effects are small for extreme event loading, in which considerable energy is dissipated through hysteresis rather than radiation, since only radiation produces stress waves. The model that is proposed in this report does not directly consider stress wave interaction effects.

Liquefaction. In the event that soil in the free field is determined through separate geotechnical analysis to have the potential to liquefy during a loading event such as an

earthquake, PoLam et al. [24] recommend that p-multipliers smaller than 0.5 be used. Such values would come from the evaluation of the strength loss in the soil from free-field pore pressures. Some guidance on these factors are available through small-scale centrifuge experiments on the behavior of piles in liquefied soil [e. g., 34, 35]. Ashford and Rollins [36] conducted very informative large-scale, slow-cyclic, field lateral-load tests on single piles and pile groups within zones of liquefied sand (produced by controlled blasting). For a four-pile (2 X 2) group of free-headed, 324-mm-diameter steel pipe piles in liquefied soil, the lateral stiffness of the group on the first cycle of loading was reduced to a value of about 0.2 times its stiffness in the same soil prior to liquefaction. For a nine-pile (3 X 3) group of the same piles, the lateral stiffness of the group in the liquefied soil on the first cycle was reduced to about 0.15 times its stiffness in the same soil mass before liquefaction. These data suggest, as PoLam et al. indicate, that liquefaction has a profound effect on lateral stiffness of the soil supporting piles in groups but that such stiffness does not decrease to zero.

The analysis method that will be pursued in this report, which is based on the p-y method, will not explicitly consider liquefied soils. The information from the Chi-Chi earthquake and similar studies have indicated that far less than half of the damaged foundations and superstructure damage resulting from excessive foundation movements occurred in liquefied soils. However, soil strength in the proposed method can be degraded and p-multipliers can be modified empirically to account for the designer's best estimate of loss of soil support due to liquefaction.

Axial Pile Stiffness Modeling. Proper modeling of axial pile response is very important in the analysis of laterally loaded pile groups. Lateral forces applied to the

superstructure mobilize axial loads in piles in two ways. First, they produce moments about the pile cap that produce rotation of the cap and therefore axial compression and tension thrusts in the piles. Second, even if the resultant of loads passes through the centroid of the pile group, any lateral component will cause the cap to translate. If the piles are fixed into the cap with any degree of fixity, "fixing" moments will be produced at the pile heads that will cause the cap to rotate, thus inducing axial thrusts in the piles. The extent to which such cap rotation can produce axial thrusts depends on the axial stiffness of the piles [37]. In turn, these axial forces affect the pile-head moments, which affect the lateral response (stiffness) of the pile group.

Norris [29] stated that axial stiffness of piles is different in compression and uplift, so that when a pile group rotates under extreme lateral loads, the center of rotation migrates, since the piles acting in compression have a different axial stiffness than those on the uplifting side of the group. One-half cycle later the piles that were in compression go into uplift and vice versa, which causes a shift in the location of the axis of rotation. If the migration of the center of rotation is not taken into account in the analysis, the motion of the pile group and the loads on the piles will be computed incorrectly. This is not easily done in a Step-1 analysis unless the method used in the analysis can incorporate different values of stiffness for axial compression and uplift loading. Most current design procedures ignore this effect, and many ignore axial stiffness altogether.

Summary

The realization that nonlinear structural and soil behavior affect the stiffness of laterally loaded pile groups during extreme events, which in turn affects the response of the structure, suggests that an improved, user friendly, nonlinear model should be

developed and employed for designing laterally loaded pile groups for DOT structures in the future. That effort was the overall goal of this research project. Because of the successful experiences of designers of offshore structures in the use of the p-y method, the p-y method was selected as the basis of nonlinear soil modeling for the pile-group-superstructure analysis method that was developed for this project. In order for that method to improve practice significantly, it must have the capability of simulating yielding of piles during the extreme event being modeled and simulating the effects of axial loads in piles in the group on lateral behavior, and, per the recommendations of Bardet et al. [12], it should permit loads to be applied to the pile-structure system through the soil. It will be possible to model liquefaction implicitly and empirically through user-supplied modifications to the p-y curves; however, the computational model will not be developed to analyze the effects of laterally spreading ground.

In order to facilitate the use of this computational model, or similar models that now exist that could conceivably be used for the same purpose, it was desirable to develop a means of defining p-y curves and correction factors for p-y curves to take account of group action, dynamic loading and similar effects. That was a major effort in this research project. The p-y curves and correction factors, such as p-multipliers, were developed through a combination of analytical modeling and full-scale dynamic field testing, and a means for deriving such factors on a site-specific basis was also devised.

RESEARCH OBJECTIVES

The underlying objective of the research reported herein was to advance the state of design-level practice for laterally loaded pile groups, with a strong focus on extreme-

event loading by utilizing and improving upon the current concepts that were described in the previous section. Specific objectives were as follows:

1. Determine experimentally the effect of method of pile installation on p-multipliers.

2. Determine appropriate p-y curves analytically, including damping factors and p-multipliers for harmonic, dynamic loading.

3. Develop a specific, user-friendly numerical model for static and dynamic loading of pile groups. This model will incorporate the capability of using the dynamic p-y curves and p-multipliers from Objectives 1 and 2 and be capable of modeling (a) extreme nonlinear structural behavior of the piles within the group and full or partial restraint at the pile heads, (b) loading of the piles through the pile cap (as for ship or ice impact loading) and from the pile cap (as for feedback from seismic loading of the foundation), (c) loading of the piles kinematically by the seismically excited soil, and (d) the presence of batter piles in the group.

4. Design, develop and deploy a reusable pile group that can be installed at various sites by state DOT's to determine directly site- and pile-type-specific dynamic stiffness and/or site- and pile-type-specific dynamic p-y curves and p-multipliers.

5. Perform repetitive impact loading tests upon the pile group (Objective 4) at two geologically diverse sites and with two geometric configurations for the purposes of evaluating the performance of the group piles and other features of the portable system, and derive experimental p-y curves and p-multipliers from those tests.

These objectives address the recommendations of the Bardet et al. report [12], except for providing a better understanding of the behavior of laterally loaded pile groups in liquefied soil and the means for modeling the effects of laterally spreading soils.

RESEARCH APPROACH

The research objectives were accomplished by performing the following tasks:

1. Review the literature on design and analysis of laterally loaded pile groups.

2. Review the state of practice in designing laterally loaded pile groups for extreme events, and develop an initial design for the reusable pile group referred to in Objective 4 in the preceding section.

3. Write an interim report covering Tasks 1 and 2 [13]. The salient points in the interim report, except for the design of the reusable test pile group, are summarized in the introduction to Chapter 1 of this report. Drawings of the reusable test pile group are provided in this report.

4. Select and test a numerical model that can be modified to meet Objective 3. Use that model to infer p-multipliers for new static lateral loading tests on pile groups, e. g., a set of massive group tests conducted recently in Taiwan. The model chosen was FLPIER, developed at the University of Florida, which employs a time domain analysis of a pile-soil-cap-pier system.

5. Modify FLPIER to include dynamic loading. The modifications are illustrated schematically in Figure 3. Included are the capability to excite the piles by exciting the supports of p-y curves according to time histories of free-field soil motion predicted off-

line by SHAKE [28] or similar methods; mass effects in the piles, pile cap and supported pier; nonlinearity and hysteretic damping in the p-y curves (soil) and the M-ϕ relations (piles and other structural elements); and the capability to model the development of gaps both in the soil adjacent to a pile after lateral movement of the pile has thrust the soil away from the pile and in the piles, in which, for example, cracks in concrete piles may need to be closed before the section can begin to develop a higher resisting moment. Test the modified version of FLPIER against well-controlled experiments, and validate it against ADINA, a well-known, comprehensive finite element program [38].

6.   Perform field load tests with the reusable pile group. First, construct, instrument and calibrate the piles; then, construct a portable cap (frame). Second, select sites for testing. The sites chosen were the U. S. 17 bypass over the Northeast Cape Fear River, near Wilmington, NC (soft-soil location), and the Spring Villa National Geotechnical Experimentation site near Auburn, AL (stiffer soil location). Third, conduct the load tests by performing static and Statnamic load tests on single reference piles and then upon the test groups. Statnamic tests applied a single-direction impulse load through an increasing sequence of load amplitudes. Fourth, reduce and analyze the test data to infer p-y curves and p-multipliers under repeated impulse loading (for use in FLPIER or similar software), and comment on the future use of the portable pile group for site-specific testing.

7. Develop the final report (this document).

30

Chapter 2: FINDINGS

INTRODUCTION

The findings for this research are given in detail in Appendices A - F. This chapter provides a summary of those findings.

EFFECT OF INSTALLATION METHOD ON p-MULTIPLIERS

Current typical modifications for p-y curves for group action using p-multipliers were reviewed in Table 2. These factors were developed from analysis of full-scale pile group tests and from centrifuge tests on pile groups. They modify p-y curves on a row-by-row basis, rather than on a pile-by-pile basis, mainly because analysis of test results did not yield a clear pattern of shear resistances among the individual pile heads within any group but did reveal clear patterns of average head shears on each row, from leading to trailing. Trailing rows tend to attract less load than leading rows because the strength of the soil mass against which a trailing row of piles pushes has been reduced by the movement of the piles in a leading row away from that soil mass. This physical effect is not reflected in elastic solutions for pile-soil interaction without artificial manipulation of elastic constants for the soil, but it is directly reflected in the p-multipliers.

One factor that may affect the values of p-multipliers is the manner in which the piles are installed. For example, the installation of a group of bored piles tends to reduce the effective stresses, and thereby the strength and stiffness, in soils surrounding piles already in place. For driven piles, the opposite effect may prevail. The values in Table 2 do not reflect installation method. During the performance of this research project, the research team had the opportunity to acquire and analyze data from a major static lateral pile group testing program in predominantly loose to medium dense silty sand that was

conducted for the Taiwan High Speed Rail Authority near the city of Chaiyi, Taiwan. Details of the test program and soil conditions are given in Appendix A.

Two pile groups were installed and tested as illustrated in Figures 4 and 5. The first group (Figure 4) was a group of six (3 X 2) bored piles 1.5 m in in diameter. The second group (Figure 5) was a group of twelve (4 X 3) driven, circular displacement piles 0.8 m in diameter. The spacing in both groups in both directions was 3 D on centers. Companion, isolated piles were also installed adjacent to the test groups to serve as references. Because of the manner in which the group piles were attached to the pile caps (thick, cast-in-place reinforced concrete caps), the bored piles were considered as being fixed (having full moment connections), while the driven piles were considered as being pinned to the cap.

In both groups, the installation order was generally from the leading row (first) to the last trailing row (last), although there were some variations in this pattern. See Figures 4 and 5 for documentation of installation order. After all of the group piles were installed, but before they were loaded, CPT and DMT tests were performed in the soil between the group piles and compared with the CPT and DMT readings before the piles were installed. These tests indicated that in the zone in which lateral soil response is important, installation of the bored pile group generally caused the strength and stiffness indicators to decrease, while the opposite observation was made in the driven pile group.

Site-specific p-y curves were determined through back-analysis of the results of the lateral load tests on the reference piles, using the computer code LPILE [25]. These p-y curves were then input into an early (static) version of FLPIER [33] and the

32

deformations of the group caps were predicted. The version of FLPIER that was used had the capacity to model nonlinear structural behavior in the piles.

Meanwhile, the group caps had been loaded to a maximum load of 1000 metric tons (1100 tons) each by one-way jacking, and the deformations of the pile caps and individual piles were measured. The loads were applied as ground-line shears in several increments of increasing load, with unloading after every increment.

The predicted and measured load-deformation relations did not match without modification of the p-y curves that had been developed for single piles at the site. p-multipliers had to be applied to both sets of p-y curves (bored and driven piles) in order for an acceptable match in predicted and measured results to be obtained. These p-multipliers were quite different for the bored and driven pile groups — lower for the bored piles than for the driven piles, which reflects, at least qualitatively, the changes in CPT and DMT readings observed in the soil within the groups before they were loaded. The values for the p-multipliers that were required to affect acceptable matches in load-deformation behavior are shown in Table 3.

On average, the p-multipliers for the bored pile group were slightly lower than those recommended by Peterson and Rollins or by FLPIER. As for the other methods, the p-multipliers were found to be larger for the first row than for the subsequent trailing rows. For the driven pile group, however, the p-multipliers were higher on average than those recommended by Peterson and Rollins or by FLPIER in all four rows. This may have been caused to some extent by the fact that the driven piles were modeled as pinned-headed. Had they been modeled as having partially restrained heads at the level of the pile cap, the p-y curves that would have been required to match the measured behavior

would be softer and the p-multipliers therefore lower. There was no evidence in the test results, however, that the piles were restrained by the pile cap.

It can be concluded form the Chaiyi tests that lower p-multipliers should be used in loose to medium dense cohesionless silty sand for modeling groups of bored piles than for groups of driven, displacement piles, in the general pattern shown in Table 3. Further research on this issue is warranted. This effect may not be true at sites where cohesion exists in the granular soil. Note is also made that the p-multipliers for these very-large-scale static tests were in the general order of magnitude of the p-multipliers that PoLam et al. recommend for seismic analysis of laterally loaded pile groups.

ANALYTICALLY DERIVED P-Y CURVES AND P-MULTIPLIERS

The development of p-y curves and p-multipliers for dynamic (e. g., seismic) loading involved several sub-studies, documented in Appendix B.

Kinematic Loading of Pile Groups

First, in order to investigate the effects of kinematic loading (loading of the piles by the soil) versus inertial loading (loading of the piles from inertial feedback from the superstructure), single piles and pile groups embedded in soil were modeled using the computer code ANSYS [39] by imposing seismic motion from a simulated bedrock base located either at the elevation of the pile toes (simulating socketed piles) or below the elevation of the pile toes (simulating floating, or "friction" piles). ANSYS is a 3D finite element code that permits the use of nonlinear soil stiffness, including damping and gapping between the soil and the piles. The piles had mass but supported no superstructure with mass or stiffness when modeling only kinematic action.

The salient results of this sub-study were that

- pile-head response resembles free-field response at low predominant earthquake frequencies,

- pile-soil-pile interaction (pspi) is not important in the frequency range of interest for seismic loading (0 - 10 Hz), and

- based on limited evidence, pspi is important in the frequency range of interest for seismic loading (0 - 10 Hz) when inertial feedback occurs, but pspi appears not to be dependent on the frequency of loading in this frequency range.

Inertial Loading of Pile Groups

Inertial (pile-head) loading of both individual piles and pile groups under harmonic conditions was analyzed using a computational model addressed in Ref. 40. A schematic of that model is shown in Figure 6. Hysteretic, hyperbolic p-y curves are used in the near-field, in the vicinity of the pile, to capture the nonlinear stiffness of the soil and the hysteretic energy dissipation that occurs in the soil near a pile. This stiffness model is placed in parallel with a damper, which is frequency dependent. The soil in the far field, away from the pile, is modeled by a separate linear spring and dashpot to represent the stiffness of the soil in the far field (which in a group is the soil between piles) and its radiational damping characteristics. The stiffness and damping parameters were evaluated from methods referenced in Appendix B. The piles were modeled with a numerical version of the dynamic bending stiffness equation. The piles remained elastic, had mass and for computational purposes were circular and vertical.

The basic near-field soil stiffness relation was taken to be the static p-y curve recommended by the American Petroleum Institute [41]. Both clay criteria and sand

35

criteria were used to develop these curves. The soil and computational models were validated by modeling Statnamic tests on piles.

Using the computational model, dynamic p-y curves were developed for a typical single pile in clay and sand profiles. Soil parameters and pile properties used in the various runs that were made are documented in Table B-1 of Appendix B. Cyclic degradation of the soil was permitted using the Idriss δ method (Appendix B), and gapping was modeled. The pile was considered to be a solid circular pile with mass. Results (after 5 cycles of harmonic pile-head loading at various frequencies) are represented by Figures 7 (soft clay) and 8 (medium dense sand). The dynamic p-y curves were all stiffer and stronger than the static p-y curves.

Simplified Dynamic p-y Expressions

The dynamic, single pile p-y curves were fit with an analytical expression, which appears to be valid for soft to stiff clay and loose to dense sand. That expression is given in Equation 3.

$$p_d = p_s \left[\alpha + \beta a_o^2 + \kappa a_o \left(\frac{\omega y}{D} \right)^n \right], \quad p_d \leq p_u \text{ at depth of p-y curve,} \quad (3)$$

where p_d = dynamic value of p on the p-y curve at depth x (e. g., in N/m),

p_s = corresponding reaction on the static p-y curve at depth x (N/m),

a_o = frequency of loading, expressed in dimensionless terms,

= $\omega r_o / V_s$,

D = pile diameter (m),

r_o = pile radius = D/2 (m),

ω = circular frequency of loading = $2\pi f$, where f = actual frequency of

36

loading (rad/s),

y   = lateral pile deflection relative to the soil at depth x, when the soil and pile are in contact (m), and

α, β, κ, and n are constants determined from curve fitting Eq. 3 to the dynamic p-y curves such as those shown in Figures 7 and 8. Values are given for various soil types in Table 4.

The fitted expressions are shown as dotted lines in Figures 7 and 8.

Equation 3 can be separated into two parts, a secant stiffness that is exactly equal to the secant stiffness to the static p-y curve at a give value of y and a damping term that is used to multiply the lateral velocity of the pile at depth x. That is,

$$p_d = ky + c\dot{y} , \qquad (4)$$

where   k   = secant modulus to the static p-y curve at pile deflection y,

     c   = damping value given by Equation 5, and

     $\dot{y}$ = velocity of the pile at the depth of the p-y curve.

The damping constant c is given by

$$c = \frac{p_s \left(\beta a_o^2 + \kappa a_o \left(\frac{\omega y}{D} \right)^n \right)}{\omega y} , \qquad (5)$$

where the factors are as defined previously. This p-y curve formulation has been incorporated as an option in FLPIER, discussed in the next section and in Appendix C. For use in FLPIER, or any similar program, ω can be taken as 2π times the predominant frequency of the earthquake for which the foundation is being designed, not to exceed 10 Hz. The dynamic p-y curve expressions, Equations 4 and 5, are most accurate for a_o >

37

0.02, since the plane strain dynamic stiffness model used to develop the far-field stiffness terms tends to become inaccurate as static conditions are approached ($a_o = 0$).

Dynamic p-Multipliers

p-multipliers for dynamic pile-head (inertial) loading were developed using the model described in Ref. 40 by comparing the response of two identical parallel piles at a given center-to-center spacing, S, with that of a single pile under comparable harmonic, pile-head loadings. In this set of computations only sand p-y curves (loose, medium and dense) were used as backbone relationships. Nonlinear near-field soil behavior, gapping and soil degradation were modeled, but the piles remained linear. The dynamic p-y curve p-multiplier is expected to depend upon several parameters, indicated in Equation 6, below, in which q is the angle between the direction of movement of a pile for which p-y curves are being computed and a line connecting the center of that pile with the center of a neighboring pile that influences the stiffness and strength of the soil surrounding the pile for which p-y curves are being calculated.

$$\textbf{p-multiplier} = f \left(\textit{S/D, y/D, } a_0, \theta \right) \quad . \tag{6}$$

The analytical work did not directly address the effect of θ; however, preliminary analyses indicated that θ had only a small effect on the p-multiplier. That is, group interaction for two side-by-side piles with this model was similar to that for two in-line piles at a comparable spacing, and the p-multiplier was not strongly dependent upon direction of loading. That is, the p-multiplier for the effect of a leading pile on a trailing pile was about the same as for the effect of a trailing pile on a leading pile. The effect of

direction of loading was not strong because the p-multipliers were determined after 5 cycles of loading, after which the model could not distinguish "shadowing" in a trailing pile from "plowing" in a leading pile.

The p-multipliers that were obtained for a medium dense sand using this model are shown in Figure 9 for several values of dimensionless spacing, S/D, dimensionless displacement, y/D, and dimensionless frequency, a_o, for in-line loading ($\theta = 0$). The soil and pile properties were identical to those used to obtain the dynamic, single-pile p-y curves (Figures 7 and 8) and are given in Table B-1 of Appendix B.

Figures similar to Figure 9 for loose and dense sand are shown in Appendix B. The values for the dynamic p-multipliers vary very little among loose, medium and dense sand profiles. It is also clear by comparing the various panels in Figure 9 that the p-multipliers are almost independent of the frequency of loading. To date, similar factors have not been developed for clay soils.

The p-multipliers were developed through a series of analyses of two interacting piles with varying spacing and varying frequency. Varying values of y were produced by varying the amplitude of applied load. The manner in which the derived p-multipliers can be used to analyze a pile group under seismic or impact loading is illustrated in Figure 10. For any given pile, its p-multiplier is obtain by successively multiplying the p-multipliers for surrounding piles (not to exceed a spacing of 6 D) together. θ is not considered in the determination of the p-multiplier; however, the p-multiplier is dependent on pile displacement, y, especially at close spacings. In theory, therefore, the computer code that uses these p-multipliers must vary the p-multiplier according to the computed lateral pile displacement. However, approximately, the dynamic p-multiplier

can be evaluated as a constant at the target value of pile head (soil surface) deflection for practical purposes.

The analytical results, which show very little dependence of the p-multiplier on θ, along with the observation that seismic motion is multidirectional as indicated in Figure 10, suggest that an acceptable approach to analysis of laterally loaded pile groups using the p-y method with p-multipliers would be to calculate the average p-multiplier from among all piles in the group and to use that average p-multiplier for each pile in the group when executing FLPIER or similar numerical models.

It is of value to compare the dynamic p-multipliers given in Figure 9 with the static p-multipliers obtained from the large-scale pile group tests at the Chaiyi site in Taiwan. The comparisons are made in Table 3. For the bored pile group, the dynamic p-multipliers were determined at a value of y corresponding to 20 mm, the largest value measured at the cap elevation in the load test, and for a value of $a_0 = 0.06$. This corresponded to $y/D = 20 / 1500 = 0.013$, which might reasonably be taking as a lower bound to the limiting deflection of this group in an earthquake. Much larger deflections were achieved in the driven pile group, and the limiting deflection for seismic action for the purpose of computing the p-multipliers was arbitrarily set at 60 mm ($y/D = 60 / 800 = 0.075$). Again $a_0 = 0.06$ was assumed (although very similar values would have been obtained for a_0 varying from 0.02 to 0.12). It is observed in Table 3 that the dynamic p-multipliers were somewhat lower than the static values determined from the load test on the leading two rows and were somewhat higher on the trailing two rows. However, the average values were nearly equal. Since the p-multipliers in Figure 9 are relatively constant beyond $y/D = 0.075$, it can by hypothesized that the average static p-multiplier

that is measured in static load tests such as the ones performed at Chaiyi is a reasonable approximation of the average dynamic p-multiplier in soil that can be characterized as a medium dense to loose sand at relatively large pile displacements that may occur in a severe extreme event. For the bored pile group, the match of average p-multipliers was not as close. This may be because the physical piles were much larger than the piles modeled analytically on an absolute scale basis (D= 1500 mm vs.D = 250 mm).

FLORIDA PIER (FLPIER(D))

A computational model for the nonlinear dynamic analysis of pile groups, group caps and supported superstructures was produced as part of this research project. The computer code is called FLPIER(D). FLPIER has been developed to its current state through an evolutionary process over a period of about ten years under sponsorship of the Florida DOT, the Federal Highway Administration, and now the National Cooperative Highway Research Program. In developing the current dynamic version of FLPIER, special attention was given to nonlinear modeling of reinforced concrete members of the pile-cap-pier system as cracking and yielding occur during a seismic or impact event. FLPIER(D) also includes nonlinear soil response in the axial and lateral directions along all piles in the system using p-y curves and t-z curves (Figure 3) and has the provision for specifying the parameters for the simplified dynamic p-y curves described in the previous section and p-multipliers that are selected by the user. While explicit values for dynamic p-multipliers based on Figure 9 are not determined internally in FLPIER, the user can select values from Figure 9, based on pile spacings and target deflections, and input them into the code. It should be noted that the dynamic p-multipliers in Figure 9 have only

41

been developed sand profiles (soils whose initial stiffness increases in proportion to depth). The applicability of these factors to clay sites is as yet unknown.

The material models and general computational methods used in FLPIER are documented in Appendix C. FLPIER runs in a Windows environment and was written in such a way that it can be used readily by designers. For information on obtaining copies of the code and instructions for its use, the reader should contact the Bridge Software Institute at the University of Florida (http://www.ce.ufl.edu/~bsi/).

One potential advantage of FLPIER(D) (dynamic version) is that it is capable of modeling the softening effects that occur in any component of the soil-pile-cap-pier system as an impact or seismic event progresses. By appropriate future application of FLPIER(D) (to model the nonlinear dynamic behavior of the soil-pile-cap-pier system), FLPIER(D) can be used iteratively with other computer codes that model the nonlinear behavior of the detailed superstructure and adjoining bridge piers. By using this simulation method in the design approach, it will not be necessary to compute the feedback loads on the pile caps computed in a linear modal analysis of the superstructure and divide those loads by a factor (in the range of 1.5 to 5), as is currently done, to reflect structural nonlinearity before analyzing the piles structurally. Since both the foundation-pier program (FLPIER(D)) and a nonlinear superstructure program will capture nonlinear effects (cracking, yielding and plastic hinges), the loads that are determined to occur in the piles will be the correct ones to be used for structural detailing.

However, FLPIER, as well as other appropriate computer pile foundation codes, can be used in the current two-step design process to compute displacement- and velocity-dependent pile group stiffness for use in analyzing the supported structure in a

modal analysis process (Step 1). The forces and moments computed at the column-cap connection by modal analysis of the structure can then be reduced by the appropriate structural ductility factors and applied back to the foundation, using FLPIER to compute the axial thrusts, shears and bending moments in all of the piles to permit structural detailing in such a manner that appropriate ductility will be provided. The simplified dynamic p-y model for laterally loaded pile groups described in the previous section and dynamic p-y curves and p-multipliers inferred from the full-scale test data reviewed in the following section are intended to improve the accuracy of FLPIER, or other nonlinear foundation analysis software, for the purpose of this design application.

The version of FLPIER(D) that has been developed for this project contains the following specific improvements relative to earlier versions of FLPIER.

1. A fiber model for modeling nonlinear bending of reinforced concrete cross sections, including hysteresis with gapping in cracked regions.

2. Distributed mass models for the piles, cap and pier for modeling dynamic loads.

3. The facility to impose dynamic loads at the level of the pile cap or motion time histories at some prescribed elevation in the soil, usually the top-of-rock elevation, for which the acceleration time history is either known or can be estimated for a given design seismic event.

4. The capability to input estimated ground acceleration time histories into the piles within the pile group at the support points of all p-y curves (equally in all piles).

5. Extension of the existing p-y models for the soil to consider unloading and gapping, to include effects of radiation damping through user-prescribed values of a

43

dashpot constant attached in series to each p-y curve (e. g., Equation 5), and to include forced movement of the reference points (supports) for the family of p-y curves needed to implement the algorithm for 4).

6. The specific formulation for p-y curves under dynamic loading given in Appendix B.

None of the p-y models currently implemented in FLPIER(D) explicitly considers soil liquefaction or lateral spreading of ground resulting from liquefaction.

FLPIER(D) was validated against a sophisticated finite element code, ADINA [38], for the case of linear piles and nonlinear soil. Details are provided in Appendix C.

Application of the new version of FLPIER(D) to structural load tests reported in the literature indicates that the proposed model for concrete is in reasonable agreement with a number of reported test results. Several comparisons of predicted and measured nonlinear structural behavior are thoroughly documented in Appendix C. A "fiber" model incorporated into FLPIER(D) (Figure 3) to consider nonlinear bending and hysteresis in reinforced concrete seems to be effective in modeling steel as well as circular and square reinforced concrete sections.

It is clear from laboratory test results that were reviewed in Appendix C that anchorage slip of reinforcement is an important concern when analyzing reinforced concrete members under cyclic loading, typical in earthquakes. Anchorage slip is not explicitly included in the reinforced concrete model for FLPIER(D); however, it is shown in Appendix C that it is possible to model anchorage slip effects by decreasing the values of the moduli of elasticity for both concrete and steel. The reduced-modulus model can be calibrated for a specific structure by performing physical tests for different structural

44

sections and adopting the corrected value for the moduli of elasticity in the analytical model. Others performed physical tests on rectangular-shaped cross-sections under various modes of loading. Those tests were modeled numerically in Appendix C, and the same values of corrected moduli of elasticity for steel and concrete gave the best results for each test on a given section, showing that anchorage slip is a function of the cross-section details rather than the type of loading.

A concrete gap was introduced into the fiber model to replicate the stiffness degradation of the section. This appeared to work very well when compared with cyclic load tests on reinforced concrete members. However, it is clear from the hysteresis diagrams for all of the tests that a steel model that includes strain hardening, and possibly cyclic degradation, should be used in addition to the modeling of anchorage slip. Strain hardening of reinforcing steel is available as an option in FLPIER(D)

The dynamic version of FLPIER (FLPIER(D)) was used to model two dynamic pile group tests where soil was present around the piles. See Appendix C. Although the computational results were generally reasonable, procedures for specifying the dynamic group effect were not well understood at the time that these tests were modeled, and factors such as dynamic p-y curves and pile-soil-pile interaction were modeled arbitrarily. However, the approximations for p-y curves that were made in the analysis of centrifuge tests and full-scale tests using FLPIER(D) (Examples 6 and 7, Appendix C) gave reasonable estimates for the displacements and forces acting in the structures from very simple soil parameters.

The dynamic field tests described in the next section of this chapter and in Appendices D, E and F provided additional insight into modeling the dynamic group

45

effect. These new field tests were performed in parallel with the development of the new version of FLPIER(D), and analysis of these new test results using FLPIER(D), documented in the following section, provided valuable guidance in modeling dynamic group effects.

FIELD TESTING PROGRAM

Objectives

The major effort in this research project was the performance of field tests on full-scale, instrumented pile groups at two sites in the United States order to accomplish the following objectives:

1. Evaluate group effects on lateral soil response against piles, specifically observing the differences between group effects that occur during static loading, which are reasonably well documented, and those for large-magnitude dynamic loading, which are not.

2. Measure and assess the effects of rate of loading on the lateral response of pile groups.

3. Develop data from these tests in such a way that these test results can be used to evaluate or provide a basis for a dynamic model for laterally loaded pile groups that employs the p-y approach to soil modeling, such as FLPIER(D) (Appendix C).

4. Develop and evaluate the benefits of a reusable pile group for possible applications at future field test sites.

In order to accomplish these objectives, a group of instrumented steel pipe piles were constructed, complete with a steel frame that was designed to serve as a both driving template and loading cap. Thirteen piles were instrumented internally with strain

46

gauges that were designed to survive and function after repeated installation by driving and extraction of the piles. The system worked generally as intended, although the frame proved to be somewhat time consuming to erect and dismantle. The future use of this part of the system will be discussed in more detail.

The tests completed for this project include both static and dynamic lateral loading tests at sites with a range of soil conditions, along with static tests on single piles that serve as controls for comparison of group effects. Static tests were performed by hydraulic jacking of the instrumented pile group against a reaction foundation. Dynamic tests were performed by utilizing the Statnamic® loading system to impart a sequence of rapid load pulses against the test group. Tests were performed at two locations at each of two sites.

Overview of the Load Testing Program

The first of the two sites was in Wilmington, NC, at the proposed location of the Cape Fear River Bridge. The use of the test pile system was incorporated into a design phase load-testing program with the cooperation of the North Carolina DOT (NCDOT). Static and dynamic load tests were performed at a location composed of very soft clay underlain by sand, and dynamic load tests were done at a second location with a depth of almost 2 m of water underlain by loose sand.

The second site was near Opelika, AL, at the Spring Villa National Geotechnical Experimentation Site (NGES) operated by Auburn University. Static and dynamic tests were performed on pile groups installed at different spacings between piles in a silty residual soil.

The following is a summary of the lateral loading tests performed for this project:

47

1. Wilmington static test on 3 (column) x 4 (row) group at 3-diameter-center-to-center (3D) pile spacing in both directions in soft clay.

2. Wilmington dynamic test on 3 x 4 group at 3D spacing in soft clay.

3. Wilmington static test on single pile in soft clay.

4. Wilmington static test on single pile over water in loose sand.

5. Wilmington dynamic test on 3 x 4 group at 3D spacing over water in loose sand.

6. Spring Villa static test on 3 x 4 group at 3D spacing in silt.

7. Spring Villa dynamic test on 3 x 4 group at 3D spacing in silt.

8. Spring Villa static tests (2 separate locations) on single pile in silt.

9. Spring Villa static test on 3 x 3 group at 4D spacing in silt.

10. Spring Villa dynamic test on 3 x 3 group at 4D spacing in silt.

The dynamic tests were generally performed by loading the pile group in the direction opposite to that of the static loading and after the static loading test was completed. Exceptions were the Wilmington test over water in sand, which did not have a static load test, and the Spring Villa 3 x 4 group test, in which the Statnamic loading was performed first, followed by the static loading in the opposite direction.

In the interest of producing a readable report, the details of the testing and test results at each site are provided in Appendices D (Wilmington tests), E (Auburn tests) and F (instrument calibrations) of this report. A summary of the test results is provided in the following sections of this chapter, along with illustrations and comparisons with computational models. These serve to provide a general sense of the observations and support the conclusions that derive from these observations.

Load Testing System and Methodology

The reusable load testing system is composed of the instrumented piles, a reusable frame, the loading systems, the external instrumentation, and the data acquisition system. The instrumented piles and frame were constructed explicitly for this project. The loading systems (hydraulic jack and Statnamic device) were rented, and the external instrumentation and data acquisition system utilized equipment this is the property of Auburn University.

Instrumented Piles

The most critical part of the load testing system is the instrumented steel pipe piles. These piles were selected to be large enough to represent field-scale piles, with an outside diameter of 273 mm (10.75 inches) and a length of approximately 12 m (40 feet). The piles had a wall thickness of 12.7 mm (½ inch) and a yield strength of approximately 300 MPa (43 ksi), so that the piles can be loaded repeatedly to relatively large displacements and bending stresses without yielding the piles. The piles consisted of straight seam pipe rather than spiral welded pipe in order that the fabrication process would have minimal influence on the instrumentation. All strain gauges were installed with the seam at 90° from the direction of loading and strain measurement.

Each of the 13 piles was instrumented with strain sensors on opposite sides of the pile at various levels. Seven of the piles were instrumented at 7 elevations (14 instruments) designed to measure the distribution of stresses along the portion of the length of the pile likely to be affected by lateral bending stresses, and the other six were instrumented at 3 elevations (6 instruments) near the top of the pile.

49

The strain sensors themselves were constructed using a system of strain transducers welded to the inside of the pile. The strain sensors consist of a square tube approximately 12 mm wide and 300 mm long that is instrumented on two opposite sides with a pair of electrical resistance strain gauges in T-rosette configuration on each side. These four gauges comprise a single strain sensor that provides a full-bridge strain gauge circuit which is stable, automatically thermal compensating, and unaffected by the resistance of lead wires. The electrical resistance gauges are used to allow for high frequency measurements during dynamic loading; vibrating wire gauges are not suitable in such conditions.

Each strain sensor was positioned over two alignment holes drilled into the face of the pile at a distance approximately 200 mm apart at the appropriate elevation, and TIG welded through these holes from the outside face of the pile. The hole left on the pile face was then filled with epoxy so that the strain indicator has no affect on the shape of the pile. These strain sensors are thus entirely within the enclosed steel pipe and protected from damage by the soil during installation.

The lead wires for the sensors were routed up through the pile and attached to a hook inside the pile near the top so that the lead wires are entirely inside the pile during driving. The leads were connected to a quick-connect type plug so that a separate independent cable can be attached from the data acquisition system after completion of pile driving.

At each measurement elevation, a strain sensor was positioned on each opposite side of the pile, with the sensor positions aligned with the direction of load. The piles have an external marking so that the pile can be aligned properly for a given loading

direction. Since each sensor is a full-bridge circuit, each provides a measure of tensile or compressive strain as a stand-alone device. Bending moments can be computed from the difference in strain between gauges on opposite sides, and axial forces can be computed from the average strain reading from gauges on opposite sides.

The completed piles with internal strain sensors were calibrated in the structures laboratory at Auburn University. This calibration was accomplished using a three-point loading system, in which the two ends of the 12-m-long pile were clamped to the strong floor and the center of the pile lifted via a cable equipped with a tension load cell. In this manner, the bending moment at each gauge location is known, and the associated strains were compared with the gauge output. The piles were loaded multiple times in opposite directions so as to exercise the gauges and verify that the signal is repeatable in both compression and tension. Details of the pile calibration are provided in Appendix F.

It is of interest to note that the gauge calibrations varied significantly from the theoretical values, with output signals smaller than anticipated by a factor of as much as 2. The signals were reproducible, reversible, and otherwise completely consistent in every case, and the calibration of the load cell was checked to verify that the calibration process was accurate and reliable. The field measurements of bending vs. depth from the single pile test results agree quite well with the expected trend near the top of the pile after adjustment of the sensors for the calibration factors. It is not clear why the gauge calibrations were variable. It is possible that the welding of the tubes to the pile on one side of the tube induced some bending in the tubes so that the strain measured on the sensor tube is not precisely that of the pipe to which the tube is attached. This is only a hypothesis for the observation, however, as the actual mechanism is not known. In any

event, so long as the strain sensor members behave elastically and the measurements are repeatable, this strain measurement system appears to provide reliable data. The strain sensors on the piles have survived 4 installations and 3 extractions with only a few lost gauges (and these generally appear to be due to wire damage near the top of the pile).

Loading Frame and Pile Installation

The steel loading frame was constructed of steel H and wide flange sections with attached steel cutouts welded to the frame to provide a guide for each pile. Dywidag bars (high-tension-capacity threaded steel rods) pass through the frame so as to allow the frame to be clamped down onto the piles after installation. Angle steel cross bracing on either side are provided to add stiffness. A schematic diagram and a photo of the frame are provided, respectively, in Figures 11 and 12.

For the typical arrangement of 4 rows of 3 piles, the center portion of the frame was erected, and cross braces were tack welded into position for the two center piles to be driven. The outside piles on the two center rows were driven next and the central portion of the frame tightened onto the piles with cross braces welded to the frame in these two bays. The leading and trailing row members of the frame were positioned next, and the center piles on these two outside rows were driven, followed by the 4 corner piles. Finally, the outermost frame members were tightened, dywidag bars were adjusted, and cross brace members were welded.

After the first such installation was completed and the system examined and evaluated, the decision was made that the piles should be tack welded to the frame guides. This decision was the result of concern that some slippage might occur if the axial loads in the pile during rotation of the group became high. Without welding the

piles to the frame, the only mechanism available to transfer axial forces through the frame would be friction at the guide contacts on the top and bottom of the frame. These guide contacts did not appear to fit so snugly as to eliminate concern that the axial forces might exceed the friction available at these points. The welding of the piles to the frame then required that these welds be cut and ground upon demobilization of the system; after three rounds of cutting and demobilization, the pile guides appear quite ragged and will need to be re-fabricated prior to another use.

External Instrumentation

Other instrumentation used during the testing program included linear potentiometers (300 mm stroke) for displacement measurement of the frame, piezoelectric accelerometers mounted on the frame for measurement of acceleration during Statnamic loading, and electronic load cells during all static and Statnamic loading operations. The potentiometers were mounted at four different locations on the face of the frame so that the overall displacements, pitching rotations, and torsional rotations could be determined. Accelerometers were mounted similarly. During single-pile tests, two potentiometers were mounted with the lower one at the elevation of the point of loading and a second one at a higher elevation, so that the slope of the top of the pile could be determined. Electronic load cells were used in every case to monitor load, with backup provided for static tests by observation of fluid pressure in the calibrated hydraulic jack. Details of the instrumentation setup and measurement locations for each test are provided in the appendices to this report which describe the specific load tests. Although each test was arranged similarly, the actual location of each instrument was measured and recorded for each individual load test.

Data Acquisition System

The acquisition of all instrumentation during the testing was accomplished using a Megadac data acquisition system, manufactured by Optim Electronics and owned by Auburn University. This system provides the needed capability to monitor over 100 channels of data at a frequency of up to 2000 samples per second. The system is controlled using a laptop computer, with data storage on the device downloaded to the computer hard drive immediately after completion of the test using an IEEE interface. For static testing, the system was typically set to monitor and record all channels of data at an interval of 2 to 10 seconds. For the dynamic tests (Statnamic loading), the system was set to record each channel at a frequency of 2000 samples per second, with a recording trigger off the load cell and storage of 0.5 seconds of pre-trigger and 4 seconds of post-trigger data. This time interval proved more than adequate to capture the pile group response during the dynamic loading events. Data stored using the Megadac test control software were exported to ASCII files for storage and subsequent analysis. Matlab® software was generally used for data presentation and analysis of test results.

Static Load Application

Static loads were applied to of the instrumented pile groups using a hydraulic jack with a load cell, pushing between the test foundation and a reaction foundation. In the case of the Wilmington, Site 1 (Ratt Island) test, the load was applied to the back side of the frame by pushing against a beam that was connected to the reaction foundation via tension cables. For the Auburn tests, the reaction and test foundations were pushed apart. In every case, hemispherical bearings were used on either side of the jack to avoid

eccentricity in the load cell/jack system. Single pile tests were performed in a similar manner.

Loads were applied and maintained at increments of load so as to include 6 to 12 load increments during the load application and define a load vs. displacement response to the static loading. At the Auburn site, some unload-reload cycles were included to measure the stiffness in such application. Each load was maintained for a duration of approximately 5 minutes. It was quite difficult to maintain the load precisely by pumping the jack, as smooth application of load in very precise amounts was not possible. Instead, the pressure valves from the jack were simply closed and the creep displacement and load was monitored. A static test was performed in typically 1.0 to 1.5 hours. The data acquisition system monitored all instrumentation and was set to record data every few seconds.

Statnamic Loading

The Statnamic loading method provides a method for generating large loads on foundations by "launching" a heavy reaction mass away from the foundation at an acceleration that can approach 20 g's. Figure 13 illustrates the typical test arrangement. The energy for the test is generated by burning special fuel pellets in a combustion chamber inside the Statnamic device, and allowing the resulting high pressure gas to vent at a controlled rate, which in turn controls the rate at which the foundation is loaded. The reaction mass is initially set up against the side of the foundation and imparts a load that ramps up to its maximum value in a finite amount of time, usually between 0.1 and 0.3 seconds, and then gradually decreases as the mass is propelled away from the foundation and physical contact between the foundation and the reaction mass ceases. The load is not

a sharp impact, but builds rapidly as a function of the gas pressure generated by fuel burning. The Statnamic loading provides a test that is quick, provides energy in a frequency band close to the fundamental frequency of the foundation, and produces significant inertial forces in the system that allows the determination of dynamic system properties. Successive Statnamic loadings with increasing load amplitudes were intended to approximate roughly the nonlinear soil response against the piles that would be experienced during a seismic event in non-liquefiable soils.

Basic Interpretation of Statnamic Test Measurements

Because the Statnamic loading involves inertial forces, the direct measurement of load and the measurements of foundation response must be considered with regard to a dynamic system. For a simple initial examination of the test data, evaluation of the dynamic response of each foundation group tested with the Statnamic loading device has been modeled using an equivalent single-degree-of-freedom (SDOF) system. The dynamic response of a SDOF system is governed by the following differential equation:

$$\mathrm{M}u'' + \mathrm{C}u' + \mathrm{K}u = \mathrm{F}(t) \qquad , \qquad\qquad (7)$$

where u'', u', and u represent the acceleration, velocity and displacement of the system, respectively, and define the physical state of the system at any instant of time, t. $\mathrm{F}(t)$ represents the forcing function vector; actual values of applied force in the load cell are measured with the data acquisition system at a frequency of 2000 samples per second. M, C and K are the generalized mass, damping and stiffness coefficients of the SDOF system. The mass and the damping coefficient are generally considered constant during a single loading event. Because soil load-displacement response to lateral loading at large strains is known to be highly nonlinear, the stiffness coefficient K is modeled with a

56

nonlinear stiffness term that decreases as a function of displacement, u within a single loading event. Equation 7 may also be expressed as follows:

$$F_{inertia} + F_{damping} + F_{static} = F_{statnamic} \quad , \tag{8}$$

where
$\quad F_{inertia} \quad$ = inertial resistance from effective mass of the foundation,

$\quad F_{damping} \quad$ = effective viscous damping resistance,

$\quad F_{static} \quad$ = effective static soil resistance, and

$\quad F_{statnamic} \quad$ = measured force on the Statnamic load cell.

The Newmark-β integration algorithm is used to solve the dynamic equation of motion numerically. Assuming the acceleration varied linearly between consecutive time steps, the response at any time could be computed using a total force balance and the state of the system at the previous step. The solution was implemented using a Matlab program with a graphic user interface whose input consisted of the measured Statnamic load vector $F(t)$ and the values of the system parameters M, C and K. The response of the system was obtained by interactively changing the values of M, C and K until a good match was observed between the measured displacement time history (signals from the displacement transducers) and the simulated response (computed by the model). The goodness of match between the model response and the measured response is judged by eye by plotting the time histories simultaneously on the same graph. In most cases, it is possible to arrive at a good match between the two with a relatively small number of trials.

The effective mass M is comprised of the total mass of the pile cap and portions of individual piles that contribute inertially to the response. The latter is usually restricted to the mass of the piles above the mud line or ground line, but it may vary slightly

57

depending on the magnitude of displacement and the degree of nonlinearity of the system. As such, this is the parameter that is easiest to define for SDOF analysis. The mass term affects the amplitude and form of the forced vibration part of the response (duration of Statnamic load), and the frequency of oscillation for the post-loading response, where the system undergoes damped free vibration.

The numerical value of the viscous dashpot, C, has relatively little effect on the response magnitude during the actual loading event but is significant in determining the amplitude decay and the damped free vibration frequency for post-loading response. In order to relate C more meaningfully to a system damping parameter, the damping constant may also be expressed as a percent of the critical damping C_c as follows:

$$\xi = C/C_c = C/[2(KM)^{1/2}] \quad , \tag{9}$$

where $\quad \xi =$ the damping ratio, and

$$F_{damping} = 2\xi(KM)^{1/2}u' \quad . \tag{10}$$

The term C is required to capture all of the rate-of-loading effects in the soil, which can be considered to result in energy dissipation in the soil through radiation, the material damping in the piles and pile cap, and the displacement-dependent hysteretic damping in the soil. Therefore, while Equations 7 and 8 are useful in visualizing the general performance of a dynamically laterally loaded pile group, a model, such as FLPIER(D) (Appendix C) is desirable to separate these distinct effects.

The magnitude of the first peak in the simulated displacement time history is sensitive to the value of the effective stiffness parameter chosen, K. The stiffness term also affects the frequency of damped free vibration at the end of the Statnamic loading event. K is also used to back-calculate a derived static load-displacement response, which

58

may be compared to the load-displacement function obtained from a conventional static test.

The simple SDOF model has been found to be extremely useful in comparing the results of Statnamic loading tests with more conventional static tests, and in visualizing the dynamic and rate-of-load effects which are present during such a test. This model is described further in Appendix D.

Test Results and Static Evaluation

This section provides a brief overview of the static evaluation of the Statnamic loading tests at each site, followed by an examination of all of the test data in comparison with the FLPIER(D) model (Appendix C). Greater details of the test measurements are provided in Appendices D and E. Complete test data are quite voluminous, but they are available from Auburn University on electronic media (CD).

Wilmington, NC, Tests

The test pile program on the Cape Fear River in Wilmington, NC, was the first use of the test piles. Two test areas were identified and used: Test Area 1 was on the shore of a land area known as Ratt Island, and Test Area 2 was in the water along the eastern edge of the channel in relatively deep water. For purposes of this evaluation, the test area 1 data will be considered in greater detail because the test provides both static and dynamic measurements to large displacements at a soft soil site. Test Area 2 included only Statnamic loading, and the great depth to the mud line resulted in the domination of the behavior of the pile group by structural characteristics of the system above the mud line, not soil behavior. At both locations the piles were driven at a

59

spacing of 3 diameters center to center, with 4 rows of 3 piles per row. These tests are described in detail in Appendix D.

Soil Conditions. The soil profile at Test Area 1 (Ratt Island) consists of an upper layer of soft organic clay, 2.5 meters thick, underlain by a 7.5-meter-thick layer of loose, alluvial sandy silts and silty sands. Below this layer is a thin layer of very soft alluvial clay just above the top of a dense, silty sand comprising the locally-termed "Peedee Formation." The test piles were entirely within the organic clay and alluvial sand. Standard penetration test values in the upper 6 meters were generally 0, with 11 to 12 blows per 0.3 m (bpf) in the lower portions of the alluvial sand. Cone penetration (CPT) tip resistance in the organic clay was close to 0 (at the lower limit of the instrument), around 3 to 5 MPa in the 3 to 7 m depth range, and above 10 MPa below 7 m. Some pressuremeter tests (PMT) were performed at this location, and these data indicate a modulus of deformation of around 2 to 3 MPa in the upper 2.5 m, around 20 MPa for the alluvial sand at the 3 to 5 m depths, and around 60 MPa for the lower portion of the alluvial sand.

Subsurface conditions at Test Area 2 (East side of River) consisted of 2 meters of water depth at high tide and 0.3 to 0.6 meters of water depth at low tide. The upper 13.5 meters consisted of loose, alluvial silty sands and loose to dense sands. The top of the Peedee Formation was encountered around elevation -15.5 meters. The piles were entirely within the alluvial sands. These sands had SPT values of 0 to 4 blows per 0.3 m (bpf) in the -2 m to -7 m elevation range, and in the range of 10 to 20 blows per 0.3 m (bpf) below. CPT tip resistance was less than 1 MPa above elevation -6 m and rose steadily to a value of around 15 MPa at a depth of around −9 m. The PMT modulus was

3 to 4 MPa in the 5 tests performed above elevation -7 m, rising to around 65 MPa at elevation -9 m. Dilatometer modulus values ranged from 1 to 10 MPa above elevation -7 m and ranged from 50 to 130 MPa below that elevation.

Load-Deflection Response. The static loading at Test Area 1 was completed first, followed by Statnamic loading in the opposite direction in 4 successively larger increments. Presented on Figure 14 is the general load vs. displacement response from the static and the derived static and total (static + damping) soil resistance from the Statnamic loading. For Test Area 2, only Statnamic results are available, as no static test was performed. These results are presented on Figure 15. In each case, the group was obviously loaded to very large lateral displacements, approximately equal to 50% of the diameter of an individual pile. The static behavior and static behavior derived from the Statnamic loading using the SDOF model compare exceptionally well for these test data. The initial loading point on the Statnamic result at Test Area 1 is likely to be somewhat softer than would be the case for a virgin loading due to residual displacement from the preceding static test in the opposite direction. The Statnamic test data indicate that a considerable damping contribution was present in the soil resistance for the two largest Statnamic loads (as indicated by the separation between the derived static and derived total load vs. displacement points). This was likely a result of large hysteretic (displacement-dependent) soil damping at those loads, which could potentially represent relatively severe seismic loading.

Interpretation of Strain Measurements. Examples of the bending moment vs. depth measurements are provided on Figures 16 and 17, for two load levels on Piles 8 and 11 during the static loading at Test Area 1. Pile 8 was in the lead row for this load

and Pile 11 was in the trailing row. One can see that the maximum positive bending moment for the trailing row pile occurs deeper than for the leading row pile.

At and above the ground line, the slope of the bending moment vs. depth relationship should provide an indication of the shear force transmitted to each pile. This interpretation of pile-head shear provides an estimate of the load distribution to the piles in the group. The load distribution estimated in this manner should be considered approximate, as measurement errors are greatly magnified when comparing differences between measurements (each of which has an associated measurement error).

Evaluations of the test data to estimate shear force distribution to the piles in the group indicate that the expected general distribution by row position was observed in these tests, with the greatest shear distributed to the lead row piles and lesser amounts to trailing rows. However, any conclusions regarding the spatial distribution of shear force must be tempered by the fact that large variations between individual piles were observed, by a factor on the order of a magnitude of 2. These variations appeared to be random and associated with spatial variations in soil resistance. In general, the piles, which were soft during the static loading, were also soft during the Statnamic loading in the opposite direction. There was no apparent pattern relating to installation order, position within a row, or any other obvious geometric factor other than row position. And, row position is only obvious when examining the average shear to the piles by row. The average of the shear distribution to piles by row position for the loadings at Test Area 1 were (by percentage of the total):

Row 1 (lead) = 29% (static)   = 33% (Statnamic)

Row 2   = 25% (static)   = 23% (Statnamic)

62

Row 3   = 21% (static)   = 21% (Statnamic)

Row 4 (trail)   = 25% (static)   = 23% (Statnamic)

One conclusion that might derive from these observations is that random variability relating to soil variations is at least as important as any other factor. Other factors such as locked-in moments in the piles due to lateral drift during driving might also effect this phenomenon.

Rotation of the group was also measured and was significant, as were axial forces in the piles. The measurement of axial force distributions to the piles is not considered particularly reliable due to the large bending strains superimposed on the strains caused by axial thrust. In principle, one can average the strain measurements across the pile cross section (there were two such measurements at each gauge level), but in practice the strains due to bending are so much larger that the derivation of axial force from such measurements cannot be taken as entirely reliable. In effect, such a measure is an attempt to use a pipe with two strain sensors as a load cell under conditions of severe bending. Even a carefully manufactured load cell will not provide a very reliable indication of axial force under such conditions. The axial forces measured appeared reasonable on the whole, although there is much scatter in the data.

Comparison with FLPIER Static Model. It is instructive to evaluate the test data using a 3D group model such as FLPIER in order to compare the observed group effects with those typically used for design. In order to isolate the group effects from other factors relating to modeling errors in predicting soil behavior, it is necessary to "calibrate" the group model using the results of tests on a single control pile. Any model prediction of group response without calibration to a single pile control is of limited use,

since the errors associated with group effects are not separated from general errors associated with predicting soil response at a particular site. The results of the static load tests on the single "control" pile (data presented in Appendix D) were used to develop soil properties such as p-y curves that accurately and reliably capture the response of the single pile loading test. Of course, there can be errors associated with spatial variability in soil response between the control and the group, so no control data set is perfect. The p-y curve profile used at Test Area 1 is composed of "soft clay" (Matlock criterion) p-y curves overlying "sand" (Reese, et al. criterion) p-y curves. The calibration of the p-y curves to the single pile test data matched not only the load vs. displacement at the loading point, but also the bending moment distribution with depth. The latter provides assurance that the general distribution of soil resistance below grade used to formulate the p-y curves is reasonable.

The FLPIER model of the pile group matched the as-built configuration, with the cap modeled as a flexural element having a stiffness roughly equal to that of a ½-meter-thick concrete cap. This cap is NOT perfectly rigid, but is thought to approximately match the stiffness of the frame. The axial stiffness of the piles proved relatively important in matching the rotational stiffness of the group, but axial loading test data were not available with which to "calibrate" the single pile axial response. The axial stiffness was simply estimated using default soil parameters within the FLPIER code and proved to match the observations reasonably well. No piles were observed to fail during static loading or during the first three Statnamic loadings. Some slippage at the pile/frame connection appeared to occur during the fourth Statnamic loading, as evidenced by popping sounds from the tack welds and jerks in the strain data while the

measurements were being taken. The fourth Statnamic loading may therefore have somewhat higher rotation than would be estimated by a model in which no pile yielding occurs.

The FLPIER model for a rectangular pile group with piles spaced at 3d center to center uses p-multiplier values according to row position to account for group effects. By default these values are 0.3, 0.2, 0.4, and 0.8 for trailing to leading row, respectively, for a four-row group. The default p-multiplier values in FLPIER are based on historical static load test experiments performed both in the field and in the geotechnical centrifuge. Using these default values and the p-y soil models developed from evaluation of the single pile test, FLPIER computed load vs. displacement and rotation, which is compared with the static test measurements on Figure 18. This model is seen to provide excellent overall agreement with the measured group response. The FLPIER analysis was performed again using a common p-multiplier for all piles equal to the weighted average for the four rows of piles in the group. The results of that analysis are also shown on Figure 18. This exercise was performed to evaluate a much more simple computational procedure. It appears that the overall response is captured reasonably well with this approach.

Continuing with the average p-multiplier concept, data are presented on Figure 19 that provide a comparison of bending moments vs. depth for the two FLPIER simulations with those measured on two piles. Pile 12 is in the trailing row, Pile 8 is in the leading row. The symbols labeled "Pm = FLP" represent the FLPIER model with the aforementioned default row-wise p-multiplier values, while the "Pm = 0.425" represents the FLPIER model with a single averaged p-multiplier applied uniformly to all piles.

Both simulations appear to capture the bending moments reasonably in the piles within the general range of acceptance for engineering design purposes. Considering the wide variations between shear distributed to piles that was unrelated to row position (and was apparently random), these computed results appear quite acceptable for design purposes.

The distribution of shear to the piles by row position computed by the FLPIER model were as follows (compared to the measured average shear by row position):

Row 1 (lead)	= 34%(FLPIER)	= 29% (static)	= 33% (Statnamic)
Row 2	= 26%(FLPIER)	= 25% (static)	= 23% (Statnamic)
Row 3	= 19%(FLPIER)	= 21% (static)	= 21% (Statnamic)
Row 4 (trail)	= 21%(FLPIER)	= 25% (static)	= 23% (Statnamic)

It appears that the default row-wise p-multiplier values slightly overestimate the variations by row position for this test. Of course, the model using the uniform average p-multiplier computes uniformly distributed shear to the piles (25% to each row).

Auburn University (Spring Villa NGES) Tests

The test pile program at the Spring Villa National Geotechnical Experimentation Site was performed in Jan/Feb., 2000, after shipment of the piles and frame from North Carolina. Two test foundations were constructed using the NCHRP pipe piles about a central reaction foundation as shown on Figure 20. The test groups consisted of a group of 12 piles at a spacing of 3 diameters center to center (similar to the Wilmington test) and a test group of 9 piles at a spacing of 4 diameters center to center. Static lateral tests on each group were conducted by hydraulic jacking, as shown in Figure 20. Dynamic loading of each pile group was achieved in the direction opposite to the static loading

using the Statnamic device. Static lateral tests were also carried out on single piles at locations adjacent to each group as shown on Figure 20.

The 12-pile group was constructed first, using the steel frame as a template. After the previous uses of this frame with tack welding of piles and welding and cutting of cross braces each time, the pipe guides and cross bracing locations had become ragged and required a large amount of cutting and grinding to match components together. The pile installation was completed and the piles welded to the frame at the contact points; however, these contact points required some additional small pieces of steel plate to be inserted to fill voids, and the process of completing this installation was very time consuming. In addition, the cross braces were placed on the outside of the panels as shown on Figure 11 rather than internally within each bay as shown in the photo of Figure 12 in an attempt to expedite completion of the test setup. The 12-pile group was tested first using the Statnamic device, followed by static loading in the opposite direction by pushing against the reaction foundation. The Statnamic loading was performed with a procedure similar to that for Wilmington, although the sled for the device rested directly on the ground rather than on steel runner beams or a barge deck.

After completion of testing of the 3D c-c, 12-pile group, the piles were extracted and re-driven for the 4D c-c, 9-pile group configuration. The extraction proved to be exceedingly difficult due to the large axial tension capacity of the piles. Note that the Wilmington tests over water had available a huge floating crane (4 MN lifting capacity), which was able to pull the piles directly. At the Spring Villa site with a typical construction site crawler crane having approximately 0.7 MN lifting capacity, it was not possible to pull the piles statically. A vibratory hammer was obtained, but in order to

"grab" the piles with the hammer it was necessary to weld a rather large plate to the tops of the piles. This entire process necessitated cutting about ½ m off the top of each pile to remove the damaged portion relating to the plate welding.

Because of the difficulties with using the frame for the 12-pile group, the fact that the frame would need to be reconfigured for the 4D arrangement, concerns that the construction time schedule had overrun the budget (the contractor was unwilling to stay on-site for the additional time necessary to re-fabricate the frame), and concerns that the frame had not proven to be as nearly rigid as anticipated, a decision was made to complete the 9-pile group test using a conventional cast-in-place concrete cap. Formwork was available from the 3 m by 3 m reaction foundation construction, and this was suitable for a 3 by 3 group of piles at 4D c-c spacing. The piles were driven and the cap cast around them after completion of the installation process. The 0.9-m-thick, heavily reinforced concrete cap was formed above grade using a plywood floor, and the supports for the floor were removed after the concrete was set. The piles were lubricated with form oil to facilitate future removal of the concrete cap, but this did not seem to result in slippage of the piles within the cap during the load tests.

The tests on the 9-pile group were performed by first applying static loading against the reaction foundation, and subsequently applying Statnamic loading in the opposite direction. The concrete cap proved to provide a very stable platform for instrumentation during the Statnamic loading. No indications of pile/cap slippage, cracking, or inelastic flexure in the cap were detected.

Soil Conditions. The two test locations at the AU site were within 20 m of each other, with no detectable differences in soil conditions between the two locations. The

soil at the Spring Villa site is a residual soil typical of the Piedmont Plateau of the southeastern United States between the Atlantic Coastal Plains and the Blue Ridge Mountains and extending from Alabama to Pennsylvania. These soils are derived from weathering of metamorphic rocks, predominantly gneisses and schists of early Paleozoic Age or older [42], and are composed of micaceous sandy silts. Commonly referred to as "saprolite," these residual soils retain the foliation and structural features of the parent rock but have the texture and appearance of soil. As is common in this geology, the clay content of the soil is somewhat higher in the upper few meters due to the more advanced state of weathering. Unified soil classification is typically CL/ML, with some soils below the 3-m depth classified as SM, as the sand content is very close to 50%. Groundwater is typically at a depth of 3 m to 4 m below the surface and varies seasonally.

Strength data include a wide range of *in-situ* tests as well as lab tests on undisturbed samples. Standard Penetration Test (SPT) N-values were typically 10 to 18 blows per 0.30 m in the upper 2 m, 8 to 12 in the 3 m to 6 m depth range, and 10 to 15 below 6 m depth. Average cone penetration tip resistance (CPT) was 2 to 4 MPa in the upper 10 m, with friction ratio values in the 4% to 6% range (generally higher at shallower depths). Undrained shear strengths from unconsolidated, undrained triaxial tests indicated considerable variability, with strengths ranging from 50 kPa to 150 kPa. The scatter in these data at shallow depths is likely due to variations in clay content and the effects of negative pore water pressures at depths above the groundwater table. Results from consolidated undrained and consolidated drained triaxial tests (mostly from samples in the 3 m to 12 m depth ranges) suggest that the soil has an effective cohesion,

69

c' = 17 kPa and an effective friction angle, ϕ' = 31°. A more complete presentation of the site geotechnical data, along with pressuremeter, dilatometer, and other test results, are presented in Appendix E and the references in Appendix E.

The many borings and *in-situ* tests on the site suggest that the soil properties are spatially variable within small (cm) distances. On the whole, the site appears to have reasonably consistent soil properties (as indicated by the CPT and SPT soundings) with the high local variability superimposed on the general pattern. The soils exhibit a trend of higher stiffness and strength in the upper 3 meters, apparently due to higher clay content and negative pore water pressures above the groundwater level.

Load Deflection Response. The measured load-displacement response from the static test, along with the derived static and total soil resistances from the Statnamic testing, is provided on Figure 21. Note that in this case the Statnamic test was performed prior to the static load test. It appears that the Statnamic loading has a more significant effect on the subsequent static loading in the opposite direction, due to the fact that there is a recoil from the inertial effects of the group during the dynamic loading that produces some prior loading in the opposite direction. Thus, the initial slope of the measured static response relationship is thought to be softer than would occur for a virgin test, and the derived static curve is likely to be more representative of an initial loading curve. The two static curves appear to converge at large displacements. Note also that large damping (indicated by the separation between the total and derived static resistance from the Statnamic loading) was present only at large loads and displacements. Most of the increased resistance mobilized by the fourth and final Statnamic loading over that of the

70

third loading appears to be related to damping, as only very small additional static resistance was generated.

The static load vs. displacement response for the tests on the 9-pile group at 4D spacing are provided on Figure 22. In this case the static load test was performed prior to the Statnamic loading. It appears that the initial Statnamic load response is probably too soft and was affected by the residual displacement from the prior static loading in the opposite direction. At large displacements these two curves appear to merge. By comparing Figures 21 and 22 it is clear that the magnitude of the load required to achieve large lateral displacement was much higher for this test foundation than for the Auburn 12-pile group. At a load of around 1600 kN, the reaction foundation failed by yielding during the static loading, so this represents the maximum static load that could be achieved.

Interpretation of Strain Measurements – 12-Pile Group. Examples of the bending moment vs. depth measurements for the 12-pile group are provided on Figures 23 and 24 for each of the 4 peak load levels during the Statnamic loading on Piles 8 and 12. Pile 8 was in the lead row for this loading, and Pile 12 was in the trailing row. As was the case for the Wilmington data, the maximum positive moment occurs deeper in the trailing row pile than in the lead row pile. However, compared to the Wilmington data these bending moment curves indicate smaller negative bending moments at the base of the frame and much larger positive *moments at depth.* The applied loads at Spring Villa were much larger than at Wilmington due to the stronger soil, and these data suggest that more bending in the frame occurred at the Auburn site. In fact, post-mortem inspection revealed that several of the welded connections between the piles and frame had broken.

71

Every indication suggests that there may have been some internal racking in the frame (between rows of piles) during these tests, such that the condition of restraint at the pile heads was less than full fixity to a rigid pile cap. The frame was fully intact and gave no outward appearance of any distortion, but these measurements suggest that the piles were not fully fixed at their heads.

As was the case for the Wilmington tests, there was a general pattern of shear distribution in which the lead-row piles exhibited higher head shear than other rows, but there was large spatial variability in head shear between piles within the group that has no apparent explanation other than random soil variations. The average of the shear distribution to piles by row position for the loadings on the 12-pile group were (by percentage of the total):

Row 1 (lead)	= 29% (static)	= 27% (Statnamic)
Row 2	= 23% (static)	= 23% (Statnamic)
Row 3	= 21% (static)	= 26% (Statnamic)
Row 4 (trail)	= 27% (static)	= 25% (Statnamic)

The proportion of load distributed to the lead row at this site is less extreme than was observed at Wilmington (e.g., the distribution here is more uniform). However, the actual variation in head shear among individual piles at this site was more extreme. It should also be noted that interpretation of shear force from the bending moment vs. depth relation is sensitive to small measurement errors, and at this site is less reliable than at Wilmington due to the stiff soil at shallow depth. At Wilmington the near-surface soils were extremely soft, so the initial slope of the bending moment vs. depth curve (which determines the shear at the top of the pile) could be determined more accurately.

Interpretation of Strain Measurements – 9 Pile Group. Examples of the bending moment vs. depth measurements for the 9-pile group are provided on Figures 25 and 26 for the front-row and trailing-row piles at the maximum load level during the static loading. Note the large negative bending moments at the tops of the piles, and the variability between piles in a given row. The large negative bending moments at the tops of the piles suggest that the piles were strongly fixed to the concrete cap and that the cap rotation was minimal (measurements of rotation of the cap indicated very small rotation). Because the ground surface was located at a small distance below the base of the cap and the shallow soils were quite stiff and strong, the determination of shear from these bending moment measurements is subject to considerable uncertainty. Interpreted average values for the leading and trailing rows of piles at this load are shown in Figures 25 and 26, respectively. The average of the head shear distribution to piles by row position for the loadings on the 9-pile group were (by percentage of the total):

Row 1 (lead) = 45% (static)   = 31% (Statnamic)

Row 2   = 36% (static)   = 35% (Statnamic)

Row 3 (trail) = 19% (static)   = 34% (Statnamic)

Note that the variation between rows observed with the static test are substantial from front to back, but this pattern did not repeat during the Statnamic loading. The third and final Statnamic loading exhibited this trend, and this load produced displacements far beyond any that may have been affected by the earlier static loading; thus the influence of the prior static loading cannot adequately explain this head shear distribution.   In addition, the head shear variation among individual piles for this group of piles was at least as large as with any other test group, and this group test utilized the concrete cap

73

cast after pile installation. Therefore, it appears that variability in shear distribution to individual piles was not affected substantially by structural details within the loading frame. On the other hand, it appears that the piles in the row that made up the lead row for static loading (and Row 3, the trailing row, for Statnamic loading in the opposite direction) were simply installed into somewhat stiffer soil relative to the average and the piles in the row that made up Row 3 for static loading (and Row 1 for Statnamic loading in the opposite direction) were in somewhat softer soil relative to the average. If one averages the two cases (thus averaging out some of the random variability), the variation by row position is 38% - 35% - 27% from front to trailing row, respectively.

These data suggest that the trend observed throughout all of the testing for this project is confirmed by this final test configuration: For actual field conditions, random variability relating to soil variations is as important as any other factor influencing head shear distribution to the piles in a group.

Comparison with FLPIER Static Model. As discussed with respect to the Wilmington data, the soil parameters for the generation of p-y curves in FLPIER were calibrated to the single pile test results in order to isolate the group effects from other factors relating to modeling errors in predicting soil behavior. The results of the two static load tests on the single control piles (data presented in Appendix E) were very similar and were used to develop a soil profile that accurately and reliably captures the response of the single pile loading tests. The p-y curve profile that was used consisted of the Reese et al. static stiff clay criterion with a higher shear strength near the surface and lower strengths below the 3 m depth. The calibration to the single pile test data matched not only the load vs. displacement at the loading point, but also the bending moment

distribution with depth. The latter provides assurance that the general distribution of soil resistance below grade is reasonable.

The FLPIER model of the 12-pile group was similar to that used at Wilmington, with adjustments for ground surface elevation and soil characteristics (p-y curve profiles). Because the pile bending moment data and observations suggest that some internal rotation occurred within the steel frame, the piles were not modeled as completely fixed to the cap. This "partial fixity" between the piles and the frame introduces some additional degree of uncertainty in the interpretation of the results. However, FLPIER has a provision to model partial fixity, and this provision was exercised with these test results. A partial fixity factor of 0.1 was used at the pile/cap connection to release some of the moment that occurs at this connection.

The 9-pile group was modeled using 9 similar piles, with the pile cap modeled using shell elements, each 0.85 m in thickness and with an elastic modulus of concrete (3 X 10^7 kPa, or 4400 ksi). The piles were modeled as fixed to the cap.

The input parameters for the axial soil model (t-z curves) were based on the CAPWAP analyses of a restrike blow on one of the piles after installation, and also upon the default parameters suggested in FLPIER. Observations of the test results suggest that none of the piles yielded (either geotechnically or structurally) in the axial direction, so the axial pile stiffness is the only relevant parameter. The shear modulus (used for construction of the default t-z curves) used for the 12-pile group was at the lower range of the FLPIER default parameters and somewhat less than used for the 9-pile group so as to reduce the axial stiffness somewhat to account for axial group effects due to the closer

pile spacing. The value for the 9-pile group is consistent with the guidelines provided in the FLPIER help manual.

FLPIER Results – 12-Pile Group at 3D Spacing. The FLPIER model for a 12-pile group spaced at 3D center to center uses p-multiplier values according to row position to account for group effects. By default these values are 0.3, 0.2, 0.4, and 0.8 for trailing to leading row, respectively. Using these default values and the p-y soil models developed from evaluation of the single pile test, the load vs. displacement and rotation relations computed by FLPIER are compared with the static test measurements on Figure 27. The computed results are seen to be somewhat stiffer than the measured response, although not by a large amount. In order to match the measurements more, the p-multipliers were scaled down by a uniform value. The computed displacements and rotations are shown to be very close to the measurements with an additional scaling factor of 0.8 applied, giving p-multipliers by row of 0.24, 0.16, 0.32, and 0.64. There is no special significance to this factor of 0.8 other than to define the magnitude of the error in the prediction for this test using default values. It appears that the default values are generally within the range of engineering accuracy for most applications. One possible explanation for this overestimation of stiffness may be related to the soil profile at the site. This profile includes a stiffer crust over a somewhat weaker underlying stratum, and this type of profile may tend to amplify the group effects, since the group is influenced more strongly by the deeper soils than is an isolated pile.

In order to evaluate the effects of a more simple model, additional analyses were performed using a uniform p-multiplier. An additional plot of lateral displacement is shown on Figures E-17 (Appendix E) for a FLPIER analysis with the p-multiplier for all

12 piles set at 0.34 (the average of 0.24, 0.16, 0.32, and 0.64). The overall response with this simple model appears to be sufficiently close to the distribution obtained using row-wise p-multipliers for general engineering and design purposes. A simple, uniform p-multiplier may have advantages for some seismic analyses in which load reversals occur in multiple directions and the consideration of directional effects makes the analysis much more complex.

Figures 28 through 30 provide plots of the computed and measured bending moments as functions of depth for two piles. Piles 8 and 10 are in the trailing row, while Pile 12 is in the leading row. There is general agreement in the trend of the measured and computed bending moment profiles, but there is a wide variation in the magnitude of the maximum moment values. The computed maximum moments in Pile 12 are somewhat less than measured on Pile 8 but significantly more than measured on Pile 10. Piles 8 and 10 are in the same row, so the computed values are identical. The results shown demonstrate the wide measured variations observed within the physical group. However, there is excellent overall agreement with the measured group shear load vs. displacement relationship. Also shown on Figures 28 - 30 are the results of static analyses with FLPIER in which all 12 piles were assigned a p-multiplier value that was equal to the weighted average for the four rows of piles in the group. This exercise was performed to evaluate a simple approach to estimating bending moments in piles within the group. It appears that the overall measured bending moment response is captured reasonably well with this approach.

The distribution of shear to the heads of the piles by row position computed by the FLPIER static model (with row-wise default p-multipliers) were as follows, compared to measured averages by row position:

Row 1 (lead)   = 38%(FLPIER)   = 29% (static)   = 27% (Statnamic)

Row 2   = 25%(FLPIER)   = 23% (static)   = 23% (Statnamic)

Row 3   = 16%(FLPIER)   = 21% (static)   = 26% (Statnamic)

Row 4 (trail) = 21%(FLPIER)   = 27% (static)   = 25% (Statnamic)

It appears that the default p-multiplier values overestimate the variations by row position for this test. Of course, when the piles are assigned the uniform average p-multiplier, uniformly distributed pile head shears are obtained with FLPIER (25% to each row).

FLPIER Results – 9-Pile Group at 4D Spacing. The p-multipliers used for the initial analysis of the 9-pile group were the default values recommended by the help file in FLPIER for a pile group with three rows. Values used for the spacing of 4 diameters c-c were interpolated between the values given in the help file for 3D spacing and 5D spacing, as values are not given for 4D spacing. These interpolated values are 0.50, 0.625, and 0.90, starting with the trailing row and ending with the leading row. As was the case for the 12-pile group, these default values produce a response that is slightly too stiff, and better agreement with the overall load-deflection behavior was again obtained by scaling the p-multipliers down by a factor of 0.8. The resulting p-multipliers are 0.4, 0.5, and 0.72 for the trailing to leading rows, respectively. The computed lateral load-displacement response at the base of the cap using these values is shown on Figure 31, along with the measured static response and the static response derived from the Statnamic test using the SDOF procedure outlined previously. Note that the static test

78

was performed prior to the Statnamic test for this pile group, and therefore the measured initial derived equivalent static test data may be slightly too soft due to the permanent set that occurred in the earlier loading in the opposite direction. In addition, the initial stiffness of the measured static response may be somewhat too stiff due to a residual load in the jack that appeared to be in place when the instrumentation was zeroed. (This was discovered upon unloading.)

As was the case for the 12-pile group, the computed lateral displacement at the pile heads using the default p-multipliers was too stiff. The adjusted p-multipliers appear to lead to slightly soft responses at small displacements (less than 5 to 8 mm), but appear to match the measured data quite well at larger displacements, which are of most interest for extreme event loadings. The stratigraphy (stiff crust over softer soil below) at the location of the 9-pile group was similar to the that at the location of the 12-pile group, which was situated a few meters away.

As with the 12-pile group, analyses were also performed using a uniform p-multiplier. The plot on Figure 31 of lateral displacements with the p-multiplier for all 9 piles set at 0.54 (the average of 0.4, 0.5, and 0.72) appears to be sufficiently close to the more realistic distribution for general engineering and design purposes, for reasons advanced for the 12-pile group.

Figures 32 through 34 provide plots of the computed and measured bending moments as functions of depth for three piles. Piles 10 and 11 are in the lead row, while Pile 13 is in the trailing row. There is general agreement in the trend of the measured and computed bending moment profiles, but the magnitude of the maximum moment values

do not match. Some error in the maximum measured moment values may be attributed to the strains superimposed from the axial pile forces.

The distribution of shear to the pile heads by row position computed by the FLPIER model were as follows (compare to measured average by row position):

Row 1 (lead)   = 45%(FLPIER)   = 45% (static)   = 31% (Statnamic)

Row 2   = 36%(FLPIER)   = 36% (static)   = 35% (Statnamic)

Row 3 (trail) = 19%(FLPIER)   = 19% (static)   = 34% (Statnamic)

Note that the agreement between FLPIER and the static test measurements (average by row) appears to be excellent. However, this result is likely to be somewhat fortuitous, as there is a distinct lack of agreement between FLPIER and the results from the third and final Statnamic loading. As for all of the previous pile group tests in this study, the measurements are influenced by apparently random variations within the group attributed to variations in soil response unrelated to spatial position.

In summary, the group effects on the 9-pile group were substantial and slightly greater than that predicted using FLPIER with default p-multipliers. The stratigraphy of stiff crust over somewhat softer underlying soil is thought to have contributed to the more significant group effects. After calibration using the single pile test data, the FLPIER model for static response of the 9-pile group appeared to capture the general load-deformation behavior reasonably well for engineering design purposes, especially when the row-wise p-multipliers were reduced by a constant factor of 0.8. The measured distribution of head shear from pile to pile was more variable than predicted by FLPIER, owing to apparently random variations in soil response that appear unrelated to spatial position of a pile in the group. The use of an averaged p-multiplier does not reproduce

the measured head shear distribution pattern, but it appears to provide overall load-displacement results, as well as maximum moments and shear, that are suitable for design purposes. The deviation of the computed pile-by-pile head shears and maximum bending moments from the measured values will require a relatively high load factor to be used when using FLPIER or similar software to design the piles structurally to account for the uncertainty in the pile stresses that are unrelated to geometric positions of the piles.

Dynamic Response of Test Foundations

This section provides a brief summary of the dynamic characteristics of the test foundations that were measured during the Statnamic loading and interpretation of the results. The Statnamic loadings, described in the previous section, represent a rapidly applied push to the foundation as gas pressure builds during the rapid burn of the propellant within the device. As the inertial mass is accelerated away from the test foundation, the gas pressure is diminished and finally vented. An example of the measured force time histories for Statnamic loading of the test foundations is provided on Figure D-30; these plots represent the force measured in the load cell between the Statnamic cylinder and the foundation during the four test loadings at Test Site 1 in Wilmington, NC. Other test loadings are similar, although the load amplitudes varied in magnitude (the Auburn - Spring Villa loads were larger).

Evaluation of Dynamic Response Using Simple SDOF Model

The simple SDOF model for the Statnamic loading event was described earlier. This model provides a simple framework for capturing the components of dynamic motion of the test foundation in terms of inertia (force proportional to acceleration), damping (force proportional to velocity), and nonlinear static stiffness (force proportional

to displacement). Although this model (in the form used for this study) does not have provisions to capture permanent set, gapping, hysteresis in the soil, combined rotation and translation, etc., the advantage of the use of the SDOF model is its simplicity and utility in placing the test results in a meaningful form for ready, direct comparison with static test results.

A direct comparison of the foundation stiffness at the rate of loading applied in the Statnamic tests is provided by comparing the total soil resistance vs. the equivalent static soil resistance for each test foundation as shown on Figures 14, 15, 21, and 22. These plots demonstrate that the damping resistance observed during the Statnamic load event was small until large displacements were mobilized, as evident by the close tracking of these two curves. At large displacements (generally exceeding 10% of the pile diameter), the damping resistance contributed significantly. The velocity was much higher at these larger displacements than it was at small displacements, but the soil supporting the pile was also subjected to considerably more hysteretic damping (energy loss) near the ground surface than would have occurred at lower displacements when the soil was still semi-elastic. Whether the damping effect is due to elastic energy dissipation or soil hysteresis, or a combination thereof, is not possible to tell from the observation that damping increases with increasing deflection, which also corresponds to increasing velocity.

However, in order to place the test observations into a useful form, the SDOF model may be used to derive a "rate effect" parameter to estimate the overall stiffness of the foundation at different rates of loading. This parameter can be considered a surrogate for the physical soil hysteresis and elastic wave dissipation effects, but it will be analyzed

82

in conjunction with the SDOF model as if it relates only to velocity. Consider that for each Statnamic load event, the effective static stiffness is defined as the soil resistance (measured force corrected for inertia) divided by the maximum displacement (at which point the velocity is zero). The average rate of displacement, V, during this loading event is defined as the peak displacement divided by the time required to achieve this displacement from the initiation of loading. The total stiffness of the foundation is defined as the peak total resistance force (static spring force + viscous damping force) divided by the displacement at which this peak force occurs. So, the total stiffness compared to the static stiffness is a measure of the increase in stiffness due to the viscous damping component derived using the SDOF model. A foundation could have a relatively large damping coefficient (force as a function of velocity), but if the velocity (or displacement) is not high during the loading event, the total stiffness will not be substantially increased above the static stiffness.

Using this concept and the average velocity for each loading event, the total dynamic stiffness normalized by the static stiffness from all of the Statnamic tests performed during this research are plotted as a function of displacement rate (average velocity) on a single plot as shown on Figure 35. This relationship is not meant to be an exact representation of the dynamic foundation resistance but is meant to serve as a guideline for estimating the resistance that might be mobilized by a forcing function that induces the system to react at different rates (or to different deflections).

The data on Figure 35 reveal some interesting aspects regarding foundation resistance to dynamic applied loads. First, the test data from a range of soils and foundation geometries suggest similar effects of rate of loading for steel piles. Larger

damping at low displacement rates might be expected for drilled shafts due to structural cracking of the reinforced concrete at these smaller displacement rates.

Second, these data might be used to infer which cases of loading might include a significant component of damping resistance such that the overall foundation stiffness computed using a static model might be low. Consider the case of a barge impacting a pile foundation group, and the barge causes the foundation to deflect laterally by 0.15 meters (about 6 inches). Assuming that the barge causes this displacement to occur within approximately 3 seconds after initiation of loading, then the average rate of displacement is approximately 0.05 m/s. The data on Figure 35 suggest that the total foundation stiffness for such a rate of displacement is on the order of 5% or less greater than the static stiffness, a trivial amount considering normal engineering practice in estimating foundation stiffness for design. For all practical purposes, such a problem can be analyzed as a static problem from the standpoint of the foundation response (obviously not from the standpoint of the barge, as the effective load is a function of the inertial forces generated as the barge momentum is altered).

Consider also the case of a seismic load with a frequency of around 0.5 Hz and a force that produces peak foundation displacements on the order of 0.1 meters relative to the at-rest position. An average displacement rate from such a loading is on the order of 0.8 m/s (0.2 m peak to peak divided by 0.25 seconds for ½ cycle). The data on Figure 35 suggest that the foundation stiffness might be on the order of 30% greater than the static stiffness for such high rates of loading, an amount which is certainly not trivial.

Of course, for cyclic loads such as seismic shaking, there may be other factors such as cyclic degradation, build up of free-field pore pressures, etc. The data and

discussion provided above merely serve as a guideline for the implication of the data from this research upon the magnitude of the differences in static and dynamic response under certain conditions and to help identify circumstance when dynamic analyses may be in order.

Dynamic Response Using FLPIER(D)

In order to evaluate the dynamic version of FLPIER that was developed for this project, FLPIER(D), the site-calibrated static p-y curves, pile geometries, cap properties, p-multipliers adjusted to average uniform static values (as described above) and the Statnamic force measurements from the load cell were sent to the computational research team at the University of Florida. In each case the pile group model arrangement that was used was identical to the arrangement for the static tests, except for the load time history provided as input. For the Spring Villa 12-pile group, the partial fixity at the pile/cap connection was used exactly as it was with the static analyses. The model used includes both velocity-dependent damping and hysteretic damping in the p-y curves, as described in Appendix C. Some minor structural damping was included, in the form of proportional damping equal to (0.015 X cap mass) + (0.01 X cap stiffness) + N[0.01 X pile mass) + 0.01 X pile stiffness], where N is the number of piles in the group. Some other parameters were varied for one test case that will be discussed. The results of these computations were returned in the form of the FLPIER(D) output files. The plots provided in this section of the report were generated from those files by the experimental research team at Auburn University.

Presented on Figure 36 are the computed and measured displacement time histories for the four Statnamic loadings of the 12-pile group at Test Area 1 (Ratt Island)

at Wilmington, NC. The computed displacement for the initial peak is somewhat larger than the measured value for all four Statnamic loadings, and the model appears to have a frequency response that is somewhat too high after the initial peak. Note that the oscillations from the LVDT measurements are thought to be the result of measurement errors related to vibration of the reference beam. Although the reference system was founded on piles, the ground was so soft that movements of this system could be visibly detected; the integrated accelerometer measurements are shown to indicate fairly high damping of the test foundation.

For the 12-pile group at Spring Villa, the inputs to FLPIER(D) were similar to those for the Wilmington test for Test Area 1, except for the differences in site-calibrated p-y curves due to the soil differences and the partial fixity parameter. Presented on Figure 37 are the computed and measured displacement time histories for the 12-pile group at the Auburn Spring Villa Test Site. For this test case, FLPIER(D) is seen to match reasonably well with the measured displacement data in terms of both amplitude and frequency. Note that the LVDT and accelerometer data are very similar for this test, indicating little movement of the reference beam. It is not immediately apparent why the model appears to provide such good agreement at this site and fares so poorly for the Wilmington data. Analyses were performed for these two test cases with the radiation damping set to zero; this made virtually no difference in the computed response as the damping component appears to be dominated by hysteretic damping.

The FLPIER(D) model for the 9-pile group are thought to provide the most realistic computed response due to the excellent measurements obtained on the concrete cap and the confidence that this cap provides a rigid and well-defined end condition.

Presented on Figure 38 are the computed and measured displacement time histories for the second Statnamic loading of the 9-pile group. The computed initial peak displacement is relatively near the measured value (although somewhat low), and the frequency response is fairly similar. Presented on Figure 39 are the FLPIER(D) results for the third Statnamic loading of the 9-pile group, computed using dynamic soil parameters similar to the previous runs. These computed data are also reasonably close to the measured response.

The third Statnamic loading of the 9-pile group was used to evaluate the effects of various input soil parameters within FLPIER(D) so as to develop some sense of the relative importance of these. Also shown on Figure 39 is a computed response for which a dynamic rate effect has been added to the soil p-y curves. This effect has been included as outlined in Appendix C, with a soil factor F2 of 0.07 and a baseline (static) loading rate of 7E-6 m/s (1 inch/hour). The effect of loading rate using these parameters is seen to be negligible, as the two computed curves are virtually identical.

FLPIER(D) was performed with mass added to the p-y curves so as to represent some contribution of participating soil mass within the pile group. Data are presented on Figure 40 which illustrate the effect of adding mass equal to ½ of the soil mass within the group, distributed evenly to the p-y curves on the group piles. The effect is seen to be most significant in extending the period of oscillation. The effect on the amplitude of motion is fairly small for this group.

Data are presented on Figure 41 to illustrate the effect of radiation damping on the overall computed response. The influence of this parameter is seen to be very minor; the computed damping in this foundation is clearly dominated by hysteresis.

The conclusion resulting from these parametric runs using FLPIER(D) is that the dynamic response of the model of the test foundation is dominated by the static stiffness, the overall mass of the system, and the hysteresis in the p-y curves.

SUMMARY

The findings from the test program in Taiwan, the analytical modeling, the numerical modeling, and the testing programs in Wilmington, NC, and Auburn University, Alabama, can be summarized as follows:

1. Analysis of static lateral load tests of a 2 X 3 X 3D-spaced group of large-diameter bored piles and a 3 X 4 X 3D-spaced group of large-diameter driven displacement piles in silty to clayey fine, saturated sand on the western Taiwan coastal plain indicated that p-multipliers for groups of bored piles are lower than those for groups of driven piles, particularly in the front or leading row. Comparative values are given along with default values from Computer Code "FLPIER" in Table 3.

2. Layered continuum analyses of the dynamic lateral loading of a single pile and of two parallel piles at varying spacings and harmonic frequencies in cohesionless soil were conducted. These analyses indicated that the harmonic dynamic lateral response of a single pile could be simulated well using static p-y curves, in particular those recommended for sands by the American Petroleum Institute [41], provided a velocity-dependent resistance is added to the static resistance at a given local pile displacement, y. The velocity-dependent stiffness can be expressed through a damping parameter, c, that is a function of several other parameters, including the frequency of vibration. This concept is expressed mathematically in Equations 4 and

5. Dynamic p-multipliers for piles in a group for cohesionless soil derived from analytical two-pile interaction analyses are given in Figure 9. With the mathematical formulation that was used, there is no difference in the p-multiplier, ρ, based on the relative position of the pile within the group relative to another pile (leading, trailing, in-between, side-by-side, or skewed). Only the center-to-center spacing, pile-head displacement and frequency of loading affect ρ. In a group of more than two piles, ρ is obtained for a given pile by multiplying together the ρ values for all surrounding piles. For a series of dimensionless frequencies, $0.02 < a_o < 0.12$ ($a_o = \pi f D / V_s$, in which f is the frequency of harmonic pile motion, D is pile diameter or equivalent diameter for a non-circular pile, and V_s is the shear wave velocity of the soil), ρ is expressed in Figure 9, which applies to medium dense sands, in terms of relative head displacement, y/D, and center-to-center pile spacing. Similar graphs for soils of different density are provided in Appendix B. For relative pile-head displacements of interest for extreme event loading, for example, 0.075 for the more flexible driven pile group in Taiwan, and for $0.02 < a_o < 0.12$, which may be typical for seismic loading as long as the soil does not liquefy, the computed values of ρ are somewhat less dispersed row by row than was measured during static testing, but the average analytical ρ-value was about equal to the average measured value of ρ. See Table 3. However, for the more rigid bored pile group tested in Taiwan, in which the maximum y/D was only 0.013, the row-by-row and average analytical ρ values were smaller than the measured static ρ values. Again, see Table 3. This "p-multiplier" effect appears to be less dependent upon frequency than on pile deformation (according to the analytical model) and method of construction (according to the test

89

program in Taiwan, Appendix A). It therefore appears tentatively that values of ρ obtained from static load testing of pile groups, or inferred from static p-y criteria and criteria for ρ for static design, can be used to analyze pile groups undergoing low-frequency, large-displacement dynamic (extreme-event) loading, provided the relative head displacements are in the order of 0.05 to 0.10 D during the extreme event. During static loading the ρ values did not appear to be highly dependent on y/D, as shown in Table A-2 in Appendix A, so the use of values of ρ obtained from static lateral group tests, or from published criteria, to model low-frequency, low-displacement (0 < y/D < 0.05, approximately) extreme event loading was not established in this study. In any event, damping must also be included in the p-y model (e. g, using Equations 4 and 5 or through explicit modeling of soil and/or structural material hysteresis. See below.).

3. The analytical layered, continuum model referred to above (Appendix B) does not consider soil hysteresis, nor does it consider non-harmonic or kinematic loading directly. To provide the designer with a versatile, user-friendly computational tool, FLPIER(D) (Appendix C), a dynamic version of the FLPIER program, was written to model dynamic laterally loaded pile groups in the time domain with hysteretic soil and structural material (cap and piles) damping, along with gapping. The value of c proposed for application to static p-y curves in Equation 5 can be input into FLPIER(D), which uses several standard static p-y models for clay and sand. FLPIER(D) also permits the modeling of both inertial loading (from the cap) and kinematic loading (through the soil), although the latter was not verified. FLPIER can consider various levels of fixity of the pile to the cap and considers nonlinear

axial behavior, which affects the lateral behavior of the group if there is any fixity at all between the piles and the pile cap. It appears that FLPIER(D) may exhibit difficulty converging under some conditions when there is partial fixity at the pile heads, but this did not occur for the field tests that were analyzed here. Overall, FLPIER(D) provided reasonable simulations of the impulse (Statnamic) tests on full-scale pile groups summarized below.

4. This and the following comments apply to the field-testing program carried out with driven pipe piles in North Carolina and Alabama. The Statnamic loading sequence (a series of lateral impulses with increasing amplitude) was used to simulate dynamic extreme event loading, such as barge impact and seismic loading. Although the relatively long time lapse between pulses did not allow for simulation of the response of soils in which high pore water pressures build up during the extreme event (e.. g., liquefiable soil), it did allow for the simulation of the effect of loading rates and displacement amplitudes produced in the soil by the movements of the piles.

5. With only a few small exceptions, the instrumentation and measurements appear to provide reliable indications of the pile group behavior. The strain gauge pairs within each pile provided generally reliable bending moment measurements, although the superposed axial forces appeared to contribute to some measurement errors in converting the measured strains to bending moment. Conversely, the superposed bending strains made the measured axial forces in the piles subject to large measurement errors. In essence, steel pipe piles do not make very good load cells when large bending stresses are imposed and measurements are obtained using only an averaged pair of strain sensors. Previous field loading tests using a pinned

connection avoid some of these measurement problems since axial and bending forces are not superposed on the piles; however, such tests are less realistic foundation models than the fully coupled foundation tests performed as part of this research.

6. The group effects were substantial for all foundations tested, including the tests in Taiwan, and slightly larger than expected at the Spring Villa Site using the default p-multipliers for both the 3D and 4D center-to-center spacing. The default p-multipliers used by the FLPIER code provided excellent agreement with the observed test results. Close agreement at the Spring Villa site was obtained between measured and computed results when p-multipliers were scaled down by a factor of 0.8. This reduction factor appears to be associated with a stiff-over-soft soil profile. The differences in overall group performance (shear load vs. lateral deformation and rotation) between the 3D and 4D center-to-center spacing predicted by using the interpolated p-multipliers in the FLPIER code appear to be approximately correct.

7. The axial stiffnesses in the piles for the 4D spacing appeared to be somewhat higher than was the case for the 3D spacing. It is suggested that designers may apply judgment and use somewhat softer t-z curves for closely spaced groups of piles (accomplished by using a somewhat smaller shear modulus within FLPIER), but the measurements of group rotation for these two test cases are insufficient to develop specific design guidelines. No piles were observed to yield either structurally or geotechnically in the axial direction during these tests.

8. The measured distribution of shear loads to the piles in the group <u>by average row position</u> was generally somewhat less extreme than computed using the row-by-row p-multipliers in FLPIER.

9. The measured distribution of shear loads to the individual piles within the group was somewhat more extreme than computed using the row-by-row p-multipliers in FLPIER. There appeared to be significant and substantial variation in individual pile stiffness that was unrelated to geometric position alone. Random spatial variability in soil response due to stratigraphic variations, installation effects, or other uncontrolled variables were at least as important as geometric position of the pile within the group in determining the actual shear distribution to an individual pile within the group. The general pattern of greater load to the leading row and less to trailing rows could only be discerned by observing average response for piles in a given row. This behavior was observed not only for the piles driven within the frame template, but also for piles driven in the free field for the 9-pile group, which had a suspended, cast-in-place concrete cap constructed after pile driving was completed. Therefore, for purposes of designing the piles and pile-pile cap connections structurally, the average row-wise moments and shears computed using a code such as FLPIER should be multiplied by a load factor. Figures 19, 28 through 30, and 32 through 34 suggest that this factor should be on the order of 1.2 for bending moment. Further tests of grouped piles at other sites are clearly justified for purposes of defining this factor more accurately.

10. The use of the steel frame for pile group testing proved to be difficult, time consuming, and led to uncertainties relating to small connection details. While the

93

difficulties with the use of this frame could be resolved, the use of a cast-in-place concrete cap proved to be much more reliable, cost effective, and provided better measurements. The use of the frame on future projects is not recommended.

11. The static FLPIER computer model using a single average p-multiplier (equal to the weighted average of all the P-multipliers by row position) provided a good prediction of overall static load-deformation behavior. Given the many other uncertainties in the actual distribution of shear and moment, this simple approach may be sufficient for many engineering design applications, provided an appropriate load factor, discussed in Item 9, is applied to the results.

12. The rotation of the cap, and to a lesser degree the lateral stiffness in translation, were somewhat sensitive to the axial stiffness of the piles. When there is any degree of fixity of the pile heads to the pile cap, attention must be paid to axial pile stiffness when experimentally deconvolving p-y curves and/or p-multipliers for the pile group.

13. The interpretation of the Statnamic loading using the simple single-degree-of-freedom (SDOF) model appears to provide a relatively good correlation with static test results for load vs. lateral translation and natural frequency of vibration. The rate of loading effects with the Statnamic loading appear to be relatively modest, although they increase with increasing displacements. The Statnamic device provided the capability to push the 9-pile group to large lateral displacements after the reaction foundation failed during the static testing, and so was a very valuable part of the test program.

14. At the rates of loading achieved in the field (similar to rates of loading in seismic events) static soil stiffness was the dominant component of soil resistance to lateral

load.   Damping adds significant additional stiffness only at relatively high displacement rate (velocity) — an increase on the order of 30% to 40% from the static resistance at a velocity of around 0.8 m/s.

15. In general, the static version of FLPIER was very successful in modeling the test results.   The partial fixity at the pile/frame connection appears to be modeled appropriately using this feature of FLPIER.   The dynamic version did a reasonable job of modeling the Statnamic loadings of the 12 and 9 pile groups at Spring Villa, capturing the peak displacements and frequency of motion reasonably well. This agreement was achieved by (1) using as inputs to the model static p-y curves for the soil, such as the Reese et al. p-y curve formulation for stiff clay with small changes to calibrate the p-y curves to the behavior of reference, or "control," piles at the test site, (2) defining (internally) unloading branches to the p-y curves in which hysteretic damping was included in the system by allowing the p-y curves to "loop," as described in Appendix C, (3) by including modest material damping (as proportional damping), as defined in this chapter, for the piles and cap, and (4) using a uniform average of the default static p-multipliers. The Wilmington model was less effective at modeling the measured response, with a computed frequency of motion that was too high.   The reasons for this poor correlation are as yet unknown, but additional evaluations of the FLPIER(D) model for this case are ongoing.

16. Sensitivity studies conducted using the FLPIER(D) model for the 9-pile group suggest that the most important parameters controlling the computed dynamic response to inertial lateral loading are the static soil stiffness (including axial stiffness of individual piles), the overall mass of the foundation, and the hysteresis damping

95

provided by the p-y curves. Radiation damping, structural damping, rate effects in soil stiffness (as defined using the default parameters outlined in Appendix C), the use of uniform average p-multipliers in lieu of row-by-row values, and the addition of a modest amount of soil mass had relatively small effects on the computed response.

Chapter 3: INTERPRETATION, APPRAISAL, AND APPLICATION

INTERPRETATION

The primary reason for initiating this study was a motivation to develop guidelines and computational vehicles for designing laterally loaded groups of piles for transportation structures. The emphasis was on extreme-event dynamic loading, such as ship impact and seismic loading. As the research developed, it appeared that this type of loading would be amenable to analysis by means that have been well-developed in the past for modeling the static behavior of laterally loaded pile groups. That is, by applying inertial effects to the structural elements, using static stiffness relationships for the soil (in the form of p-y curves), adding soil damping either through a viscous damping factor or hysteresis and gapping in the p-y model, using p-multipliers developed from previous, full-scale and centrifuge static load testing, and employing minor structural material damping, solutions to inertial loading events (loading through the pile cap) could be obtained that are sufficiently accurate for design purposes.

A computational model, a dynamic version of the computer code FLPIER, was developed to include these characteristics. This code was then verified against a series of full-scale static and impulse-type dynamic tests performed in the field at two sites. The impulse loading events used in the field tests can be classified as "inertial" in the sense that loading was applied through the cap, rather than "kinematic," where the loading would be applied to the piles to the soil. Seismic loading is a combination of inertial and kinematic loading. Although FLPIER was not verified for the case of loading through the soil, it was programmed with the capability to model such loading through time-domain motion of the supports for the p-y curves that mimics free-field ground motion.

In neither the field tests nor in FLPIER was any attempt made to model explicitly the effects of liquefying soil, although it should be possible in include a liquefaction model in the p-y curve formulation.

This approach to modeling the test groups appeared to give results that are sufficiently accurate for the design of pile groups in non-liquefying soils at a limited number of sites and should be generally applicable to the design of pile groups in non-liquefying soil as the number of sites at which the method has been calibrated increases. It should be pointed out that this approach is not limited to the code used here (FLPIER) but should apply to any structural program that includes the inertia of structural elements and uses hysteretic p-y curves that can be modified by p-multipliers.

APPRAISAL

Using the general inputs described above, and using no viscous damping factor for the soil, the computational tool FLPIER(D) provided reasonable predictions of the field test behavior, with two exceptions. First, the program did not give reasonable results when the pile heads were specified to be partially fixed (rotation permitted with some resisting moment developing) to the pile cap. The program also did not predict accurately the distribution of either head shears or bending moments among the various piles. The first deficiency is likely due to a "bug" in the program that has not yet been located. In due time it is expected that this problem will be solved, but it could not be solved in the time frame available to the research team. The second issue appears not to be a deficiency in the program but rather to be a result of variations in lateral soil resistance spatially among the locations of the individual piles in the group that is not associated with group action. For example, it was shown that extreme differences in the

installation method (boring and casting piles in place versus driving displacement piles) produced rather large differences in soil resistance against both individual piles and pile groups at an independent test site in Taiwan. For this reason, it is recommended that the ideal (computed) maximum shears and moments in the various piles be multiplied by a load factor before the piles are designed structurally.

The field test program included only two sites, that although dissimilar, do not represent geotechnically all of the soil types of concern in designing laterally loaded pile groups for extreme events. When using the approach described here, it is expected that the most accurate designs for impact or seismic loading will be achieved when full-scale pile group tests are tested at the site of interest. In the event that large, portable inertial vibrators become available in the future, using vibrators instead of the Statnamic device will undoubtedly prove more appropriate for simulating seismic loading. The test piles that were developed for this project would be appropriate for future field studies. However, the steel frame should be abandoned in favor of using a cast-in-place concrete cap.

APPLICATION

The results and analyses of the field load test program suggest the following engineering guidelines for the design of pile groups subject to lateral loading.

Pile-Soil-Pile Interaction and Group Effects

The use of p-multipliers derived from static testing, as implemented in FLPIER, is an effective means of modeling the effects of group action on the soil resistance. In granular soils, consideration should be given to reducing the default values of the p-multipliers (Table 3) when bored piles (drilled shafts) are used by about 40 percent on the

leading row if row-by row p-multipliers are used, or about 20 percent if a single, average p-multiplier is used for all rows of piles. The default values provided in FLPIER (Table 3) appeared appropriate from the soils at the field test sites for 3-diameter and 4-diametrer center-to-center pile spacing when the piles were driven displacement piles. For the rare case where closer spacings (2.5 D) are used and granular soil is present near the ground surface, the p-multipliers that are approximated from Figure 9 are recommended for use.

Although the general trend of distribution of shear and moment to the piles within a group is reasonably similar by row position to the trend predicted by the row-position-based p-multipliers in Table 3, the actual distribution of shear and moment that might be expected among the piles in the row considered on a realistic, full-sized pile group foundation is subject to significant random variations due to variations in soil properties. This unpredictable variability is at least as significant as any geometric variability. Designers should therefore provide accommodations for variability of computed maximum bending moments in the piles by multiplying the computed average maximum moment for a pile in a given row by a load (moment multiplication) factor of about 1.2 before completing the structural design of the piles.

The use of a simple average p-multiplier for all piles in the group based on a computed weighted average of the individual piles based on row position provides a computed response which is equally suitable for design purposes. Given the uncertainties related to the above-noted variability, and to the unknown, reversible and likely variable direction of loading from a seismic event, it appears sufficient for design purposes to use this simplified approach.

The test data and the modeling efforts both indicate the strong coupling between lateral and rotational stiffness. The axial pile stiffness has a major influence on the rotation of the cap and this stiffness is strongly coupled to the lateral stiffness. The use of group models such as FLPIER or other computer codes that include axial stiffness of the piles are recommended. The use of uncoupled analyses could significantly underestimate or overestimate the lateral stiffness, particularly if the pile cap is assumed not to rotate.

Dynamic Behavior

The lateral dynamic response for large lateral loads similar to extreme event loading is strongly nonlinear, even when the structural response of the piles and cap is within the linear elastic range. The damped resonant frequency is reduced and the damping increases with increasing displacement amplitudes. Therefore, damping needs to be included in the design model (e. g., FLPIER).

If funds are available at a bridge site, Statnamic loading of a test group should be strongly considered, especially in the case of critical structures. The Statnamic loading device provides a mechanism to apply large lateral loads to a test foundation with a force time history that is reasonably close to the resonant frequency of a full-scale test foundation. Except for the largest pile groups, this system is effective at inducing large-amplitude dynamic motions in test foundations and provides a means of obtaining meaningful dynamic measurements of the system response. The Statnamic loading mechanism is limited in producing the cyclic degradation in soil strength and stiffness that might be expected during a seismic or repeated loading event and could be replaced with a portable vibrator. At present, however, inertial vibrators with force amplitudes large enough to produce lateral deformations in the piles equivalent to those that are

expected in major seismic events in full-scale pile groups are not available. When they become available, they may be employed in place of the Statnamic device.

However, a simple SDOF model for evaluating the dynamic response of a pile group due to Statnamic impulse loading can be very useful for identifying fundamental system properties and extracting nonlinear static stiffness, which is the most important parameter in predicting dynamic response. SDOF modeling can be done independently of computer simulations and may in certain circumstances be sufficient in itself for evaluating the response of the pile group.

For more in-depth analysis, FLPIER(D) or a similar code should be used to simulate the behavior of the group. Modeling the dynamic response of the soil using hysteretic, static p-y curves and static p-multipliers seems to capture the most important aspects of foundation behavior during dynamic loading reasonably well. The inertial effects of the structure above grade are straightforward, and must be included in the simulation because they are important to the overall system response. Some small amount of system damping, which can be modeled with additional participating mass, may be considered, but this damping does not appear to be a major influence on the foundation. Compared to the static response, the most important elements in the dynamic soil response are the gapping and hysteretic damping and rate effects in cohesive soils. Radiation damping may contribute to overall damping, but it is difficult to separate the effects of radiation damping from that of hysteretic damping. For this reason, all damping for low-frequency, large-displacement (y/D > 0.05) loading is modeled has hysteretic for seismic loading conditions.

The static stiffness is the dominant component of resistance to lateral load for the low-frequency motion characteristic of a full-scale group of piles or shafts (in the 2 to 4 Hz range). Damping adds significantly to the resistance at higher amplitudes of motion (in excess of 20 to 30 mm), with increasing effect at larger amplitude. For vessel impact loads, which may occur at a much lower rate of loading than seismic loading (e.g., load times on the order of several seconds to peak), the static response is likely to dominate most cases and a static analyses should be only slightly conservative (unless inertial components of the structure are substantial).

APPLICATION OF FLPIER(D) TO THE ANALYSIS AND DESIGN FOR SEISMIC LOADING

FLPIER(D), the dynamic version of FLPIER, was developed in this study to facilitate interpretation of the field test results and to serve as a design tool for those who wish to use it. It is emphasized that FLPIER(D) is one of many suitable tools that can be used to analyze pile groups under lateral loading.

The following is a summary of the process used to analyze a bridge pier for earthquake loading. This process assumes that the reader is familiar with the Florida Pier program (FLPIER) and how to develop models of bridge piers using the *Flpier_gen* graphics generator. *FLPier_dyn_gen* is the equivalent generator in the new code, FLPIER(D). Some hand editing may be necessary, since all of the capabilities for the FLPier_dyn engine are not available in the *FLPier_dyn_gen* generator.

Before executing the program it should be downloaded from http://www.ce.ufl.edu/nchrpdemo.html. A help file can be found on this download. This program will be disabled after Dec. 31, 2001, as a precaution against propagating a new program that may have bugs. If the program has never been installed before, the user

should understand that the graphics interface uses a font that most Windows 98 and new NT systems do not have. Users are encouraged to go to http://www.ce.ufl.edu/ssoftware/software.html and download the font for their operating system, following the instructions given at that site.

In order to illustrate the use of FLPIER(D), the following example is given. The analysis process is based on the results from the Statnamic field tests for this project and the ensuring dynamic model results using FLPIER(D).

Consider the following soil properties, which are assumed to apply to all of the piles at the location of the pier to be analyzed.

Layer	Thickness (in.)	Modulus (k/in^2)	Unit Weight (k/in^3)	Undrained shear strength (k/in^2)	ε_{50}	ε_{100}	Shear Modulus (k/in^2)	Poisson's Ratio	τ_f (k/in^2)	Tip Bearing Capacity (k/in^2)
1	360	0.5	0.000066	0.003	0.020	-----	1.5	0.3	0.15	
2	480	0.5	0.000071	0.030	0.005	0.03	1.5	0.3	0.15	
Tip							1.5	0.3		0.27

Note: 1 k = 4.45 kN; 1 in. = 25.4 mm

These properties were taken from soil borings near the subject pile group. The soil profile is similar to that at the Wilmington site (Cooper River Bridge) described earlier in this report and elaborated upon in Appendix D. From these data, an initial pile system was developed. Note that the parameter τ_f is the ultimate unit side resistance used by FLPIER or FLPIER(D) to produce axial unit load transfer curves. A very high value was used in this example analysis to force the response of the pile group to be translational in the lateral direction of loading, rather than to be both translational and

rotational. In most cases this value would be the estimated value of maximum unit side resistance.

The following step-by-step procedure is then followed to develop the input file:

Step 1: *Estimate an equivalent static load for initial sizing of the piles.*

Use 10% of the pier + bridge weight. 2000 kips (8.9 MN) was used for this example.

Step 2: *Create a pier model with a trial size and number of piles.*

The "Pseudo Dynamic Curve" option is used. This option that requires an approximate fundamental period of the structure (17 cycles/sec was chosen for this example) and the shear velocity of each soil layer. 2000 in./sec (50.8 m / sec.) was used for soil shear wave velocity for this example.

Step 3: *Run this pseudo-dynamic option and iterate on the size and number of piles until the displacements of the pile head and the pile and pier moments are within design tolerance.*

First set the piles to "linear" with "properties," obtain convergence on the soil, then change the pile to "nonlinear" and finalize the pile configuration. The file used for this analysis is included with the example files as part of the FLPier_dyn install and is named "design_stdyn.in". That file is presented in hard copy form in Appendix G for completeness in documentation.

Note: The "nonlinear" option of the program automatically checks the moment capacity of the piles and pier elements due to the nonlinear bending. If the program converges, the pile sections have sufficient capacity.

During the execution of this pseudo-dynamic phase of the analysis, FLPIER(D) used:

- The default p-y curves for the soil types encountered (Matlock soft clay criteria in Layer 1 and Reese stiff clay below-water-table criteria in Layer 2).

- The simplified pseudo-dynamic reduction (damping) model in Appendix B for the p-y curves, which was turned on for the pseudo-static analysis (preliminary sizing of the piles achieved in this phase). This provides an estimate of damping and was assumed to apply to clay p-y curves (this case) as well as to sand p-y curves (conditions assumed in Appendix B). A different approach was used in the next phase, as described subsequently.

- A pile cap that was assumed to be flexible, but elastic. It was assigned a Young's modulus of 4400 ksi (30.3 GPa). Cap-soil interaction was not modeled. The piles were rigidly framed into the pile cap. [Note that at this time only rigid framing and pinned connections should be assumed at the pile heads in FLPIER(D), as FLPIER(D) may have difficulty converging when partial pile-head fixity is specified.]

- The default p-multipliers. That is, values of 0.8, 0.4, 0.3, 0.2 and 0.3 were used from front row to back row in the 5 row X 4 column group that was finally developed. [These would be appropriate for a driven pile group but not possibly for a drilled shaft group in cohesionless sands below the water table,

as is demonstrated in Appendix A. Because the shear wave velocity of the soft clay at this site is low, the natural frequency of the bridge high, and the pile radii large, a_o is very high (> 1). Thus, the p-multipliers that are given for sand with value of a_o up to 0.12 in Figures B-41 through B-43 are not appropriate.]

- For axial loading the maximum unit skin friction (t_f) and unit tip resistance are specified as shown in the table, and the default t-z curves in FLPIER for clay are applied automatically. No damping was assumed to occur due to axial loading of the piles as the cap rotates in response to a lateral load.

The pile group that was found to be satisfactory was a 5-row X 4-column group of steel pipe piles, each with a diameter of 60 in. (1.524 m), a wall thickness of 1.5 in. (38.1 mm), and a center-to-center spacing of 3 diameters in both directions. A layout of this group is shown in Figure 42.

For that group the final displacements given below were obtained. X is the displacement in the loading direction; Y is the transverse displacement; Z is the vertical displacement.

SUMMARY OF DISPLACEMENTS AT PILE HEADS ONLY:

NODE	X (in)	Y (in)	Z (in)
1	4.9487	-0.0001	-0.5371
2	4.9484	0.0001	-0.0060
3	4.9479	0.0002	0.5431
4	4.9487	0.0001	-0.5371
5	4.9484	-0.0001	-0.0060
6	4.9479	-0.0002	0.5431

Note that 1 in. = 25.4 mm.

Since the problem converged using the "nonlinear" option, the piles have sufficient capacity. The preliminary design has now been completed. The full time domain analysis using an actual or assumed earthquake record can be run next to provide a final check on the pile group system.

Note that alternate approaches could have been taken in this step, which results in preliminary sizing of the group. Static codes such as FLPIER or, for example, a simple program known as PIGLET [43], could have been employed using an estimated peak dynamic load. However, use of FLPIER(D) in this step is expected to save time in the overall design process.

Step4: *Convert the static model to a time-domain dynamic model by adding damping, mass and an earthquake record.*

The file used for this analysis is included with the example files as part of the FLPier_dyn install and is named "design_dyn_gap.in". That file is also included in Appendix G for completeness in documentation.

In this phase of the analysis (time-domain analysis) damping is handled differently from the way in which it was handled in the previous phase (pseudo-dynamic analysis, Step 3). In the pseudo-dynamic analysis, soil damping was handled in FLPIER(D) by using the approximation developed in Appendix B. However, in this step hysteretic damping in the soil under lateral loading (with the p-y curves) was modeled in FLPIER(D) using the gap model described in Appendix C. There is no hysteretic damping associated with axial loading of the piles as the cap rotates in this example. Radiation damping in this step, for both lateral and axial loading of the piles, was handled in FLPIER(D) by specifying

Rayleigh damping. The axial load-movement curves were generated in FLPIER(D) using McVay's driven pile model for unit load transfer curves.

In this phase an earthquake record (acceleration time history) was input as a discrete time history at the origin of coordinates (middle of the top of the pile cap). The acceleration time history used in this example was the El Centro record of 1940. Any saved acceleration record can be captured by the user interface for FLPIER(D) and placed in the input file. At present two records are saved for use by the program: El Centro and Northridge.

The results of the field Statnamic tests summarized in Chapter 2 and covered in detail in Appendices D and E were used to infer input parameters for this phase of the analysis. From the field Statnamic tests, the following parameters appear to work well in the FLPIER(D) model:

Damping: Raleigh damping can be used to replicate radiation damping in the pile group system. Such damping is expressed in FLPIER(D) by (α X mass of the cap and pile system + β X lateral group stiffness). In the field tests conducted with steel piles, good matching was found with FLPIER(D) using the following, with the exception (for soil) described in the following:

	α	β
Structure (Pier)	0.04	0.01
Piles	0.001 (steel)	0.001 (steel)
Soil	0.015	0.015

In the analysis of earthquake motion, additional damping is required that was not found in the Statnamic tests. This is because the Statnamic device applies a short pulse of energy followed by a period of free vibration response. An

earthquake acceleration record, however, causes continuous energy input, and the response is more sensitive to damping.

It is estimated that the soil damping is about 10 times that of a steel pile. As a result of Step 3, the damping values shown in the preceding table were used, and the pier and pile group shown in Figure 42 was analyzed.

Additional Input Options:

For the dynamic time domain analysis, the following options were specified:

P=2,1,4 – Print displacements for the analysis for Nodes 1 & 4 (pile heads). This will create the *name*.DS1 and *name*.DS2 files, which contain the six displacements at Nodes 1 and 4, respectively, for each time step. These are text files and best viewed using a spreadsheet like MS Excel.

W=1,1,1 – Print the forces for Pile # 1, Element #1, and Node 1 (bottom of the element) for each time step. Only one end of a single element can be printed per run. The forces are saved in the file *name*.DFO.

All the plots in the list given below were executed using Excel. To read the results files into Excel, do the following:

1) Start Excel by using the File->Open command.

2) Change to all files (*.*).

3) Select the file to read (name.DS1 or name.DFO, etc.).

4) On the pop-up dialog, select finish (to read the data).

5) All data are now in columns and can be plotted using normal Excel functions.

Principal Results from Time-Domain Analysis:

From the dynamic time-domain analysis, plots were made for the pile-head translation in the direction of loading (X) and induced bending moment in the direction of loading for Pile # 1 for the time window of the analysis. These plots are given in Figures 43 and 44, respectively. In both of these figures, time is expressed in seconds.

The maximum displacement in the analysis is seen to be a little over 2 inches (51 mm). Notice that the earthquake response has several significant peaks during the modeled time window of response. Unlike the free vibration response from the Statnamic test, the response does not decay.

The moment at the head of Pile #1 is given in Figure 44. Likewise, several peaks occur, and the maximum moment is slightly over 15,000 in.-K (1695 kN-m), which is less than the moment at which plastic behavior occurs.

Since converges occurs in FLPIER(D), the piles have sufficient moment capacity. The gap model causes the structure flexibility to increase as time increases since less and less of the soil is in contact with the piles.

Completing the Design Process:

This analysis should be conducted using a range of values of soil properties that covers the associated uncertainties, including damping and p-multipliers. For example, it would be prudent to vary the default p-multipliers by about ± 25% and to reduce the front-row values to as low as 0.5 for bored piles in cohesionless soil. For critical structures the design process should include site specific dynamic pile-group loading tests with a large-force exciter to calibrate the program to site conditions.

Chapter 4: CONCLUSIONS AND RECOMMENDATIONS

CONCLUSIONS

The research confirmed the viability of the reusable pile testing system with the Statnamic activator; however, the original plans for a steel frame cap proved infeasible for repeated use, and cast-in-place caps are recommended in any future experiments.

From a design perspective, the research demonstrated that laterally loaded pile groups in non-liquefying soil, exposed to low frequency (2 - 4 Hz) / high-displacement-amplitude (≥ 20 mm) loading can be simulated using a code such as FLPIER(D), which models the soil with hysteretic, static, p-y curves and which uses p-multipliers that are derived from static tests [such as the default values in FLPIER or FLPIER(D)]. Evidence was presented that the average p-multipliers were about 10 percent lower for bored piles in cohesionless soil than the average default values given in FLPIER / FLPIER(D). Inertial effects must be included in the method; however, structural damping has a minor effect on pile group behavior and may be included and omitted, as the designer chooses.

Random variations from the maximum bending moments and shears that were computed for each row of piles by FLPIER(D) were observed in the field experiments. This behavior appeared to derive from random variations in soil stiffness within the group and to other random factors, such as random small batters in the piles. This variability should be accounted for in designing the piles structurally by applying a load factor of approximately 1.2 to the computed maximum moments and shears.

RECOMMEDNATIONS FOR FURTHER STUDY

Some modifications to FLPIER — dynamic version [FLPIER(D)] are in order:

1. The default parameters in FLPIER(D) tend to overestimate damping, based on comparisons with the impact-type field tests in this study. Adjustments to the unloading branches of p-y curves may improve modeling of hysteretic damping for this type of loading. Further studies of the effects of high-amplitude, cyclic dynamic loading should be undertaken to determine whether the FLPIER(D) damping model is suitable for seismic loading without modification.

2. FLPIER(D) appeared to give unexpected results at certain times when the displacement is large and when the piles are prescribed to have partial fixity with the cap. This effect appears to be due to convergence of the mathematical solution and to the sensitivity of the solution to the value of the rotational restraint at the pile head. Corrections have been made in the program to minimize this effect; however, users should proceed with caution when analyzing piles with partial head fixity. This behavior should be investigated further and the formulations corrected if necessary.

3. FLPIER(D) has not been verified for the case in which loading is generated against the piles from the soil (kinematic loading with inertial feedback from the superstructure). Further physical data should be collected, perhaps using shaking table tests or full-scale tests with significant explosive charges, against which to verify FLPIER(D) for this application.

4. An appropriate p-y model should be developed to handle liquefying soil.

5. A formal research project should be undertaken to evaluate methods for determining pile-head shear accurately from bending sensors in the piles or by other means and to evaluate the flexural stiffness of pile heads for piles of differing types (pipe, prestressed concrete, H, circular reinforced concrete) with varied procedures for

attaching the piles to the caps. This project, if successful, should make it much easier to perform and interpret the results of field tests on laterally loaded pile groups.

With respect to the field testing program, it is noted that the test piles that were instrumented and developed for this study, as well as the Statnamic testing device, which is the property of the Federal Highway Administration, are available for further testing on other sites. The major conclusions of this research, stated above, should be verified by further field tests in other geologic settings (stiff clay; loose, clean water-bearing sand; loose, dry sand; and soft-over-stiff soil layering). This can most conveniently be accomplished in conjunction with highway construction projects.

The applicability of this research to seismic loading can be enhanced by repeating these experiments, using a large vibrator, to correlate damping inferred from Statnamic tests to damping under continuous loading with nonlinear displacements. Such a vibrator should be designed, constructed and deployed.

IMPLEMENTATION PLAN

A brief plan for the implementation of this research is as follows.

1. An appropriate federal agency should identify state DOT design projects in which seismic or vessel/ice impact is a major concern in the design of the foundations.

2. Two to four such projects should be selected for research implementation. The selected projects should cover a variety of soil sites (saturated sand, soft clay, very stiff clay or rock) and more than one type of loading event (e. g., seismic and vessel impact).

3. The custodian of the testing equipment from this project should then be directed to make such equipment available to the state DOT's whose design projects are selected,

114

and those states should conduct full-scale field tests, with a Statnamic device, as was employed here, or with a very large vibrator.

4. The state DOT's or their consultants should, in parallel with the field tests, perform mathematical modeling of the test pile group using either FLPIER(D) or other suitable software, taking advantage initially of the recommendations developed in this report and modifying the input parameters as necessary to affect acceptable matches with the observations. The same software should then be used to design the pile foundations for the subject structure.

5. During this process the responsible federal agency should compile the results of the field tests and of the designers' interpretations for input parameters (damping values, p-multipliers, etc.) and make the information available to the national community of DOT structural and geotechnical engineers through a sponsored conference or short course.

6. The use of the field testing system developed for the current project and the software that is used in the above process should then be evaluated by a select panel of experts and a decision made by the responsible federal agency, with the advice of the panel of experts, whether to continue with further field experiments, to standardize the input parameters (so as to use them without field testing) or take some other approach to the design of laterally loaded pile groups.

REFERENCES

1. EERI, "Loma Prieta Earthquake Reconnaissance Report," *Earthquake Spectra, Supplement to Volume 6*, Chapter 6, Bridge Structures (1990), pp. 151-187.

2. Buckle, I. G.. *The Northridge, California, Earthquake of January 17, 1994: Performance of Highway Bridges*, National Center for Earthquake Engineering Research, Technical Report NCEER-94-0008 (1994).

3. EERI, "Northridge Earthquake of January 17, 1994, Reconnaissance Report," *Earthquake Spectra, Supplement to Volume 11*, Chapter 6, Highway Bridges and Traffic Management (1995), pp. 287-372.

4. Kiremidjian, A. A. and N. Basoz (1997). *Evaluation of Bridge Damage Data from Recent Earthquakes*, NCEER Bulletin, National Center for Earthquake Engineering Research, Volume 11, Number 2 (1997), pp. 1-7.

5. Buckle, I. G., "Report from the Hanshin-Awaji Earthquake: Overview of Performance of Highway Bridges," *NCEER Bulletin*, National Center for Earthquake Engineering Research, Vol. 9, No. 2 (1995), pp. 1-6.

6. Costantino, C., "Report from the Hanshin-Awaji Earthquake: Overview of Geotechnical Observations," *NCEER Bulletin*, National Center for Earthquake Engineering Research, Volume 9, Number 2 (1995), pp. 7-10.

7. Ishihara, K., "Geotechnical Aspects of the 1995 Kobe Earthquake," *Proceedings*, XIV ICSMFE, Hamburg, Vol. 4 (1997), Balkema, Rotterdam, pp. 2047 - 2073.

8. Matsui, T., Kitazawa, M., Nanjo, A., and Yasuda, F., "Investigation of Damaged Foundations in the Great Hanshin Earthquake Disaster," *Seismic Behavior of*

Ground and Geotechnical Structures, Ed. by P. S. Sêco e Pinto (1997), Balkema, Rotterdam, pp. 235 - 242.

9.   Lin, M-L, *Geotechnical Hazard Caused by Chi-Chi Earthquake*, Department of Civil Engineering, National Taiwan University, (2000).

10.   NCREE, *Chi-Chi Earthquake Database Analysis and Management System (CEDAMS)*, NCREE, Taipei, Taiwan, (2000) published on web site: http://gisdb.ncree.gov.tw.

11.   Chang, K-C, Chang, D-W, Tsai, M-H, and Sung, Y-C, "Seismic Performance of Highway Bridges," *Earthquake Engineering and Engineering Seismology*, Vol. 2, No. 1 (2000), pp. 55 - 77.

12.   Bardet, J. P., Adachi, N., Idriss, I. M., Hamada, M., O'Rourke, T., and Ishihara, K., *Proceedings*, North America - Japan Workshop on the Geotechnical Aspects of the Kobe, Loma Prieta, and Northridge Earthquakes, Chapter 7, Performance of Pile Foundations, National Science Foundation, Air Force Office of Scientific Research, Japanese Geotechnical Society (1997).

13.   O'Neill, M. W., Brown, D. A., Anderson, D. G., El Naggar, H., Townsend, F., and McVay, M. C., "Static and Dynamic Lateral Loading of Pile Groups," *Interim Report*, NCHRP 24-9, National Cooperative Highway Research Program, Transportation Research Board, Washington, D. C. (1997).

14.   Budek, A. M., Priestley, M. J. N., and Benzoni, G., "The Inelastic Seismic Response of Bridge Drilled-Shaft RC Pile/Columns," *Journal of Structural Engineering*, ASCE, Vol. 126, No. 4 (2000), pp. 510-517.

15. Davisson, M. T., "Lateral Load Capacity of Piles," *Highway Research Record 333*, Highway Research Board, Washington, D. C. (197), pp. 104 - 112.

16. DM-7, *Foundations and Earth Structures – Design Manual 7.2*. Department of the Navy, Naval Facilities Engineering Command, NAVFAC DM-7.2 (1982).

17. CFEM, *Canadian Foundation Engineering Manual*. Canadian Geotechnical Society, 2nd Edition, Bitech Publishers Ltd. (1985), Vancouver.

18. AASHTO, *AASHTO Bridge Design Specifications*, American Association of State Highway and Transportation Officials (1996), Washington, D. C.

19. ASCE, *Design of Pile Foundations – Technical Engineering and Design Guides No. 1*, American Society of Civil Engineers (adapted from the Corps of Engineers) New York (1993).

20. Poulos, H. G., and Davis, E. H., *Pile Foundations Analysis and Design*. John Wiley, New York (1980).

21. PoLam, I., and Martin, G. R., "Seismic Design of Highway Bridge Foundations – Volume II: Design Procedures and Guidelines," U.S. Department of Transportation, Federal Highway Administration, *Report No. FHWA/RD-86/102*, (1986).

22. ATC-32, *Improved Seismic Design Criteria for California Bridges*. Applied Technology Council, Contract 59N203 (1996), p. 123.

23. Williams, M. E., Fernandes, C., Jr., and Hoit, M. I., "Comparison of Dynamic Analysis Methods for Bridge Piers," *Journal of Bridge Engineering*, ASCE, in review (2000).

24. PoLam, I., Kapuskar, M., and Chaudhuri, D., "Modeling of Pile Footings and Drilled Shafts for Seismic Design," *Technical Report MCEER-98-0018* (1998), Multidisciplinary Center for Earthquake Engineering Research, SUNY Buffalo, Buffalo, New York.

25. Reese, L. C., and Wang, S-T, *Computer Program LPILE Plus*, Version 3.0, Technical Manual, Ensoft, Inc., Austin, Texas (1997).

26. PMB Engineering, Inc., *PAR: Pile Analysis Routines: Theoretical and User's Manuals*, PMB Engineering, Inc. (1988), San Francisco, CA.

27. WashDOT, *Design Manual for Foundation Stiffnesses Under Seismic Loading*, prepared for Washington State Department of Transportation, by Geospectra, Pleasanton, CA (1997).

28. Schnabel, P. B., Lysmer, J., and Seed, H. B., "SHAKE: A Computer Program for Earthquake Response Analysis of Horizontally Layered Sites," University of California Earthquake Engineering Research Center, *Report No. EERC 72-12* (1972).

29. Norris, G. M., "Seismic Bridge Pile Foundation Behavior," *Proceedings*, International Conference on Design and Construction of Bridge Foundations, FHWA, Vol. 1 (1994), pp. 27 - 136.

30. Ashour, M. A., Norris, G., and Pilling, P., "Lateral Loading of a Pile in Layered Soil Using the Strain Wedge Model," *Journal of Geotechnical and Geoenvironmental Engineering*, ASCE, Vol. 124, No. 4 (1998), pp. 303 - 315.

31. Ashour, M. A., and Norris, G., "Modeling Lateral Soil-Pile Response Based on Soil-Pile Interaction," *Journal of Geotechnical and Geoenvironmental Engineering*, ASCE, Vol. 126, No. 5 (2000), pp. 420 - 428.

32. Peterson, K., and Rollins, K. M., "Static and Dynamic Lateral Load Testing of a Full-Scale Pile Group in Clay," *Research Report No. CEG.96-02* (1996), Department of Civil Engineering, Brigham Young University, Provo, UT, 223 pp.

33. McVay, M., Hays, C., and Hoit, M., *User's Manual for Florida Pier, Version 5.1* (1996), Department of Civil Engineering, University of Florida.

34. Dobry, R., Abdoun, and O'Rourke, T. D., "Evaluation of Pile Response Due to Liquefaction Induced Lateral Spreading of the Ground," *Proceedings*, Fourth Caltrans Seismic Design Workshop, Caltrans, Sacramento, California (1996).

35. Wilson, D. W., Boulanger, R. W., Kutter, B. L., and Abghari, A., "Soil-Pile Superstructure Interaction Experiments with Liquefiable Sand in the Centrifuge," *Proceedings*, Fourth Caltrans Seismic Design Workshop, Caltrans, Sacramento, California (1996).

36. Ashford, S. A., and Rollins, K., "Full-Scale Behavior of Laterally Loaded Deep Foundations in Liquefied Sand: Preliminary Test Results," *Preliminary Report* (1999), Department of Structural Engineering, Univ. of California, San Diego, La Jolla, California.

37. Randolph, M. F., and Poulos, H. G., "Estimating the Flexibility of Offshore Pile Groups," *Proceedings*, 2nd International Conference on Numerical Methods in Offshore Piling, Austin, Texas (1982), pp. 313 - 328.

38. Bathe, K. J., *ADINA* User's Manual, ADINA R and D, Inc., Watertown, MA (1998).

39. *ANSYS* , "General Finite Element Analysis Program," Version 5.4, ANSYS, Inc. Houston, PA (1996).

40. El Naggar, M. H., and Novak, M., " Nonlinear Analysis for Dynamic Lateral Pile Response," *Journal of Soil Dynamics and Earthquake Engineering*, Vol. 15, No. 4 (1996), 233-244.

41. American Petroleum Institute, "Recommended Practice for Planning, Designing and Constructing Fixed Offshore Platforms," *API Recommended Practice 2A* (RP 2A), 19th Ed., Washington, D.C. (1991), pp.47 - 55.

42. Sowers, G.F., and Richardson, T. L., "Residual Soils of the Piedmont and Blue Ridge." *Transportation Research Record No. 919*, National Academy Press, Washington, D.C., (1985), pp. 10-16.

43. Randolph, M. F., "PIGLET: A Computer Program for the Analysis and Design of Pile Groups Under General Loading Conditions," *Soil Report No. TR91 CUED/D*, Cambridge University, Cambridge, UK (1980). (Currently available from the Department of Civil Engineering, University of Western Australia, Nedlands, Western Australia).

Table 1. Subgrade Modulus Reduction Factors from DM-7, CFEM-1985, and ASCE

Pile Spacing in Direction of Loading, D = Pile Diameter	DM-7 and CFEM Subgrade Reaction Reduction Factors, R	Corps of Engineers/ASCE Group Reduction Factor, R
8D	1.00	1.00
6D	0.70	0.56
4D	0.40	0.38
3D	0.25	0.33

$E_{subgrade}$ (lateral soil subgrade modulus) for a group pile = R $E_{subgrade\ isolated\ pile}$

Table 2. p-Multipliers Commonly Used for Static Loading

Pile Row	p-Multipliers from Peterson and Rollins S/D = 3	Default p-Multipliers from FLPIER S/D = 3
Lead	0.6	0.8
First Trail	0.4	0.4
Second Trail	0.4	0.2
Third Trail	0.4	0.3
Average	*0.45*	*0.43*
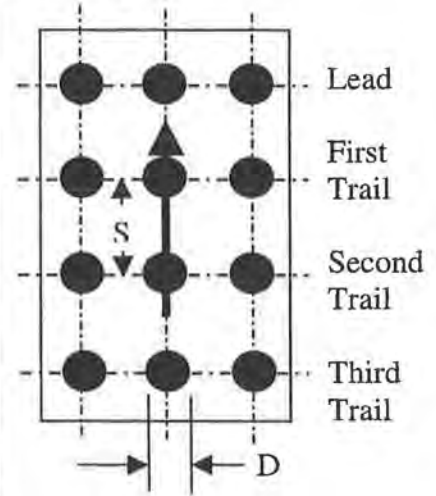
Table 3. p-Multipliers for Chaiyi Lateral Group Load Tests

Pile Row	Inferred p-Multipliers from Chaiyi Load Tests		p-Multipliers from Peterson and Rollins S / D = 3	Default p-Multipliers from FLPIER S / D = 3	Dynamic p-Multipliers from Figure 9	
	Bored Pile Group	Driven Pile Group			Bored Pile Group (y/D = 0.013)	Driven Pile Group (y/D = 0.075)
Lead	0.5	0.9	0.6	0.8	0.28	0.67
First Trail	0.4	0.7	0.4	0.4	0.18	0.61
Second Trail	0.3	0.5	0.4	0.2 (0.3)[1]	0.28	0.61
Third Trail	-	0.4	0.4	0.3	-	0.67
Average	*0.40*	*0.63*	*0.45*	*0.43 (0.50)[1]*	*0.25*	*0.64*

[1] Value is 0.2 for a 4-row group and 0.3 for a 3-row group. Average is 0.43 for a 4-row group and 0.50 for 3-row group

Table 4. Dynamic p-y curve parameter constants for a range of soil types
(D = 0.25 m, L/D = 40, $0.015 < a_o = \omega r_o/V_s < 0.225$).

$$P_d = P_s\left[\alpha + \beta a_o^{\,2} + \kappa a_o\left(\frac{\omega y}{d}\right)^n\right]$$

SOIL TYPE	DESCRIPTION	α	β		κ	n
			$a_o < 0.025$	$a_o > 0.025$		
SOFT CLAY	$C_u < 50$ kPa $V_s < 125$ m/s	1	-180	-200	80	0.18
MEDIUM CLAY	$50 < C_u < 100$ kPa $125 < V_s < 175$ m/s	1	-120	-360	84	0.19
STIFF CLAY	$C_u > 100$ kPa $V_s > 175$ m/s	1	-2900	-828	100	0.19
MEDIUM DENSE SAND (saturated)	$50 < D_r < 85$ % $125 < V_s < 175$ m/s	1	3320	1640	-100	0.1
MEDIUM DENSE SAND (unsaturated)	$50 < D_r < 85$ % $125 < V_s < 175$ m/s	1	1960	960	-20	0.1
DENSE SAND (saturated)	$D_r > 85$ % $V_s > 175$ m/s	1	6000	1876	-100	0.15

125

Rheological model of p-y curve

Static, single pile p-y curve

Degraded, single pile p-y curves

gap
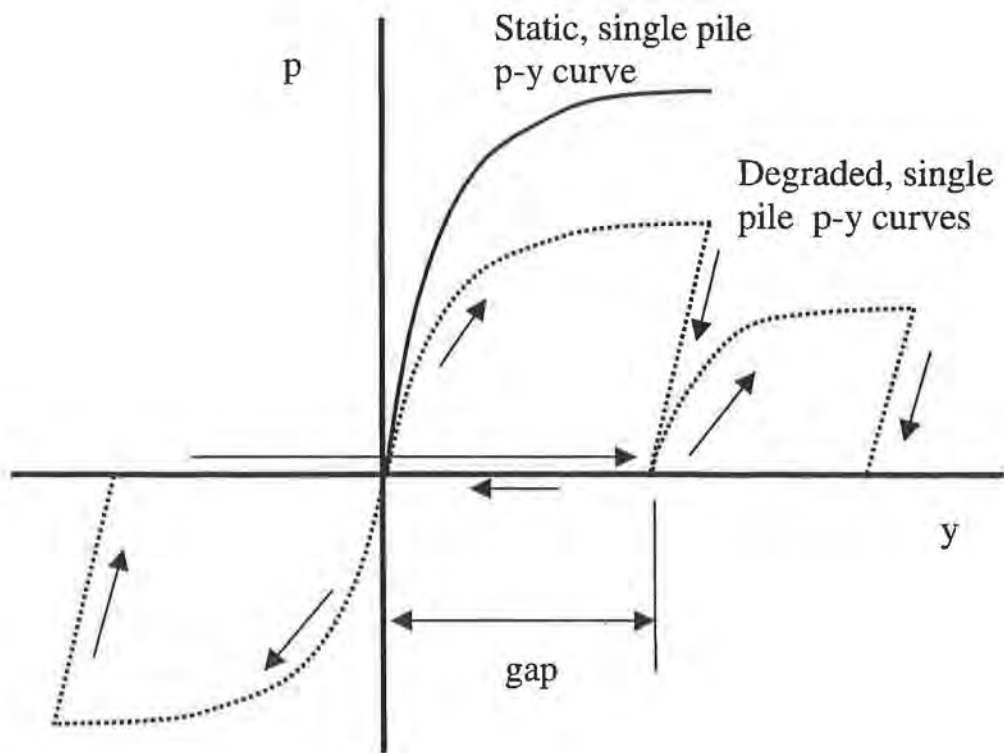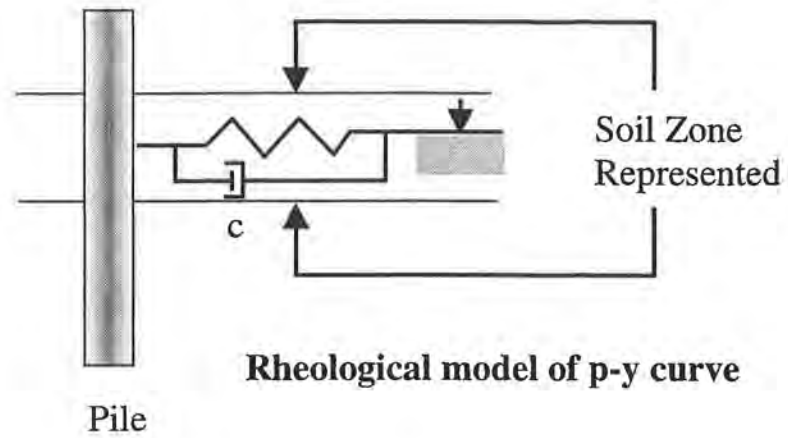
Figure 1. p-y Method for Modeling Cyclic Degradation and Hysteretic Damping in Soil

126

Soil resistance per unit
of pile length, p

p_1

$p_g = \rho\, p_1$

Single pile

Group pile

ρ is the "p-multiplier" that is applied
to all points on every single-pile p-y
curve to give a set of p-y curves for
a group pile.

Local lateral soil
displacement, y
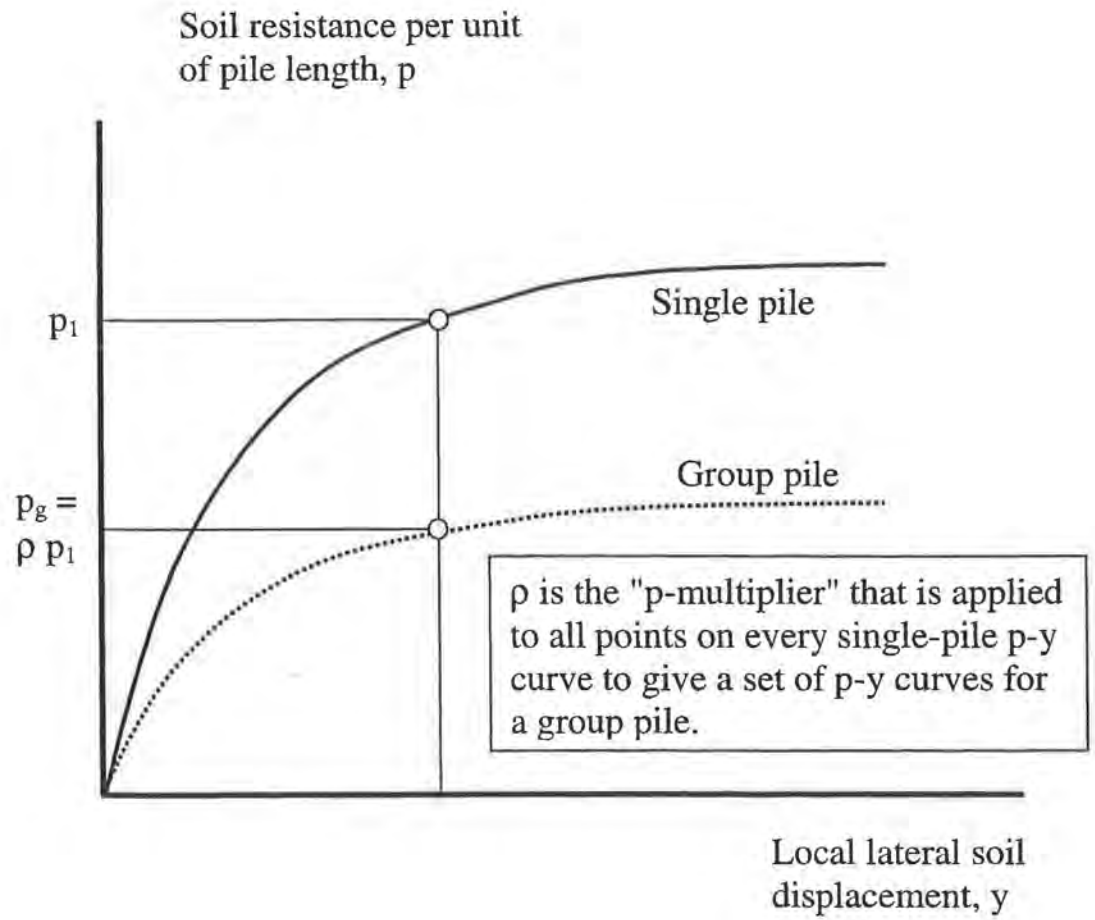
Figure 2. Definition of the p-y Curve and the p-multiplier

127
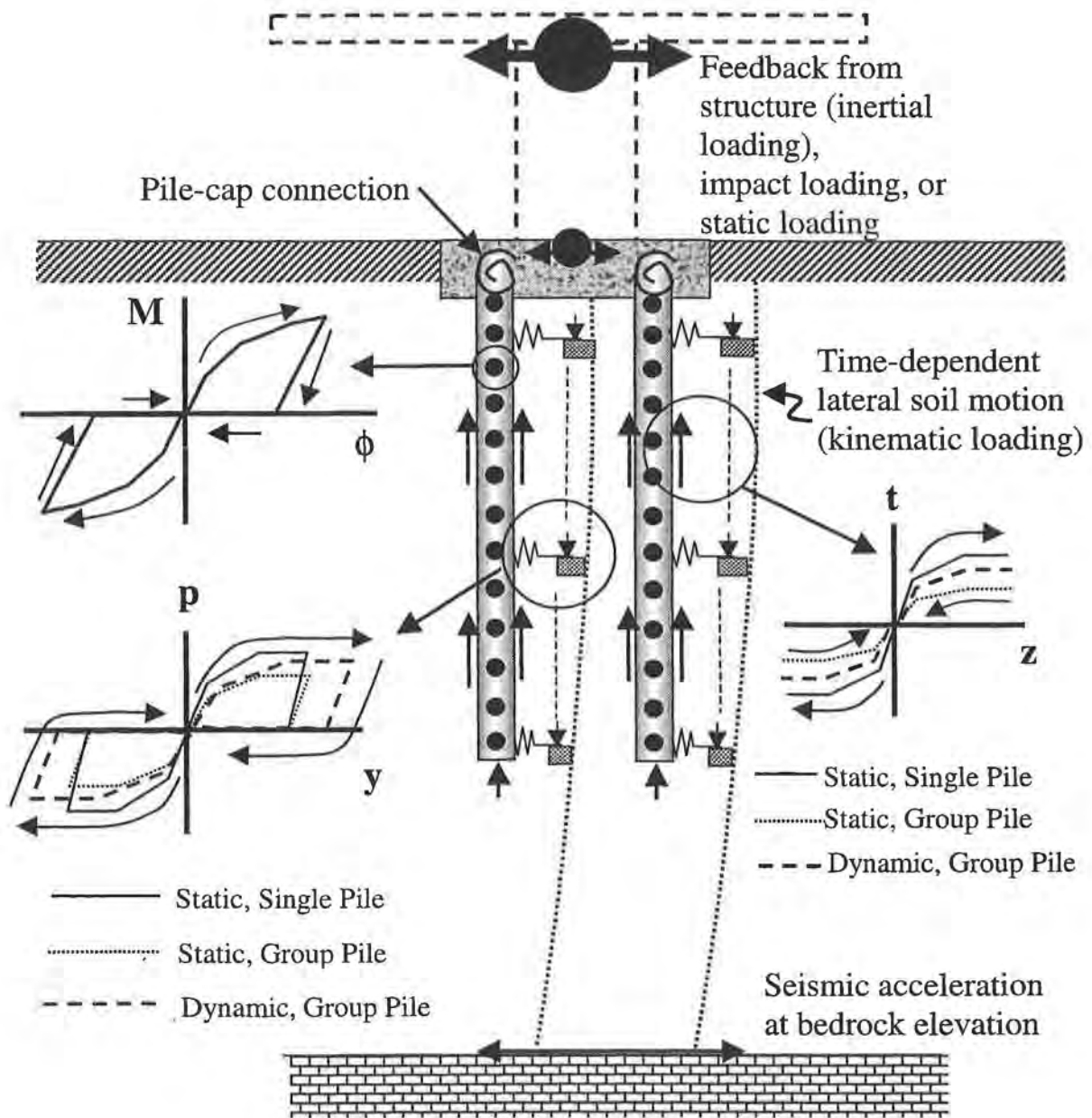
Figure 3. *Schematic Model for Laterally Loaded Pile Groups for this Project*

128
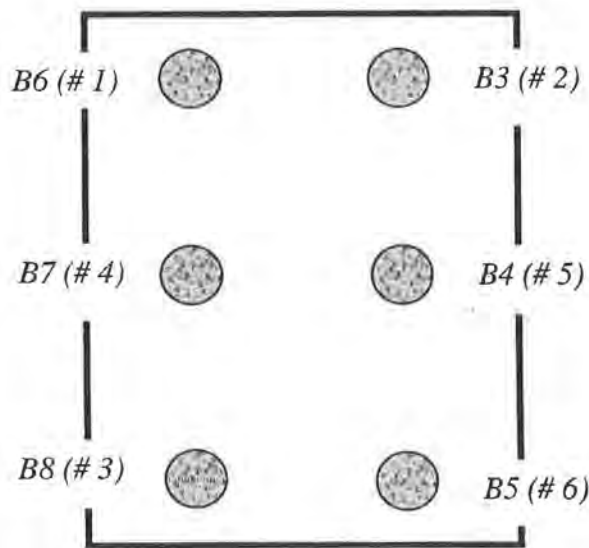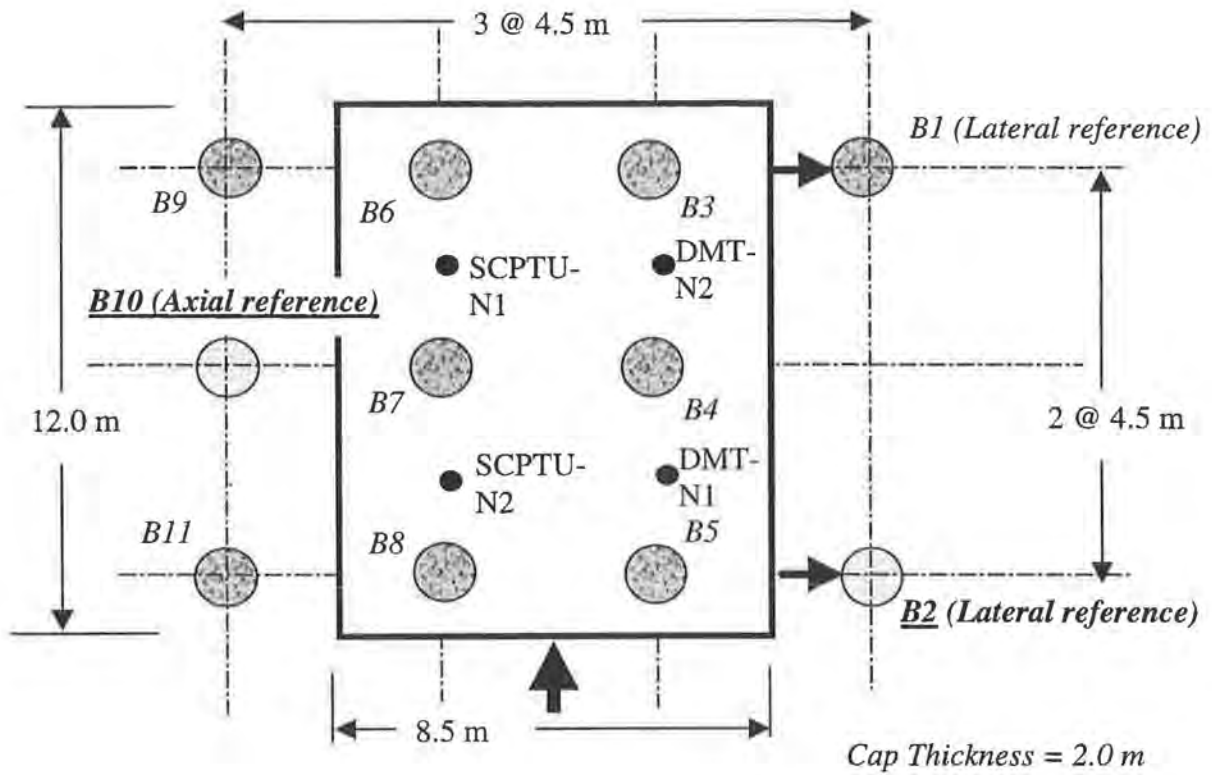
(b) Order of Installation for Bored Piles in Test Group

Figure 4. Plan View of Test Group for Bored Piles and Reference Piles (Not to Scale)
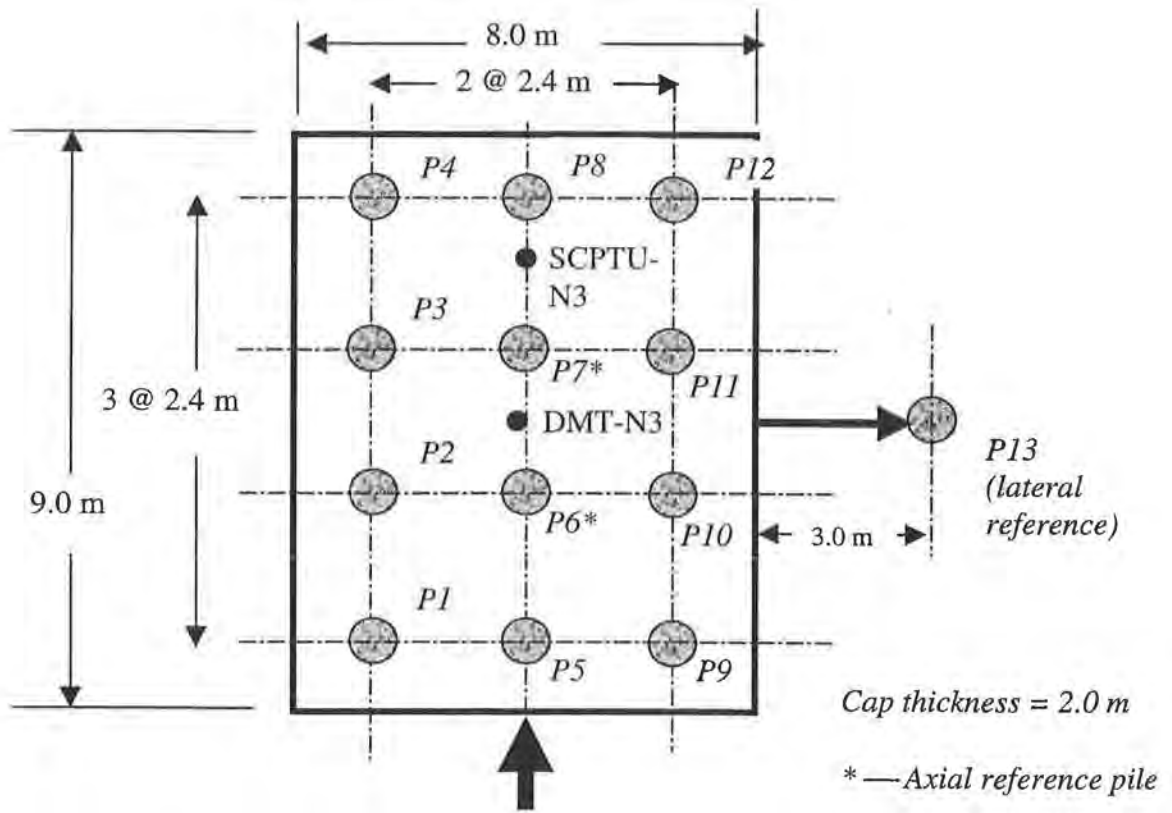
(a) Driven Pile Group Layout
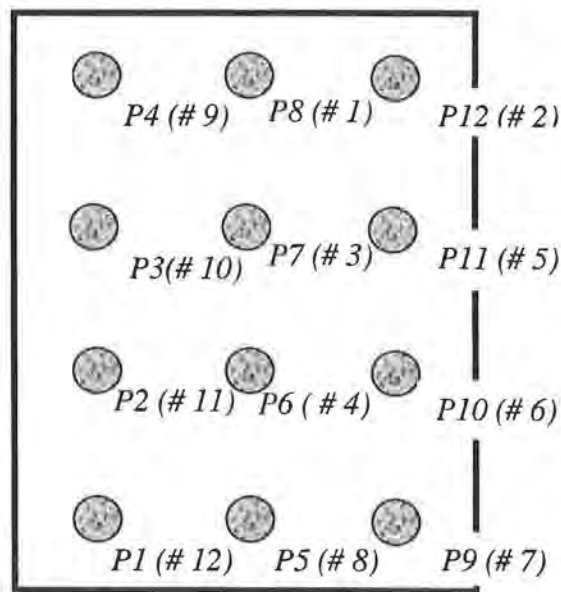
(b) Order of Installation for Driven Piles in Test Group

Figure 5. Plan View of Test Group for Driven Piles and Reference Piles (Not to Scale)
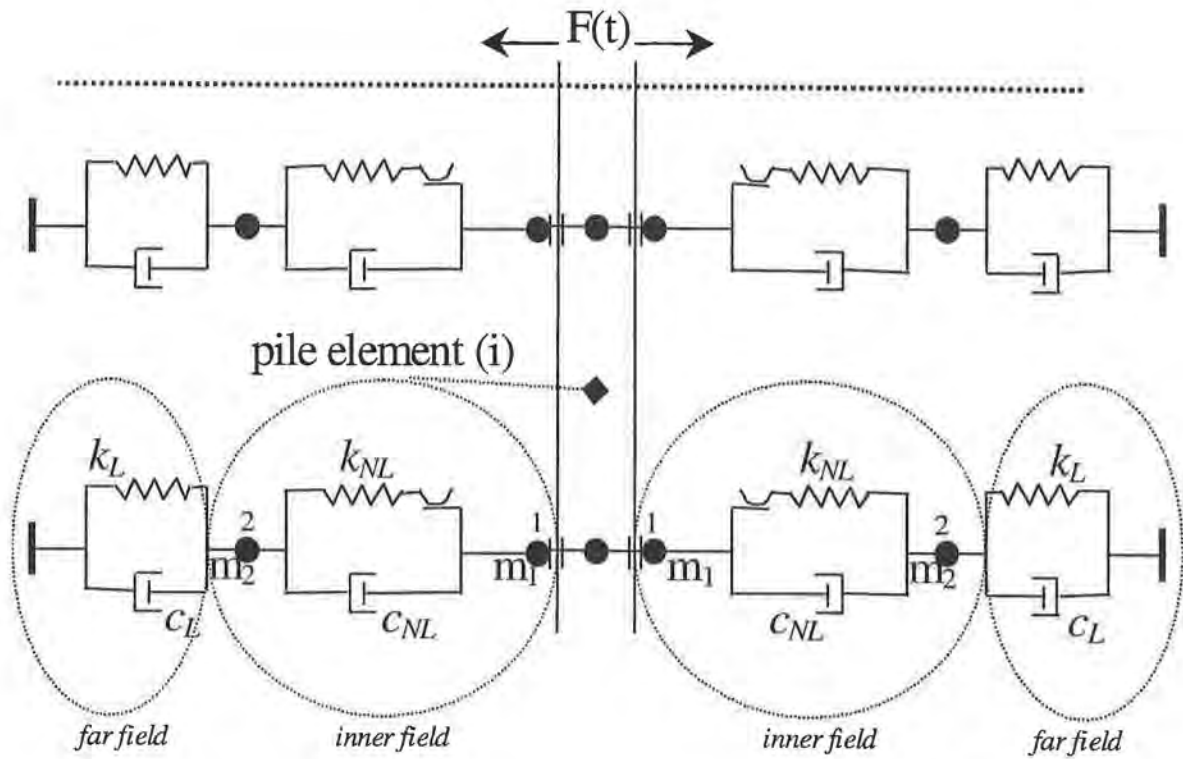
Figure 6. Schematic of Model Used for Deriving Dynamic p-y Curves and p-Multipliers
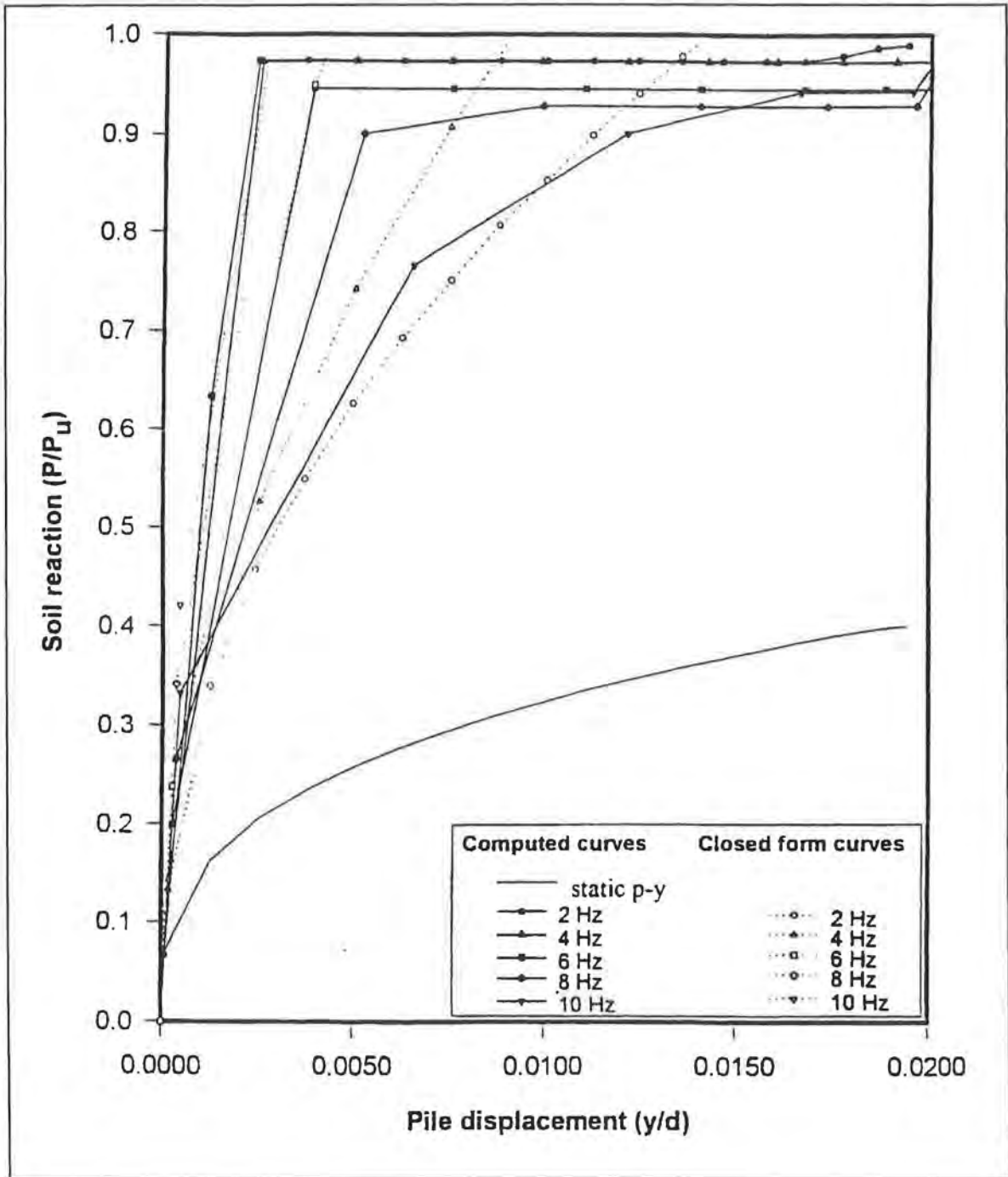
Figure 7. Static and Dynamic p-y Curves for Clay (1 m Depth)
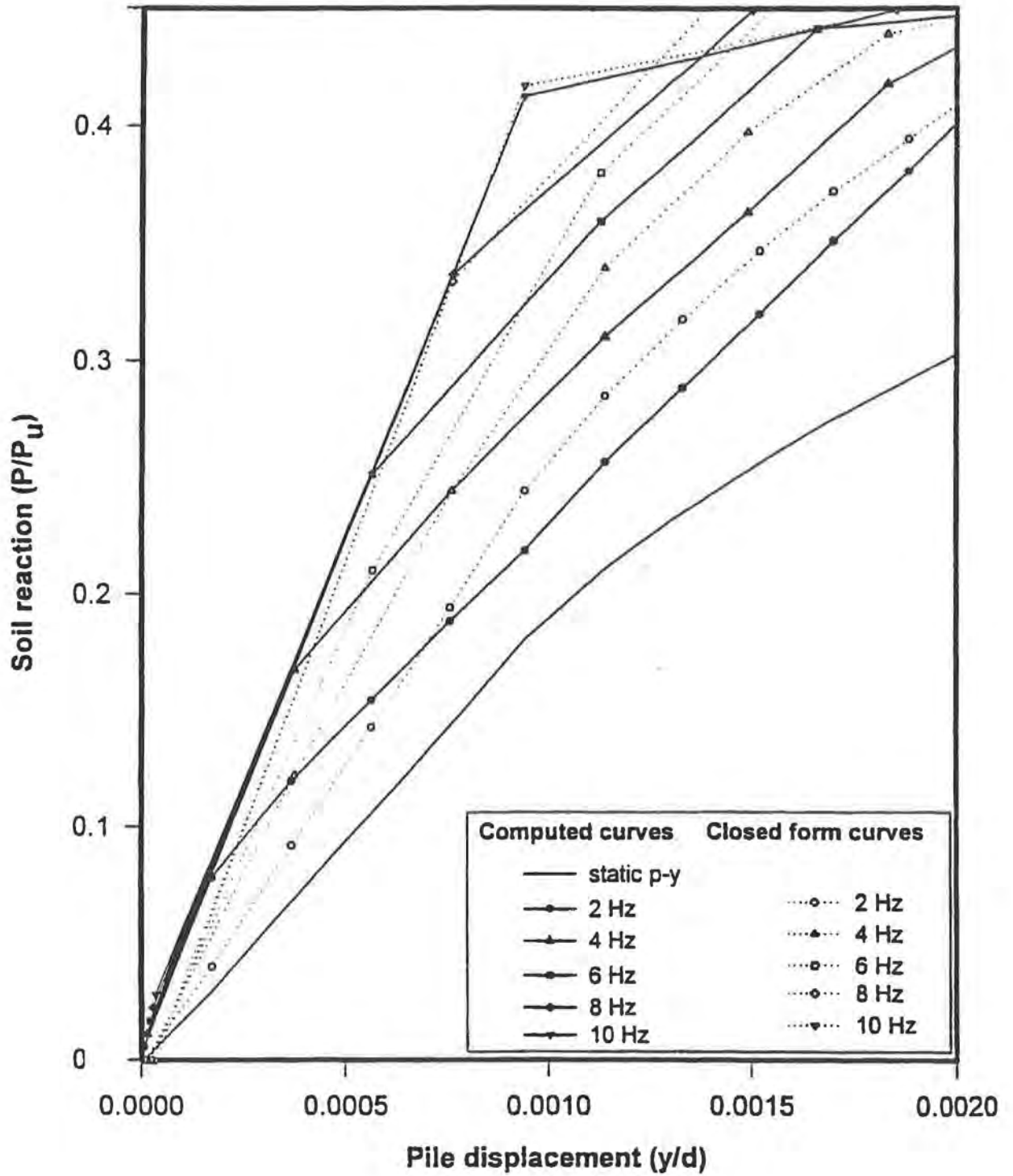
Figure 8. Static and Dynamic p-y Curves for Sand (1.5 m Depth)

133
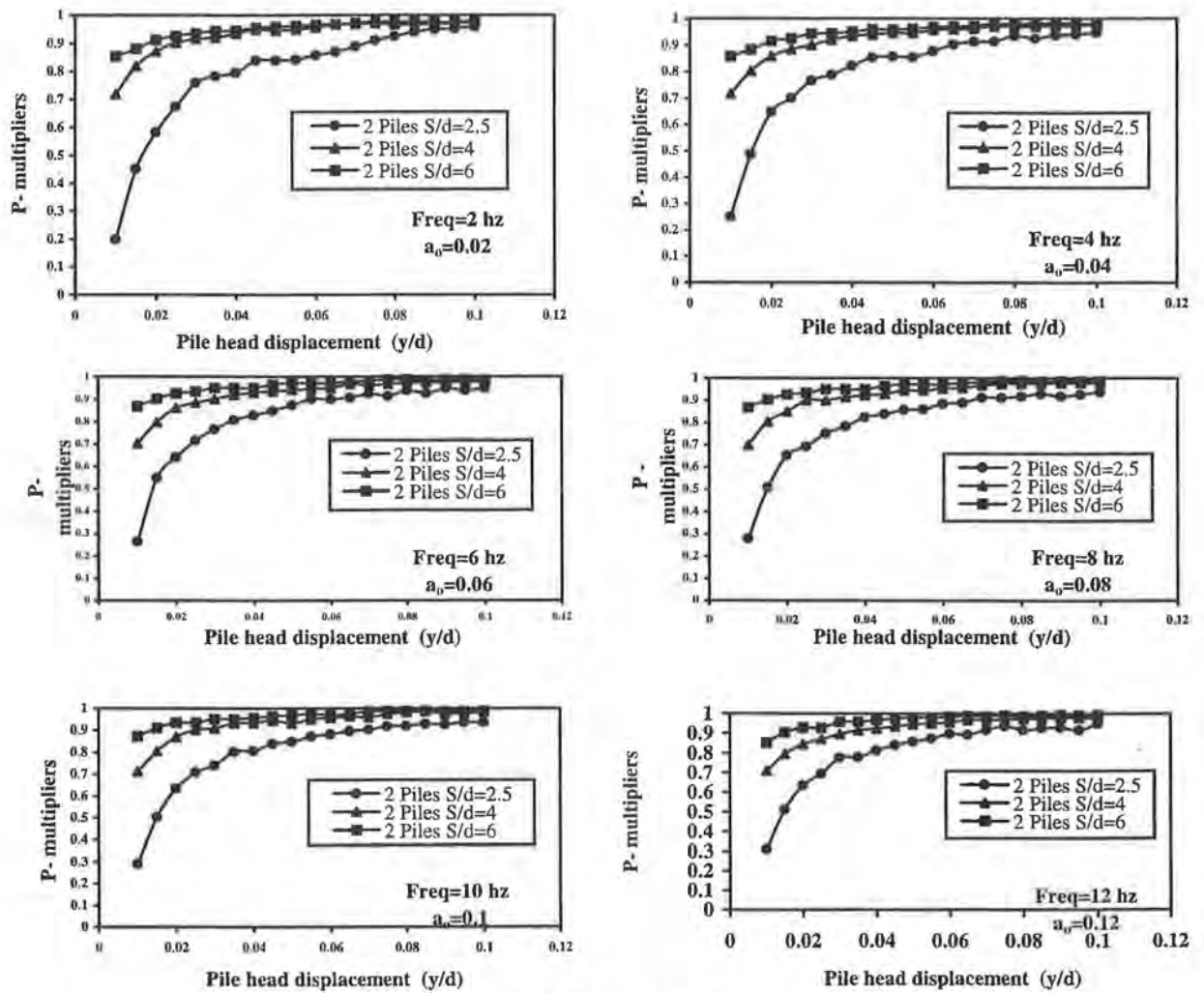
Figure 9. Dynamic p-multipliers versus Pile-Head Displacement for Medium Dense Sand

Ignore spacings over 6 D

Example:

3 D spacing

3.5 D spacing

ρ_{X-Y} = Dynamic p-multiplier for effect of Pile X on Pile Y (or *vice-versa*) at spacing S_{X-Y} / D [e.g., Figure 9]

A1   A2   A3

S_{A1} S_{A2} S_{A3} θ

B1 S_{B1} **B2** S_{B3} B3

S_{C1} S_{C2} S_{C3}

C1   C2   C3

Row D

Ignore all piles on this row, S > 6 D

D

Seismic Loading — Cyclic and Multi-Directional
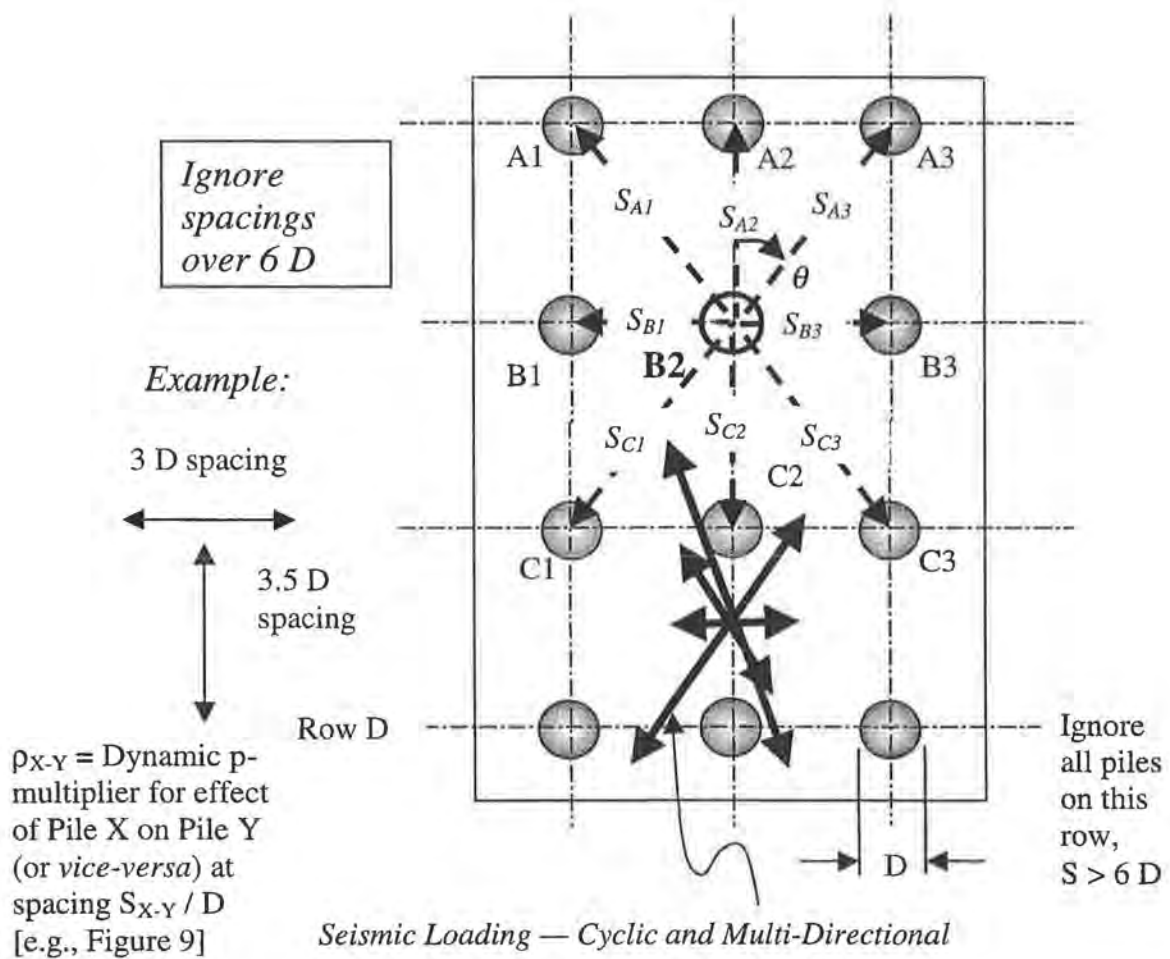
p-multiplier for Pile B2 = $[\rho_{A1-B2}]$ $[\rho_{A2-B2}]$ $[\rho_{A3-B2}]$ $[\rho_{B1-B2}]$ $[\rho_{B3-B2}]$ $[\rho_{C1-B2}]$ $[\rho_{C2-B2}]$ $[\rho_{C3-B2}]$

Figure 10. Calculation of Dynamic p-Multiplier for Typical Pile in Group
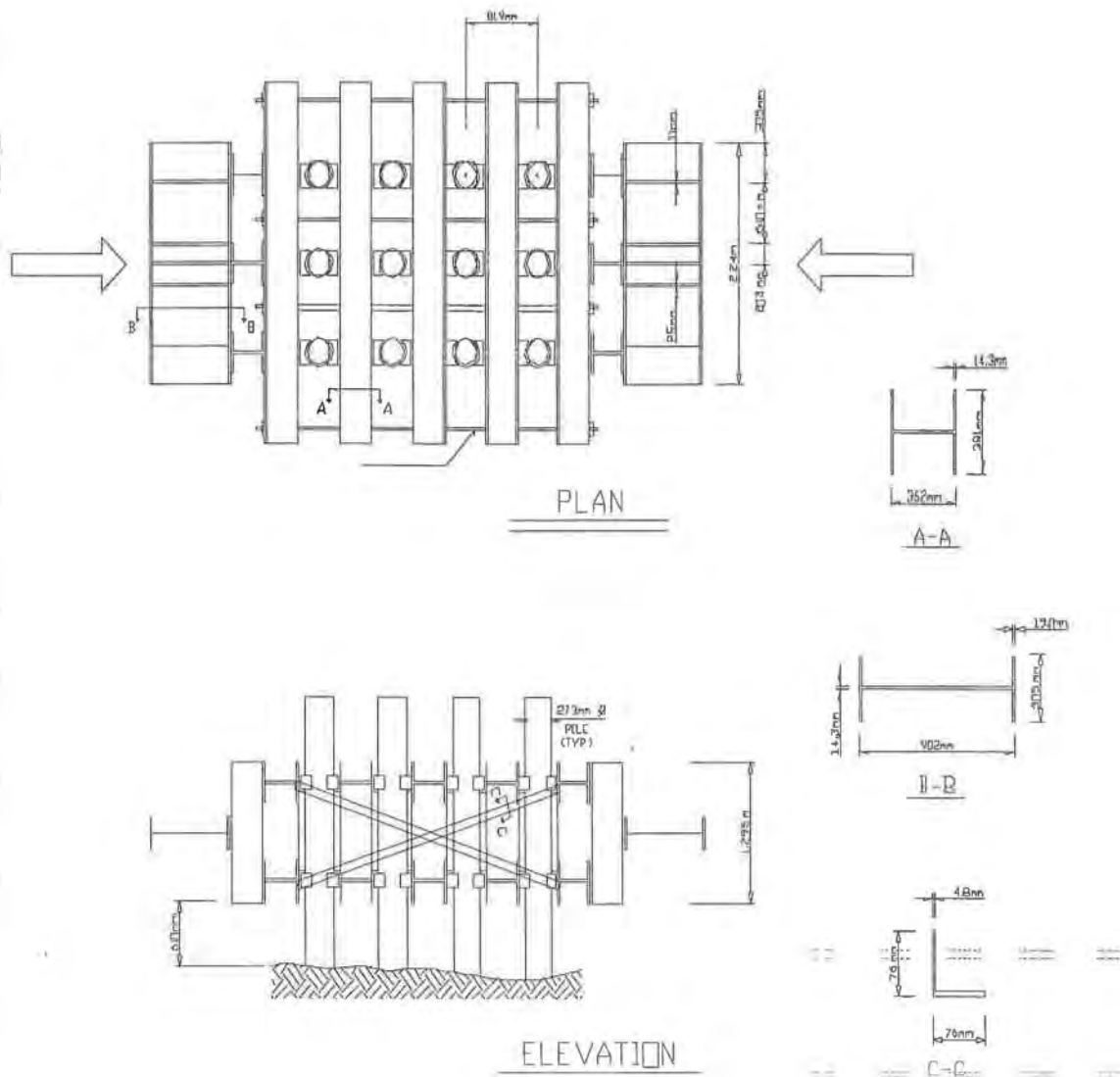
Figure 11. Schematic of Loading Frame with Pile Group

Figure 12. Photograph of Loading Frame at Wilmington Site

Hanger Beam

Reaction Mass

Test Foundation

Hemispherical Bearing Plate

Statnamic Slec

Support Frame for Statnamic Device
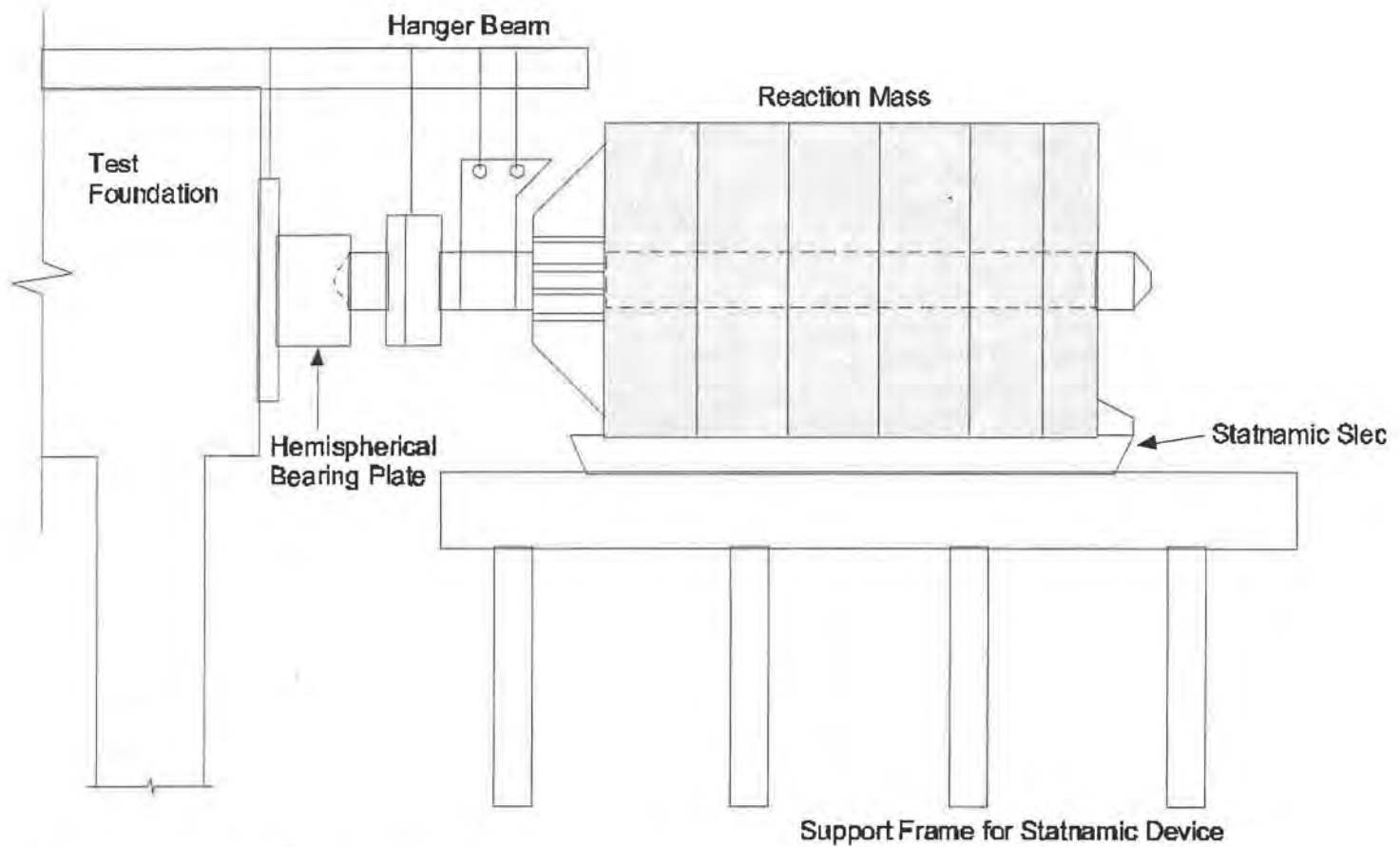
1. Statnamic device is placed against test foundation
2. Pelletized fuel inside piston is ignited
3. Expanding gases push reaction mass away from foundation imparting equal and opposite thrust on the foundation

Figure 13. Schematic of Statnamic Load Test

Load vs Displacement
Pile Group - Test Area 1
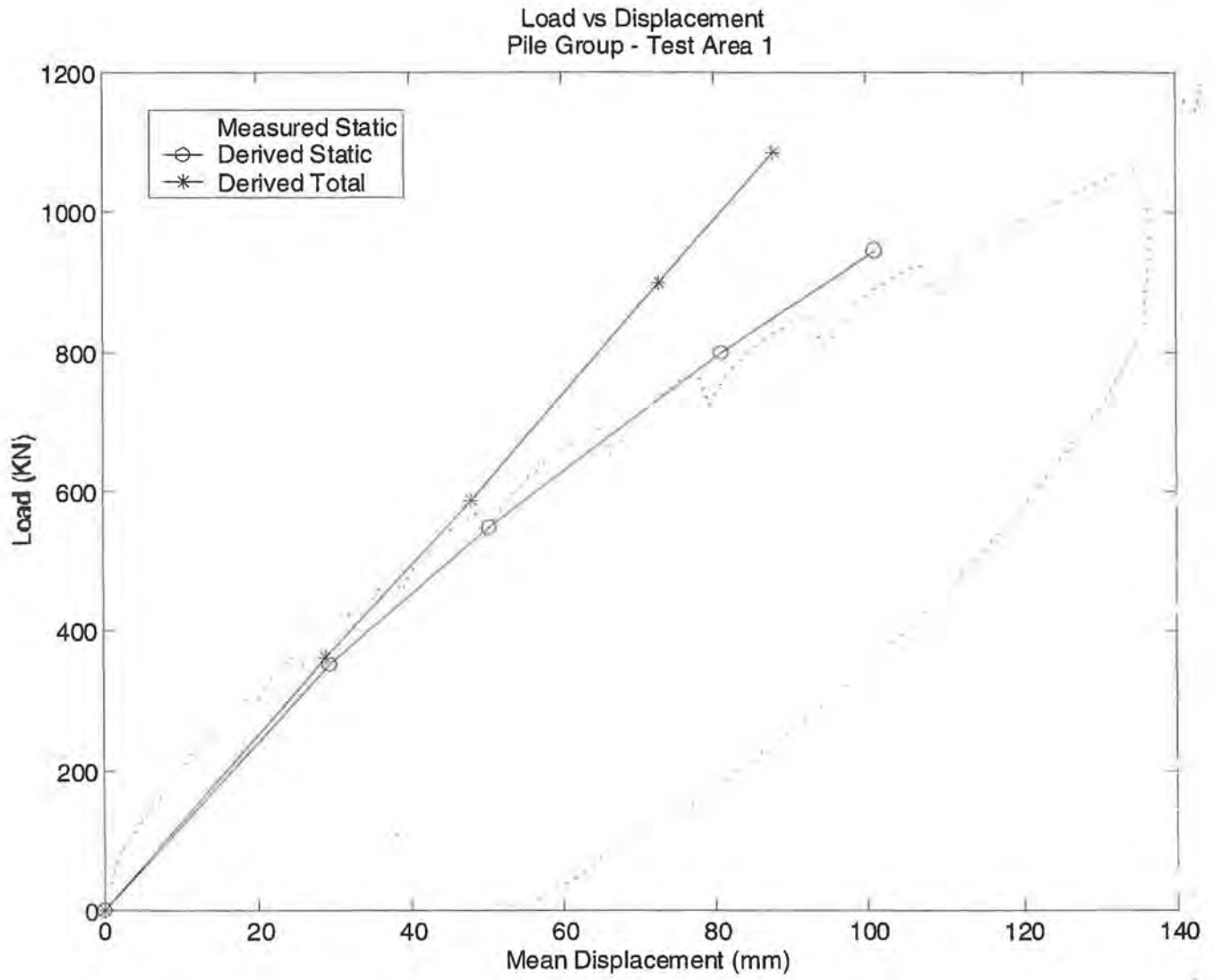
Figure 14. Derived Static Load-Deflection Response, Wilmington Test Area 1
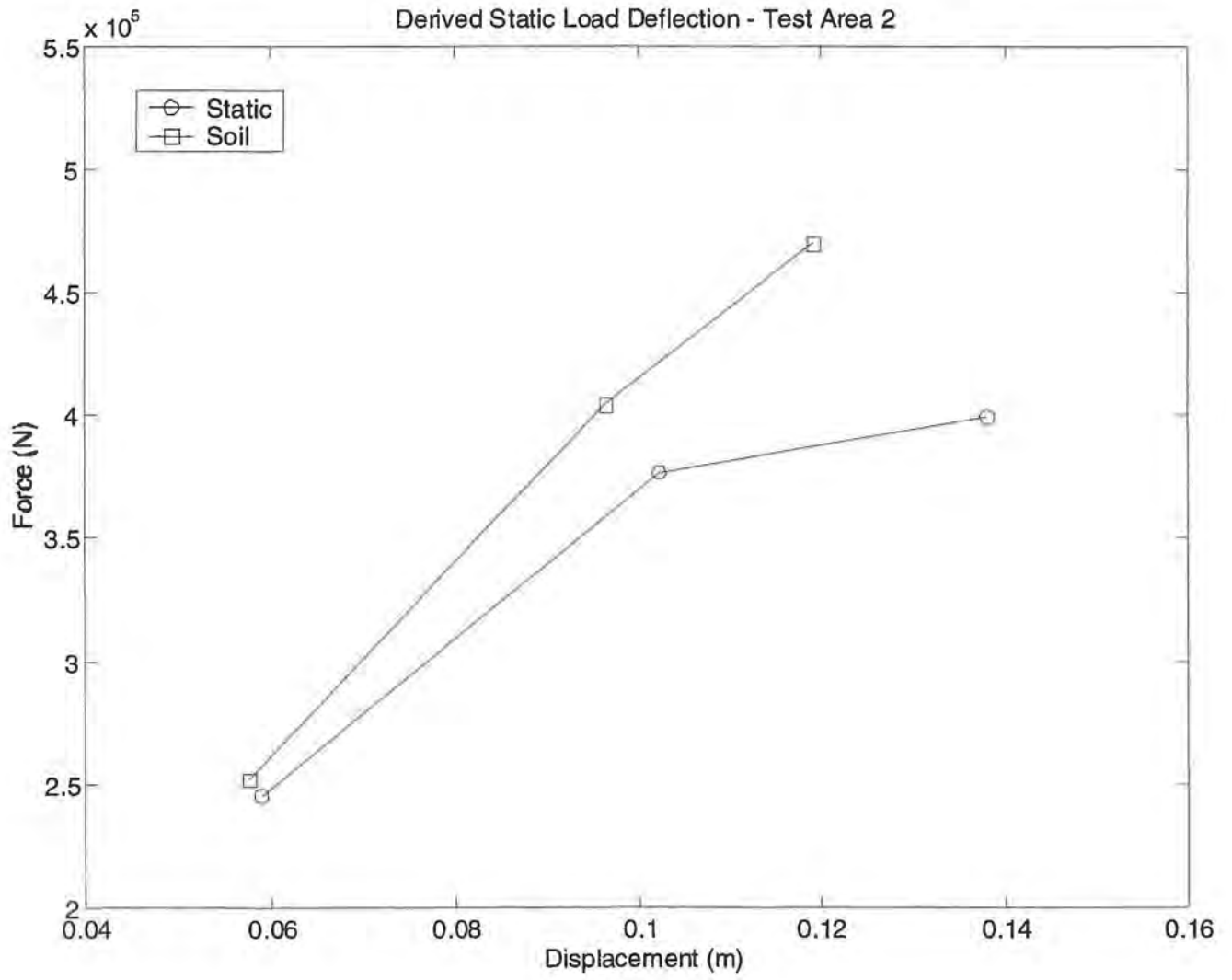
Figure 15. Derived Static Load-Deflection Response, Wilmington Test Area 2
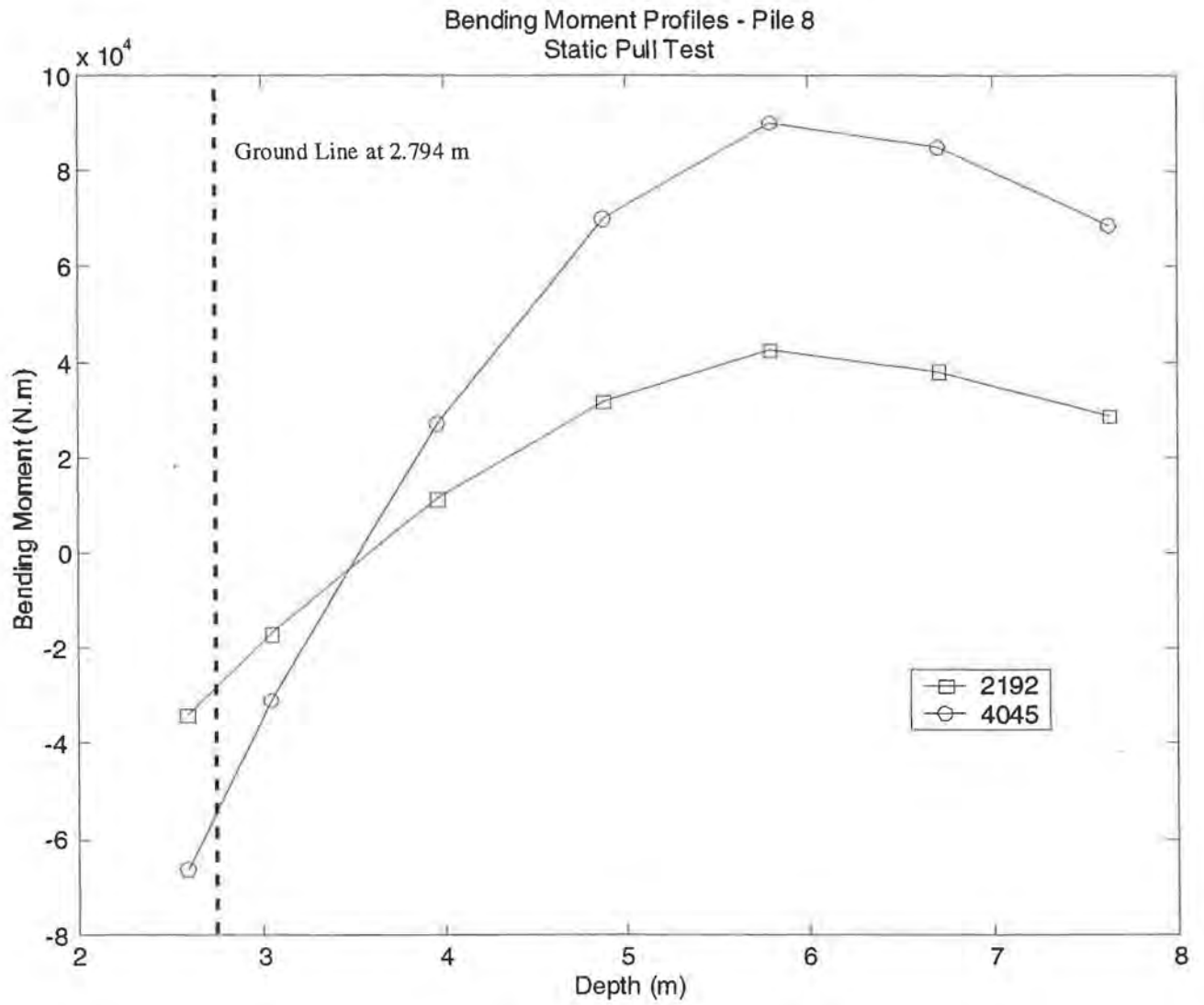
Figure 16. Bending Moment Profiles, Lead Row Pile, Wilmington Test Area 1

141
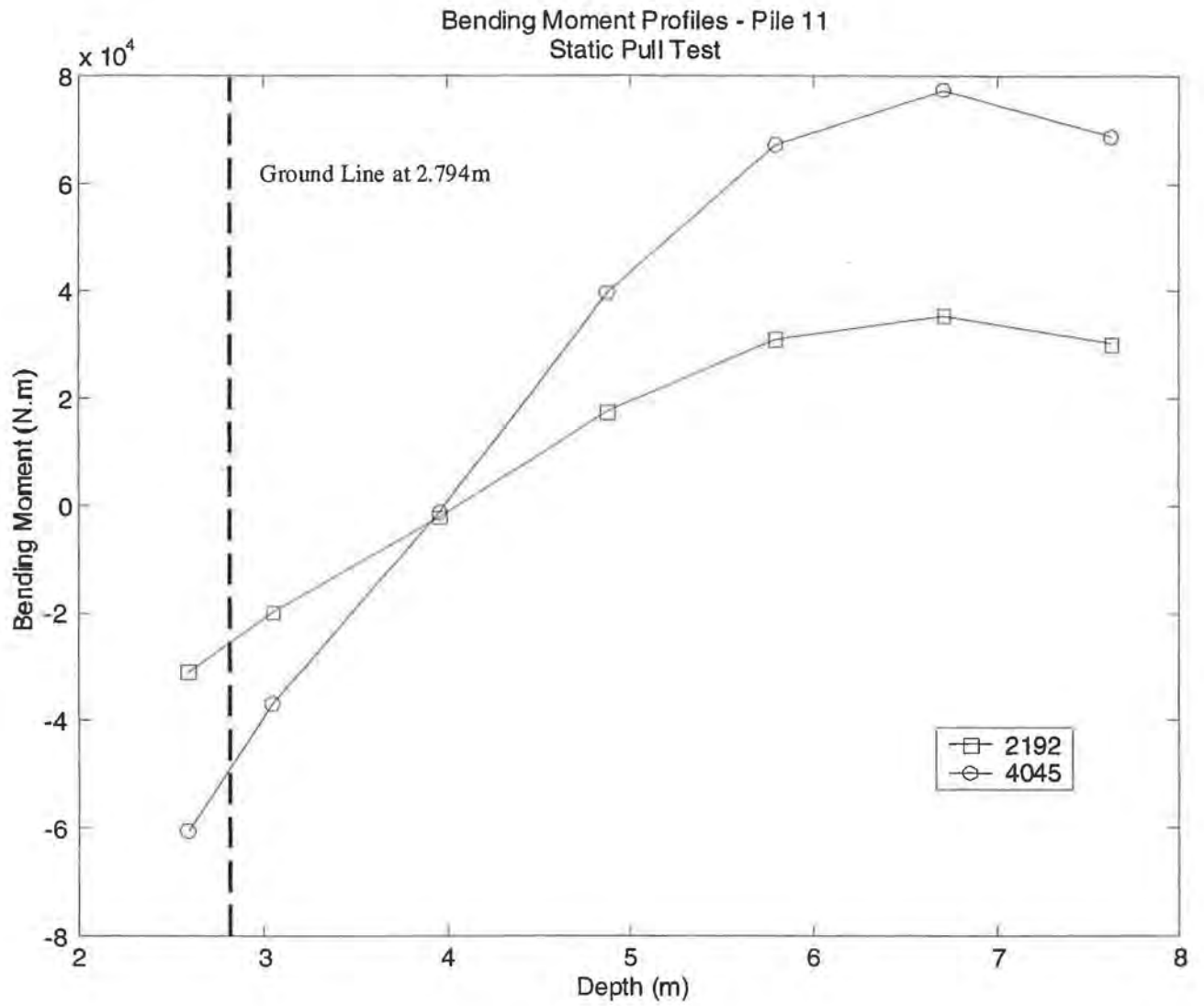
Figure 17. Bending Moment Profiles, Trailing Row Pile, Wilmington Test Area 1
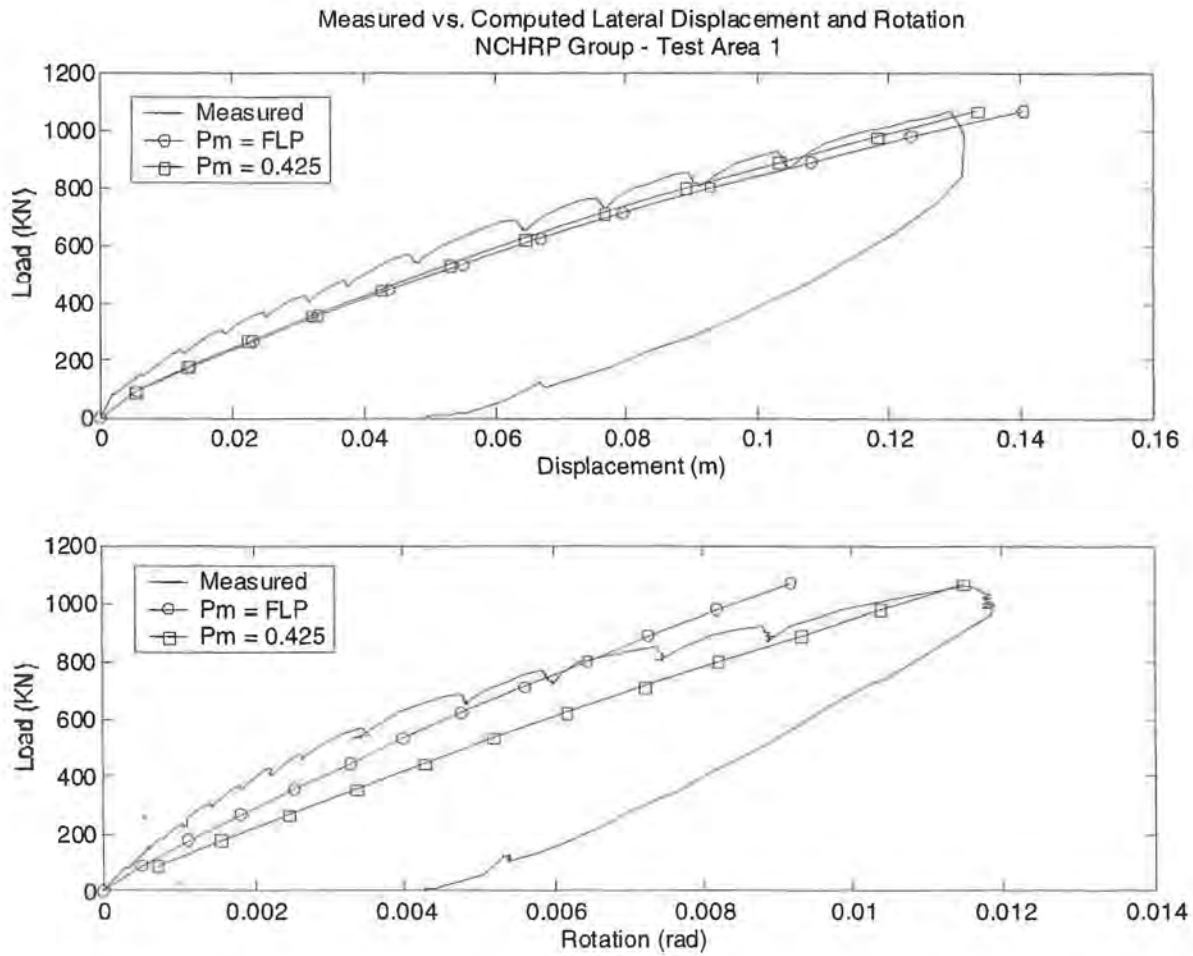
Figure 18. Measured vs. Computed Lateral Displacement and Rotation, Wilmington Test Area 1
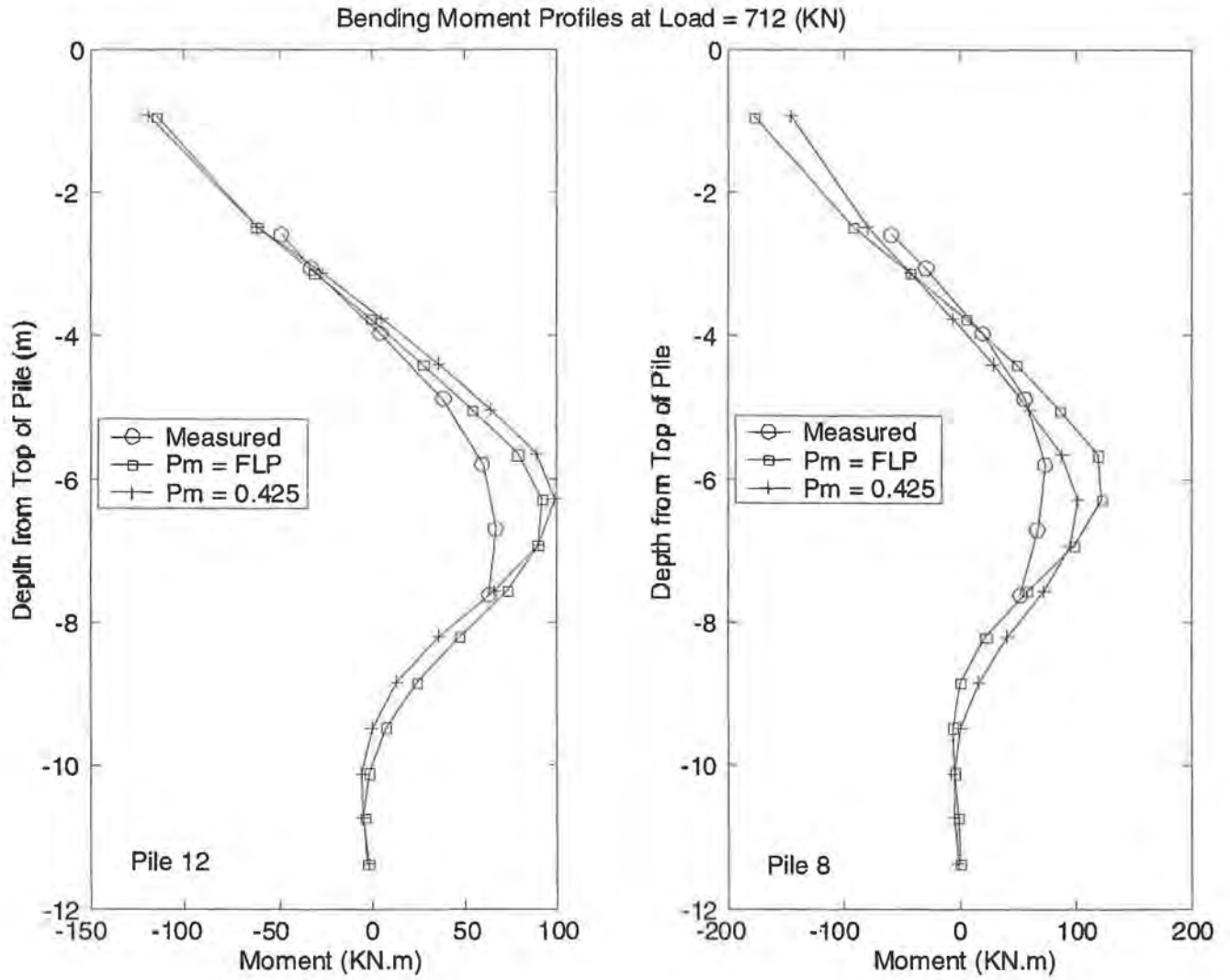
Figure 19. Bending Moment Profiles at Load = 712 kN, Wilmington Test Area 1

Static Push

Statnamic Load

Static Push

Static Push

Static Push

Statnamic Load

N

Note :
All dimensions are in meters;
Pile 1 to 7 has 6 strain gauges; pile 8 to 13 has 14 strain gauges.
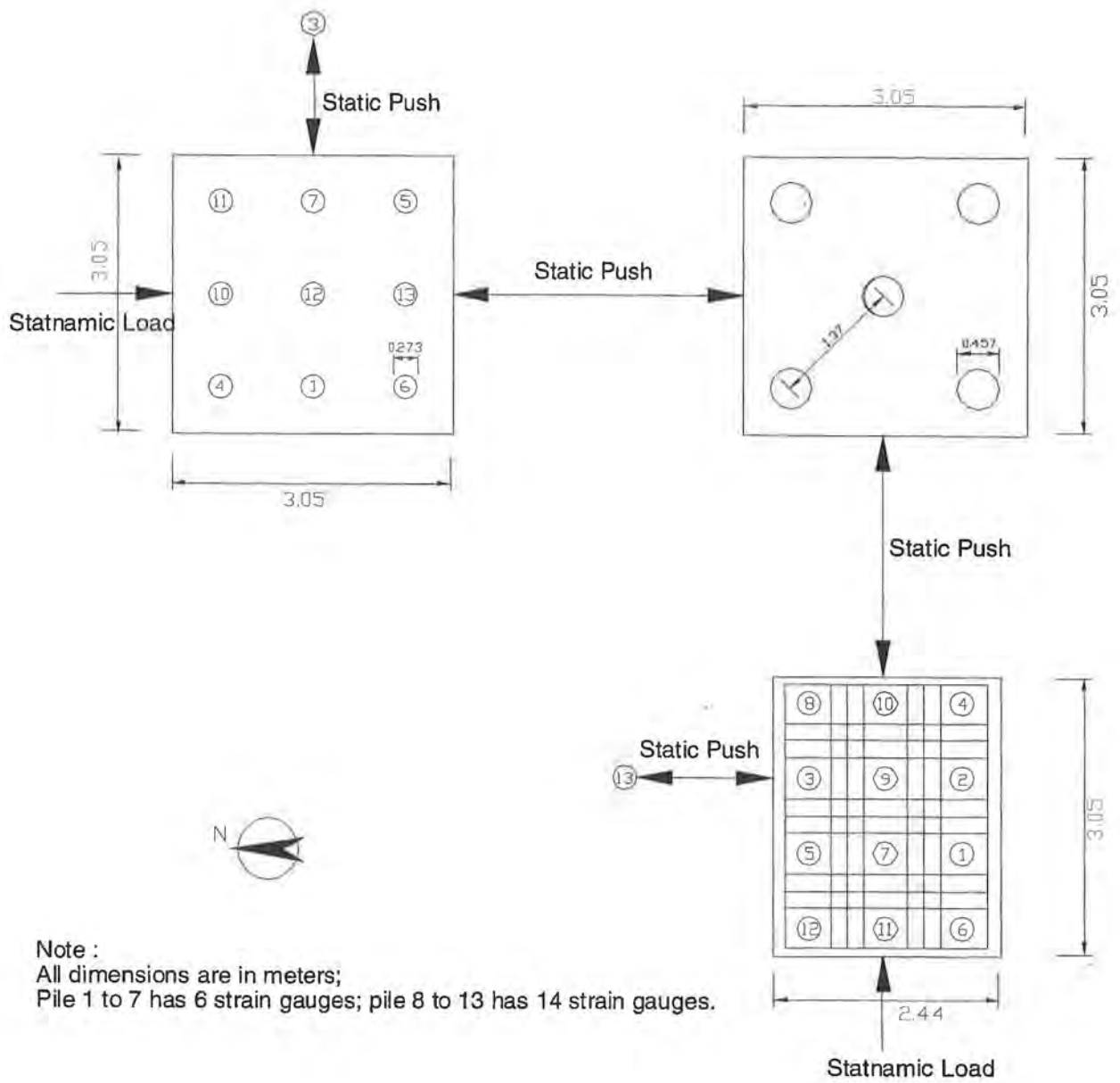
Figure 20. Site Plan of Testing at Spring Villa (Auburn) Test Site

145
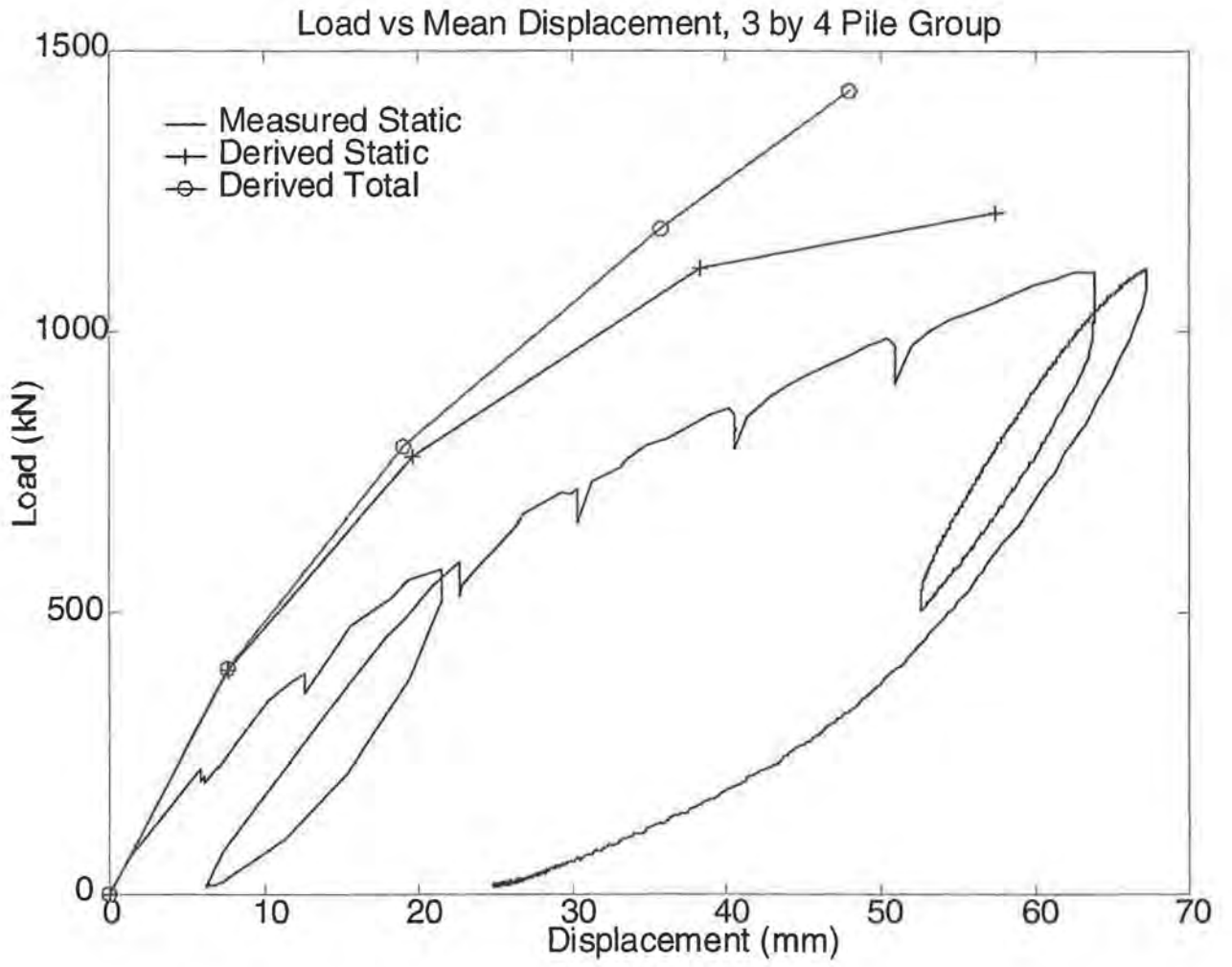
Figure 21. Load vs. Displacement, 3 by 4 Pile Group and Spring Villa Site
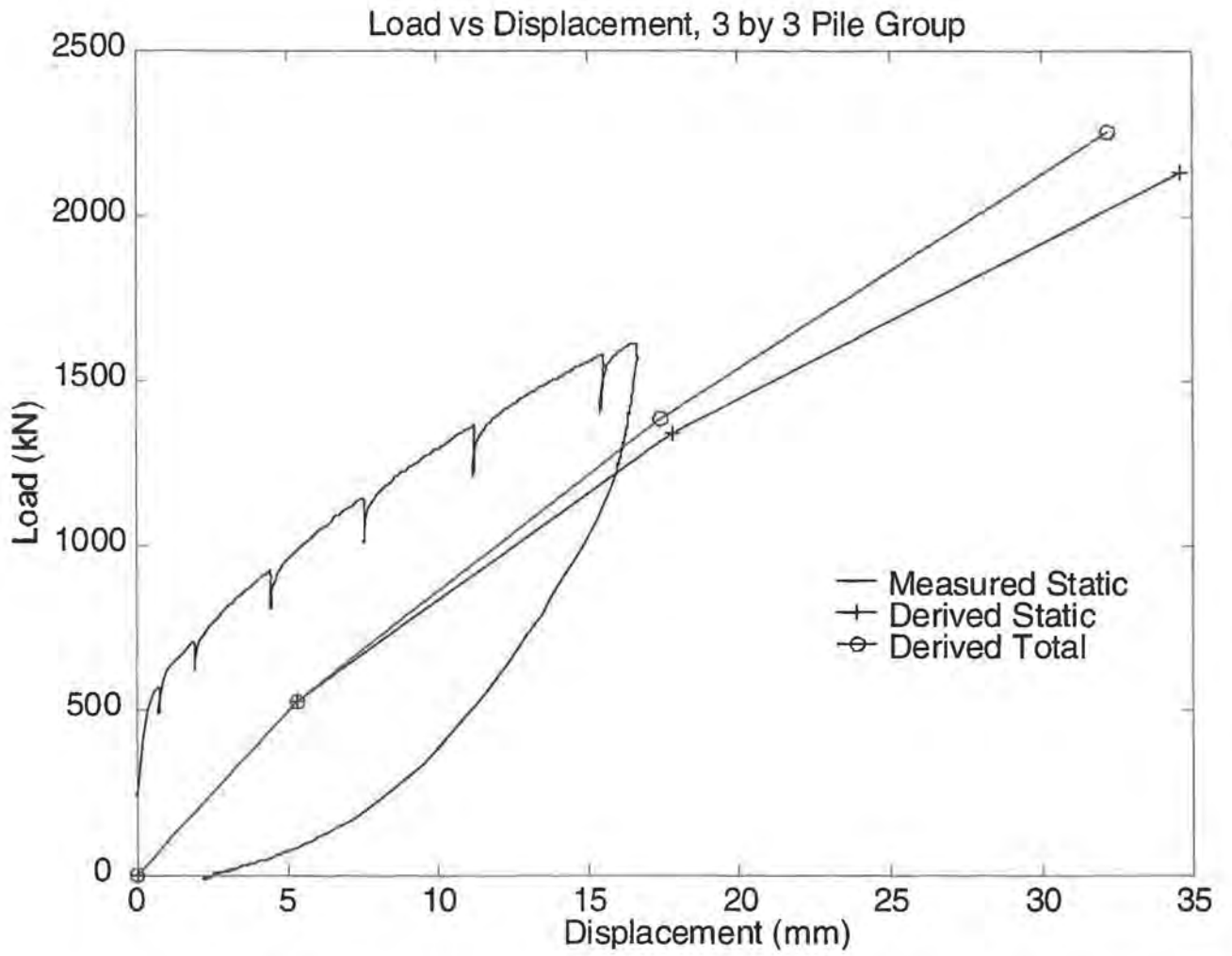
Figure 22. Load vs. Displacement, 3 by 3 Pile Group at Spring Villa Site
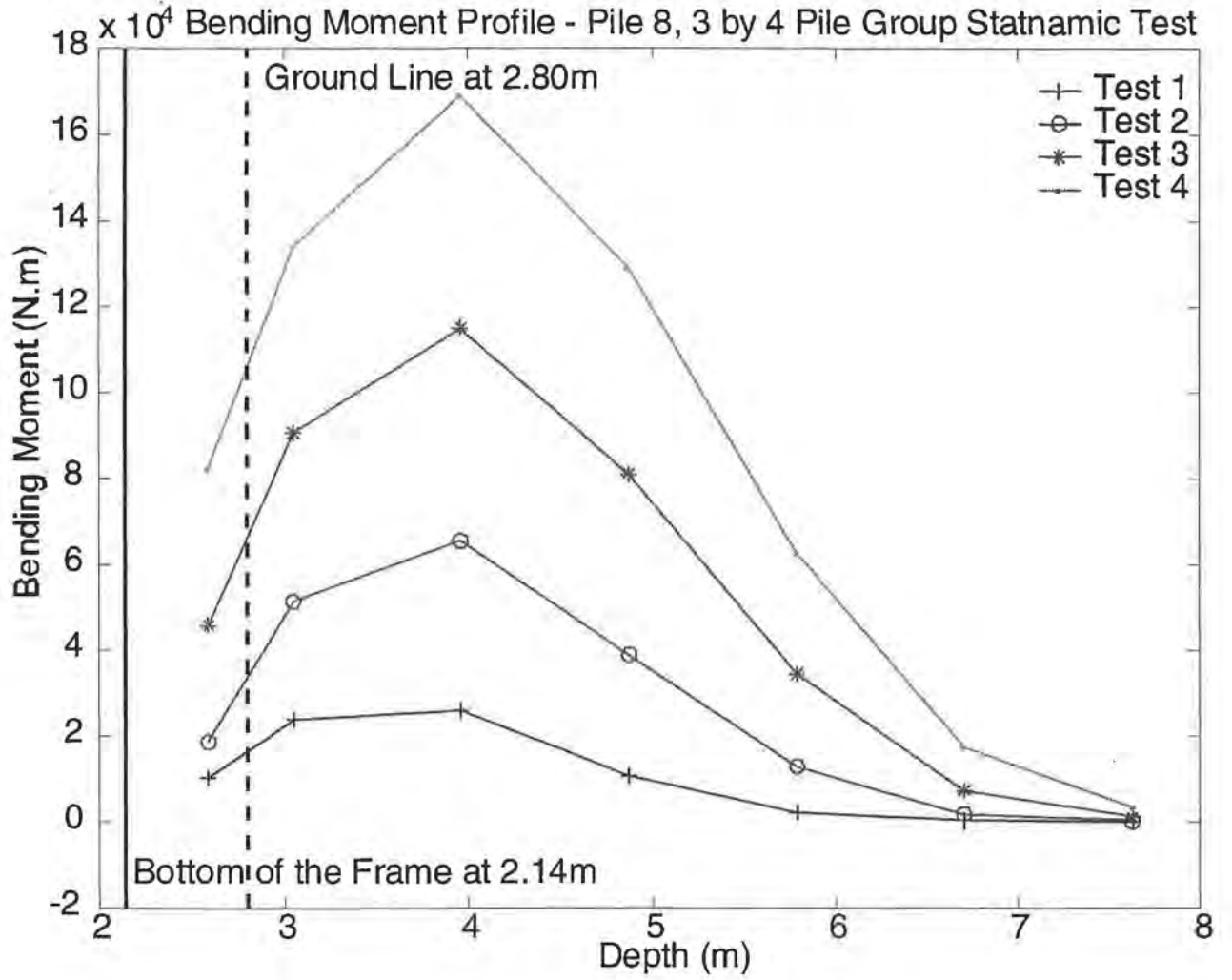
Figure 23. Bending Moment Profiles, Lead Row Pile, 3 by 4 Pile Group at Spring Villa Site
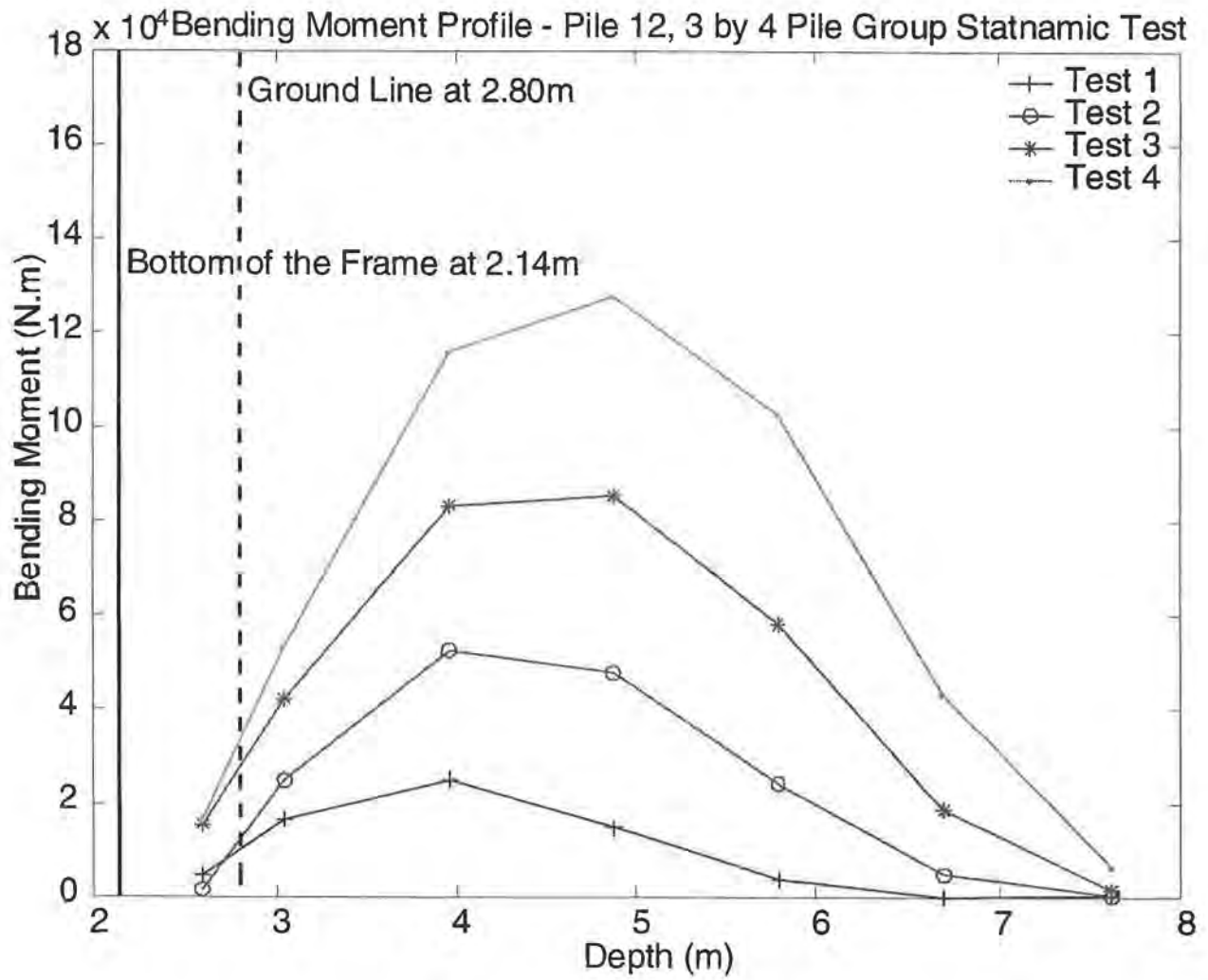
Figure 24. Bending Moment Profiles, Trailing Row Pile, 3 by 4 Pile Group at Spring Villa Test Site

149
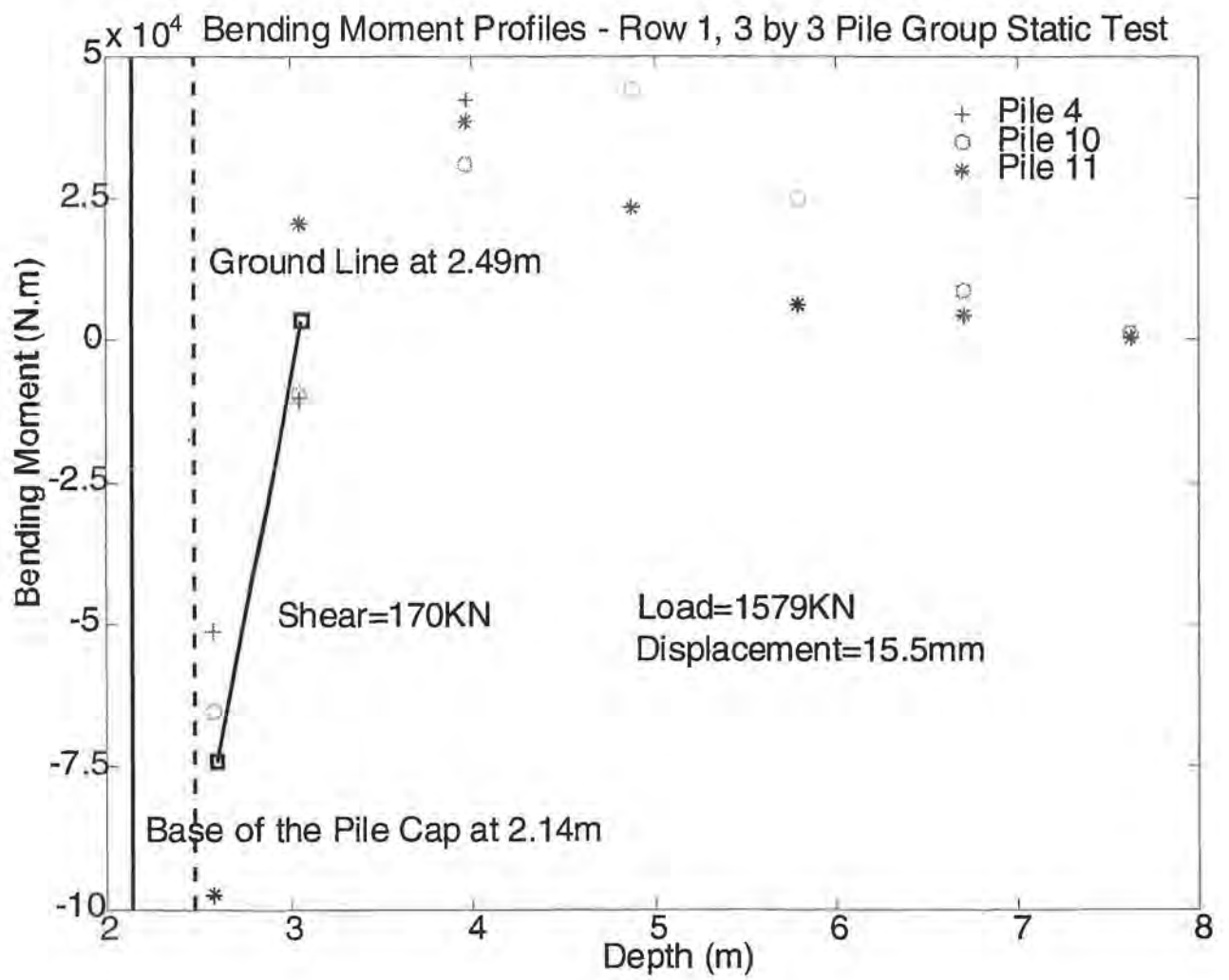
*Figure 25. Bending Moment Profiles, Lead Row Piles, 3 by 3 Pile Group at Spring Villa Test Site*
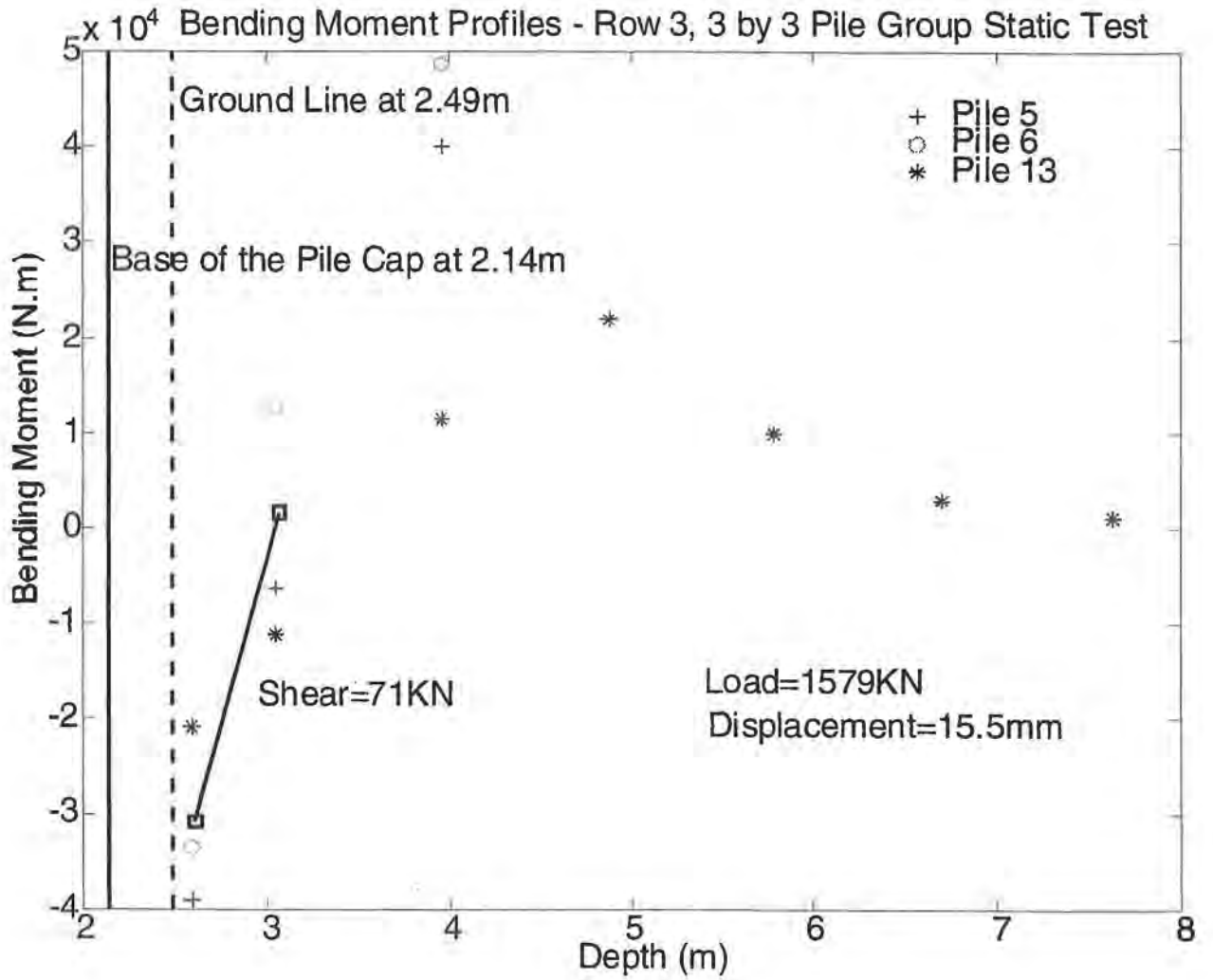
Figure 26. Bending Moment Profiles, Trailing Row Piles, 3 by 3 Pile Group at Spring Villa Test Site

151
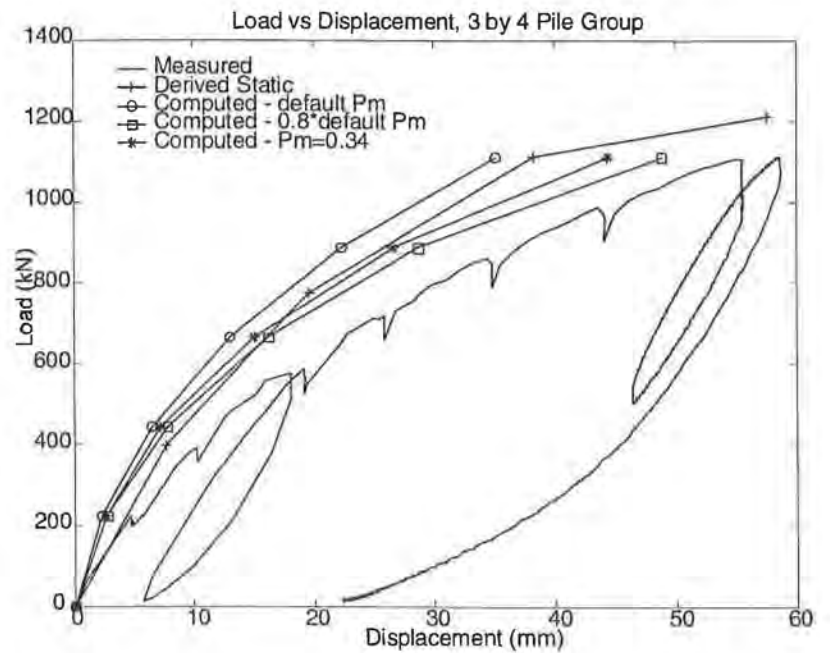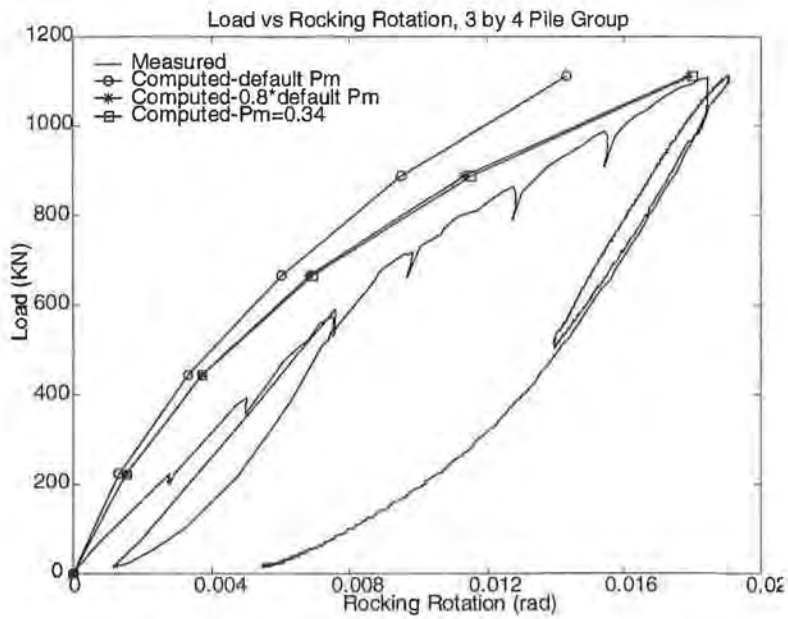
Figure 27. Measured vs. Computed Displacement and Rotation, 3 by 4 Pile Group at Spring Villa Test Site

152
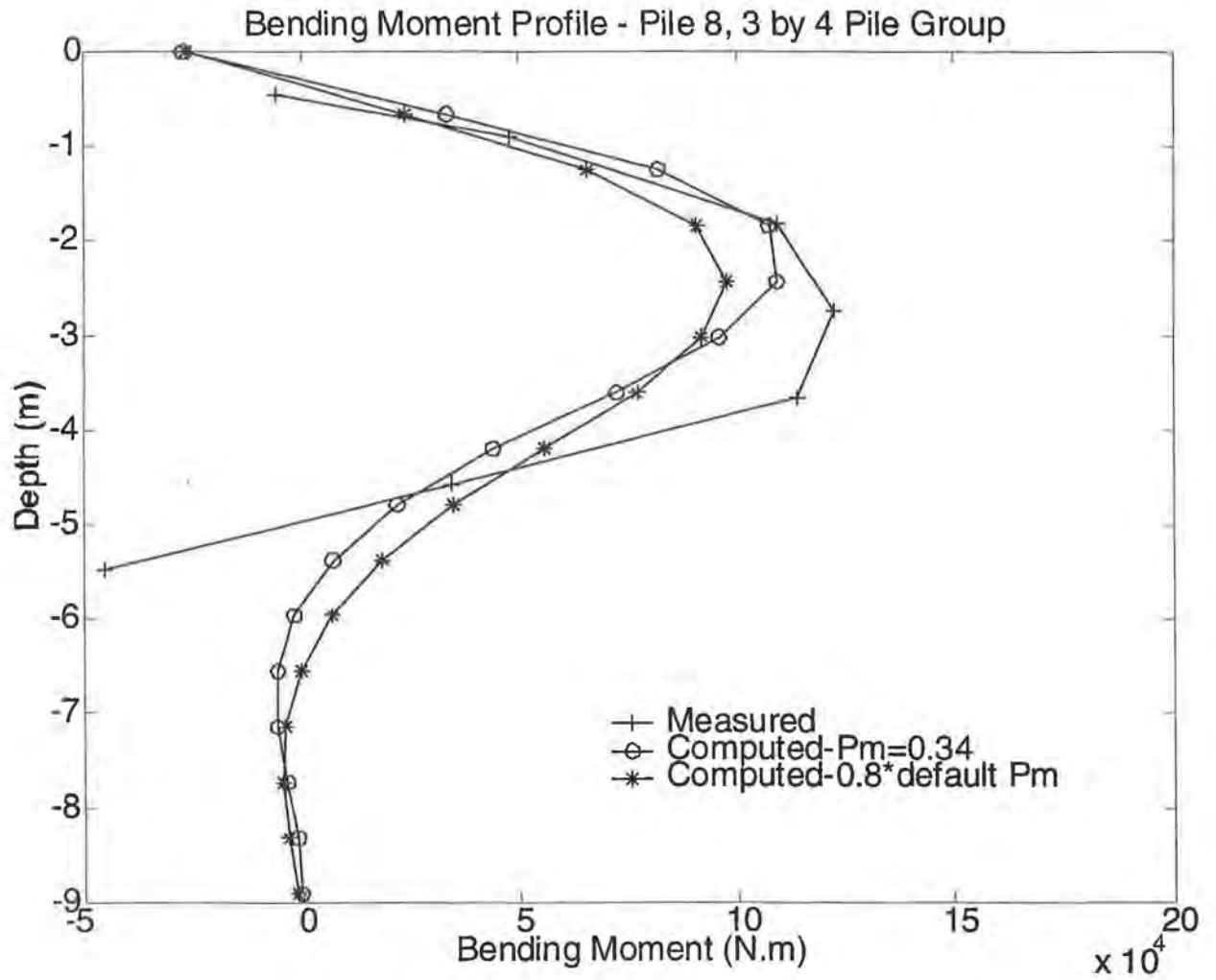
*Figure 28. Bending Moment Profile, Trailing Row Pile, 3 by 4 Pile Group
at Spring Villa Test Site, Group Load = 1111 kN*
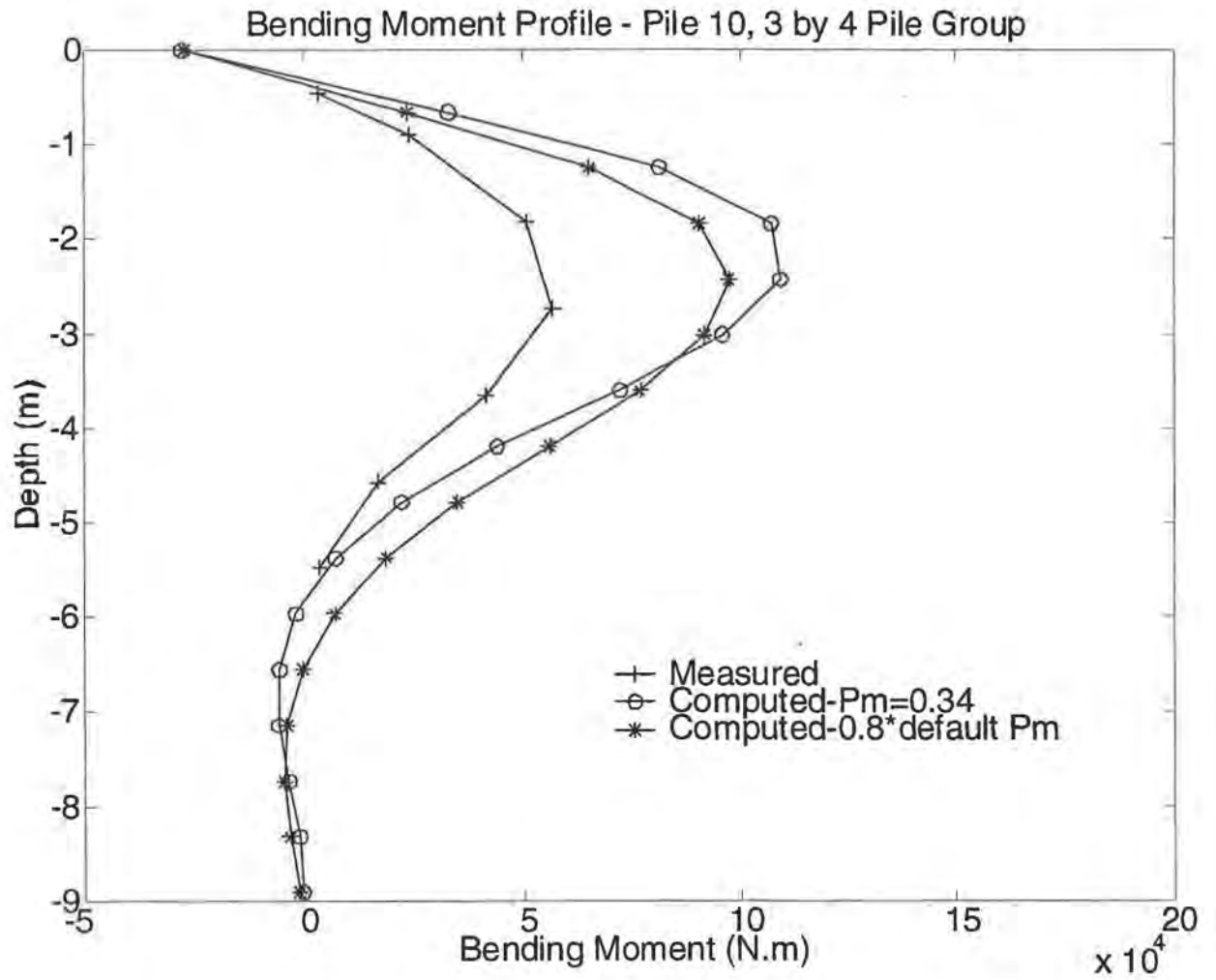
*Figure 29. Bending Moment Profile, Trailing Row Pile, 3 by 4 Pile Group
at Spring Villa Test Site, Group Load = 1111 kN*
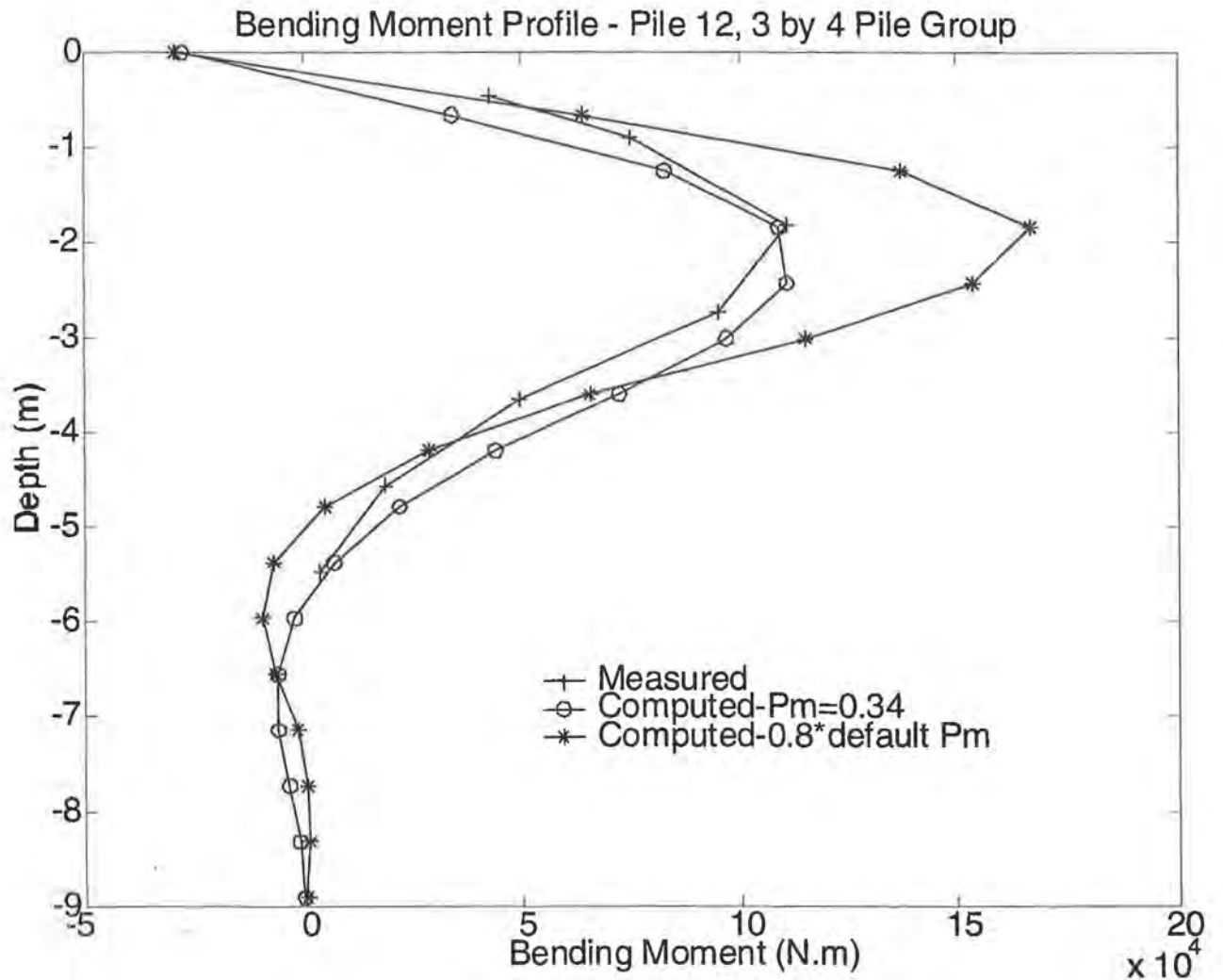
Figure 30. Bending Moment Profile, Lead Row Pile, 3 by 4 Pile Group at Spring Villa Test Site, Group Load = 1111 kN

155
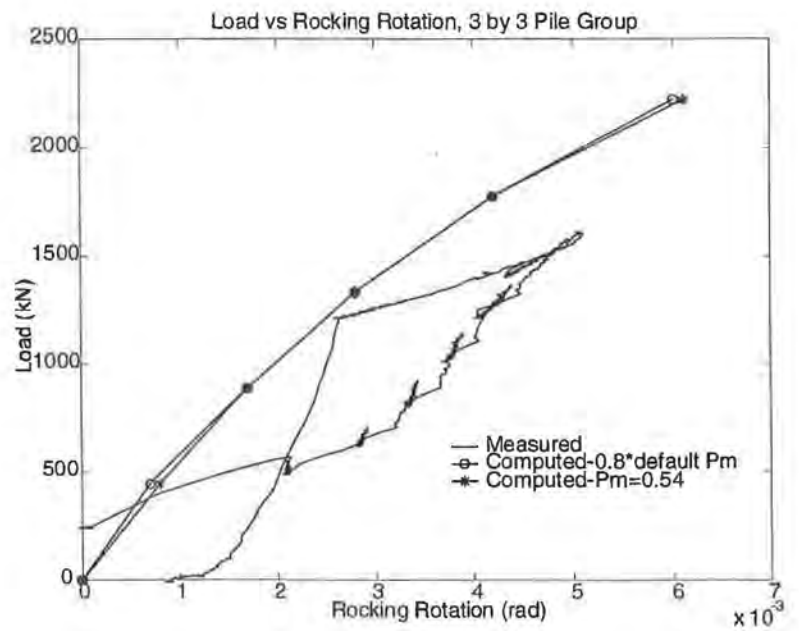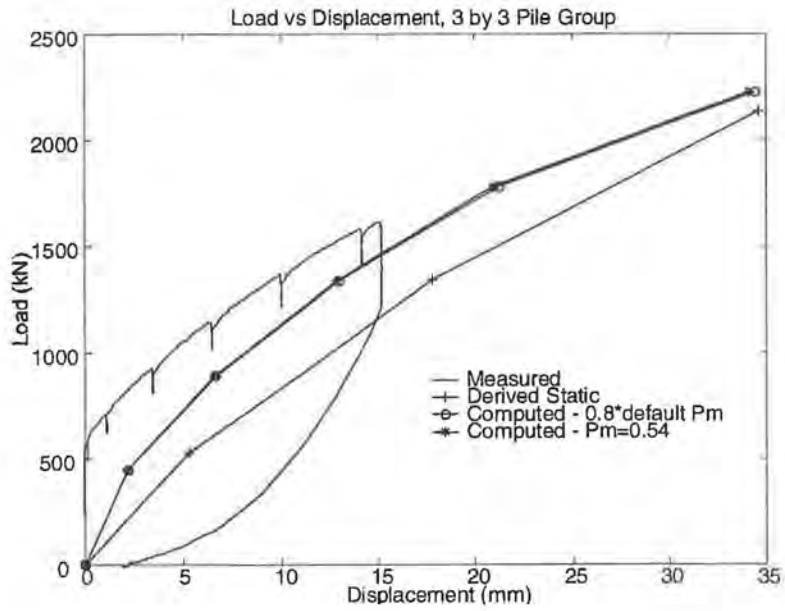
Figure 31. Measured vs. Computed Lateral Displacement and Rotation, 3 by 3 Pile Group at Spring Villa Test Site

156
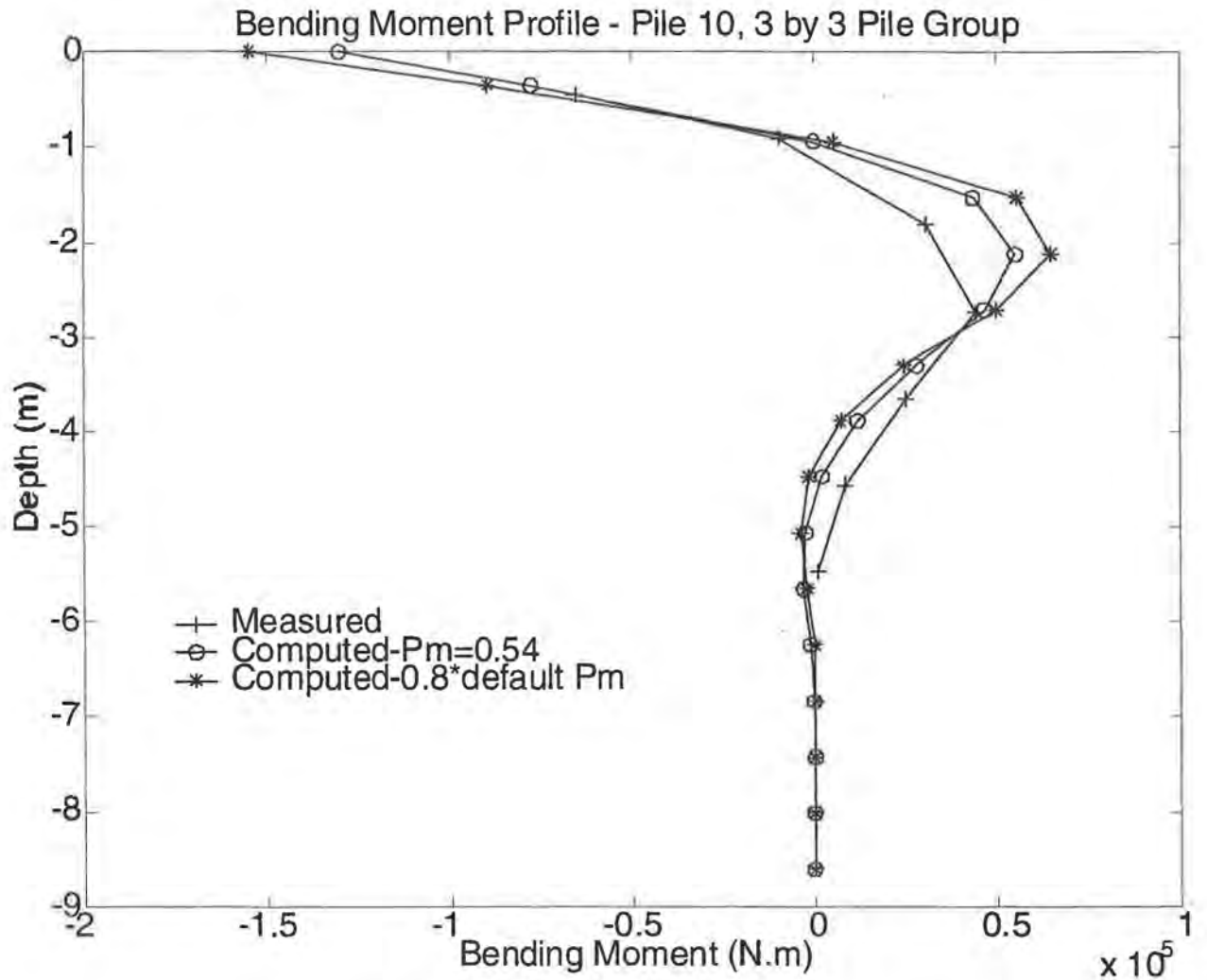
*Figure 32. Bending Moment Profile, Lead Row Pile, 3 by 3 Pile Group
at Spring Villa Test Site, Group Load = 1333 kN*
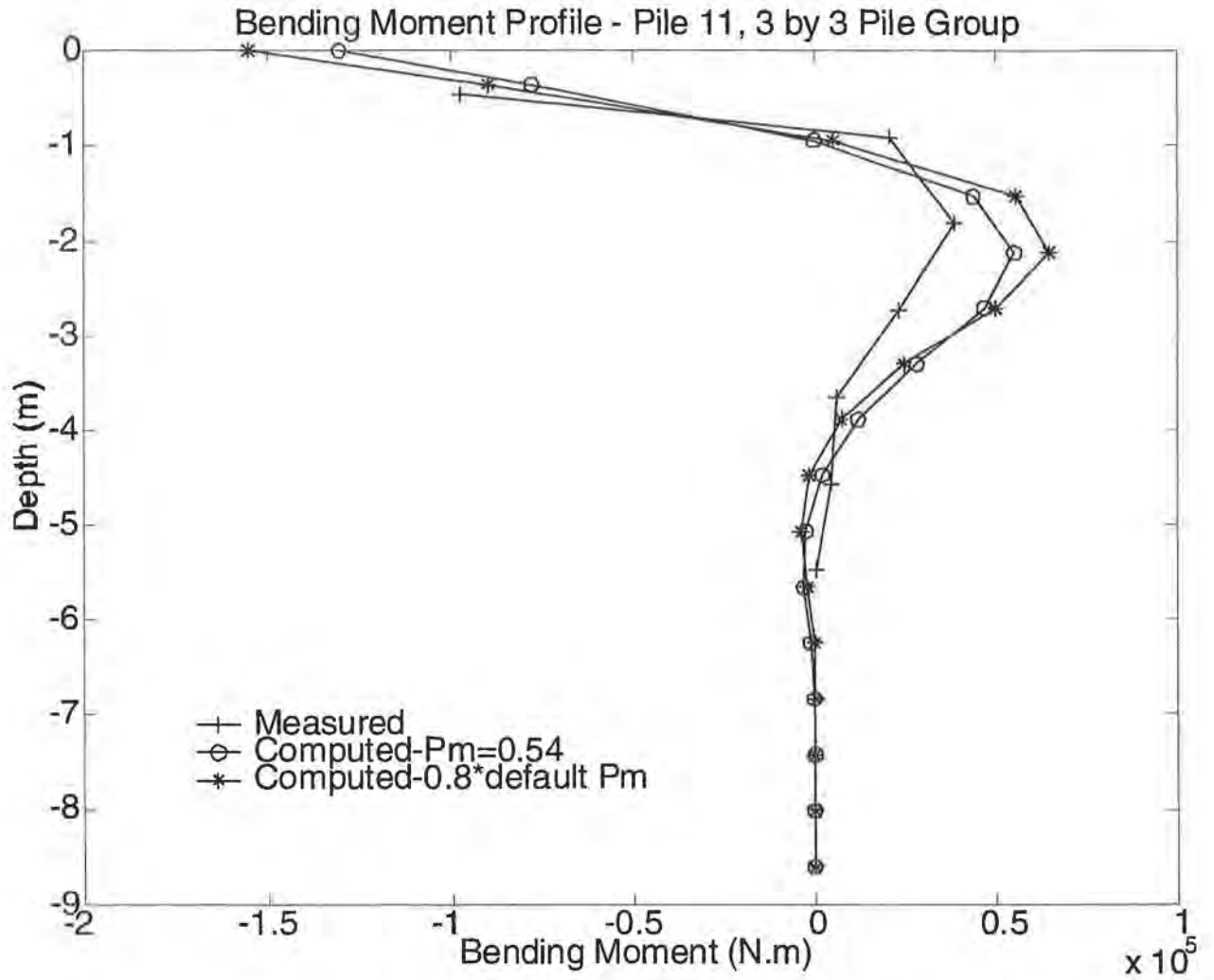
Figure 33. Bending Moment Profile, Lead Row Pile, 3 by 3 Pile Group at Spring Villa Test Site, Group Load = 1333 kN
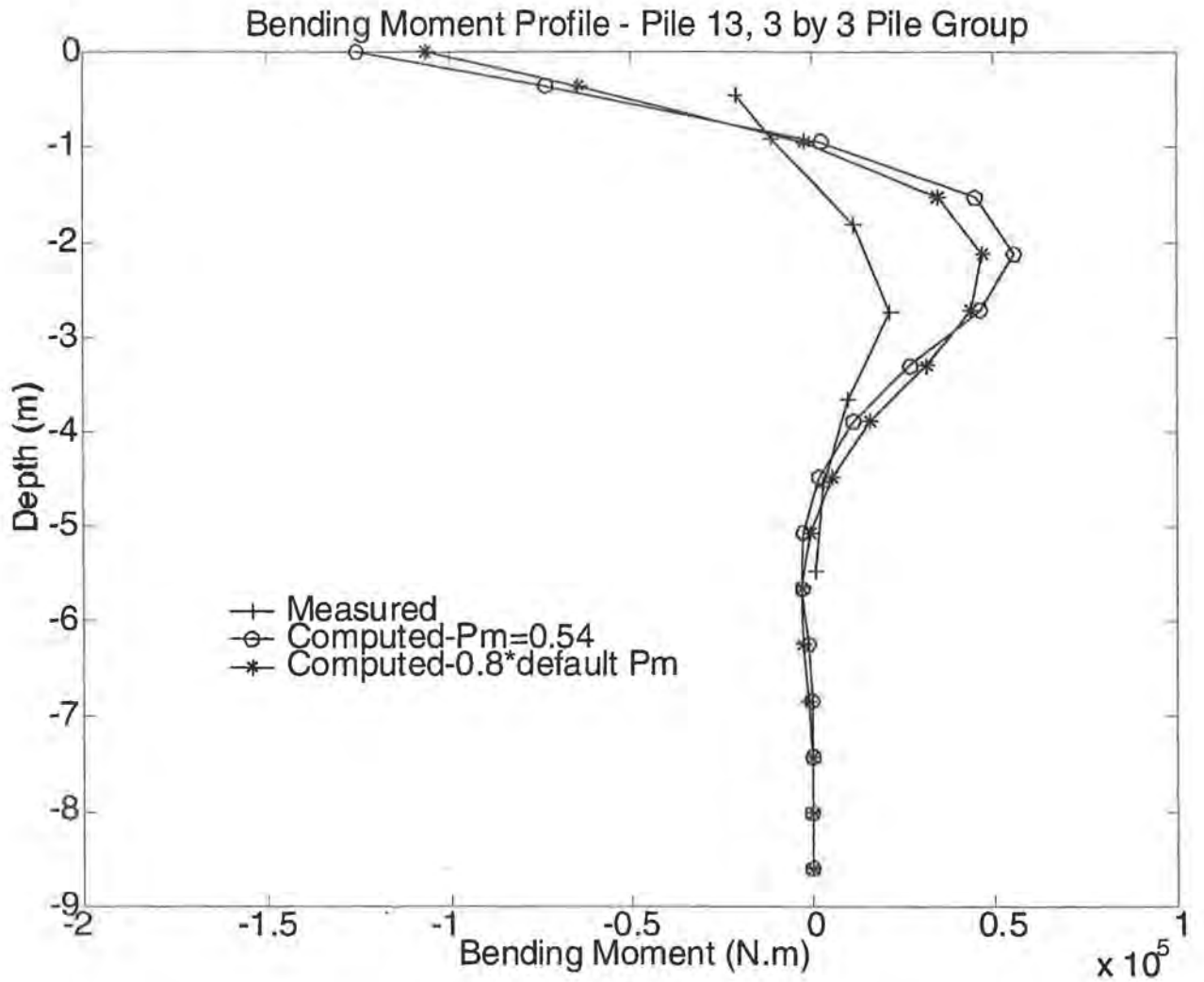
Figure 34. Bending Moment Profile, Trailing Row Pile, 3 by 3 Pile Group at Spring Villa Test Site, Group Load = 1333 kN
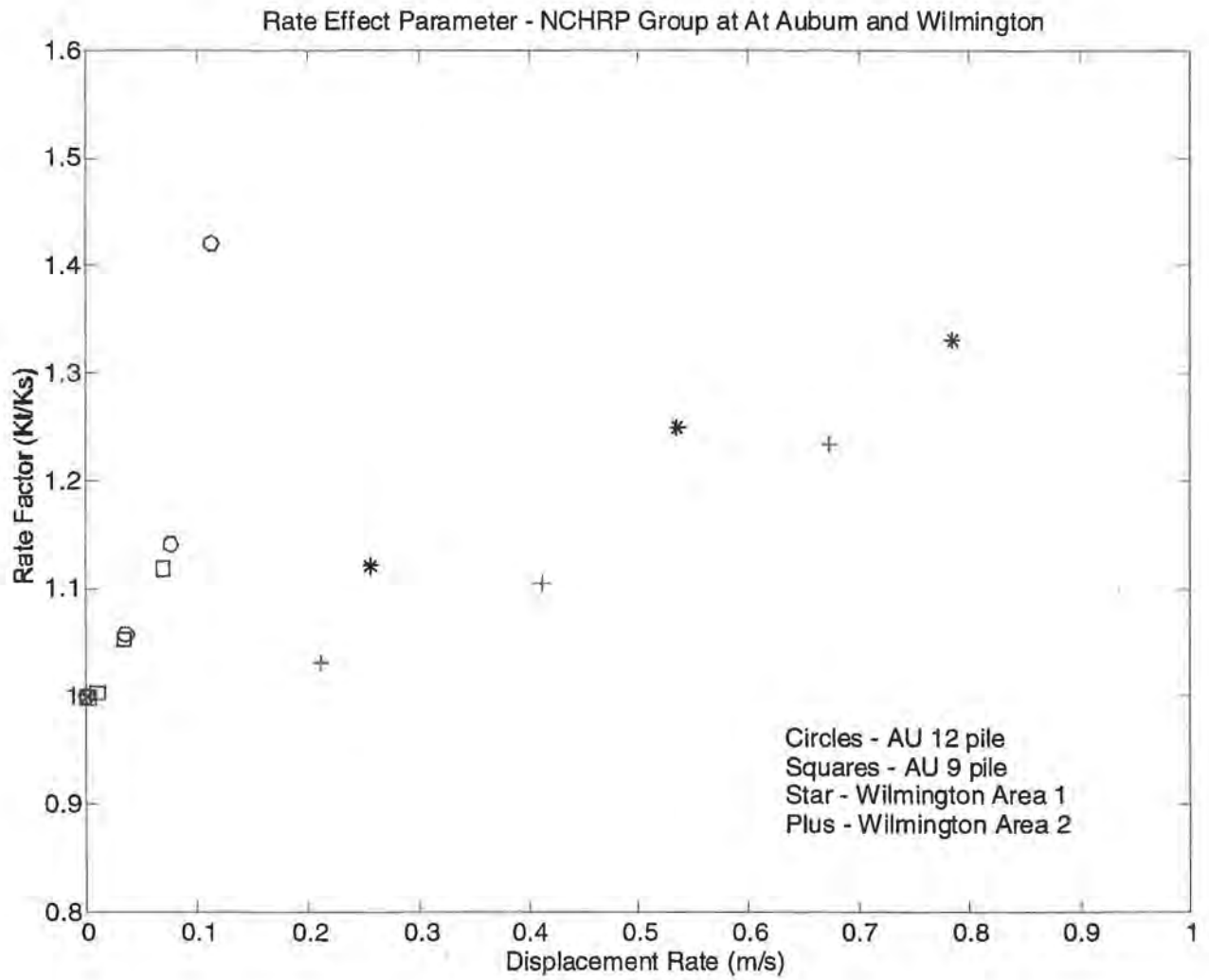
Figure 35. Effects of Displacement Rate on Foundation Stiffness

Displacement Response - Test Area 1 - Statnamic 1-4
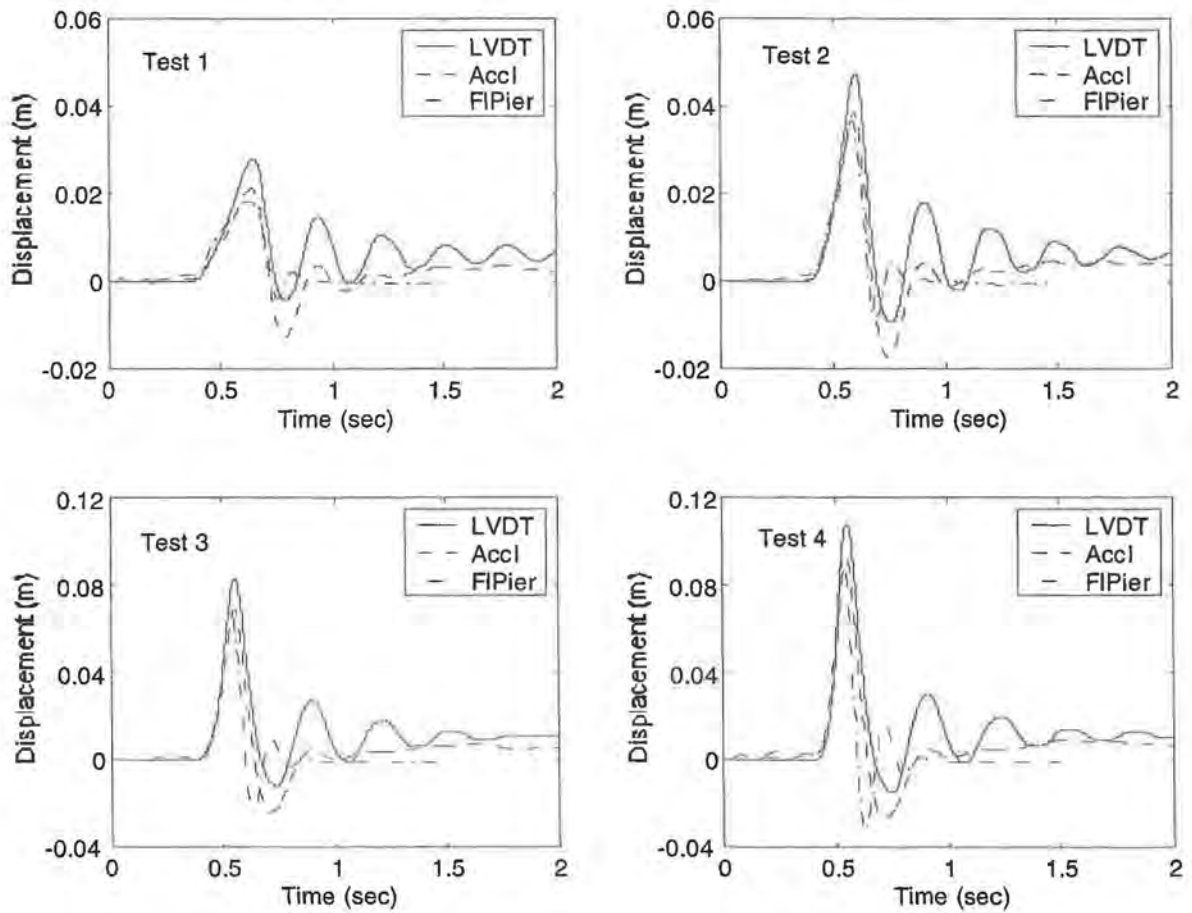
*Figure 36. Computed and Measured Dynamic Response, Wilmington Test Area 1*

161
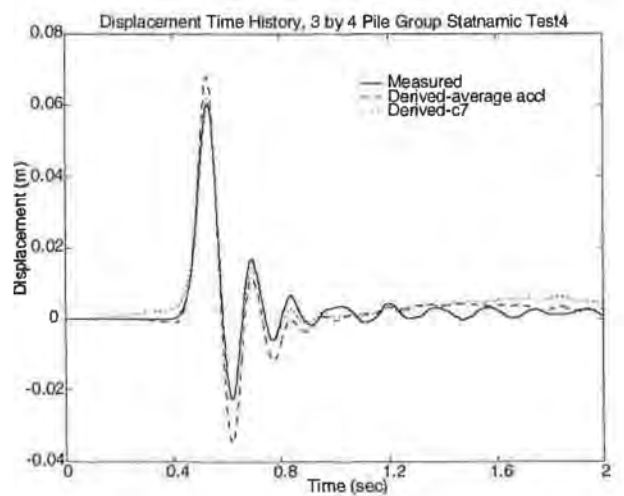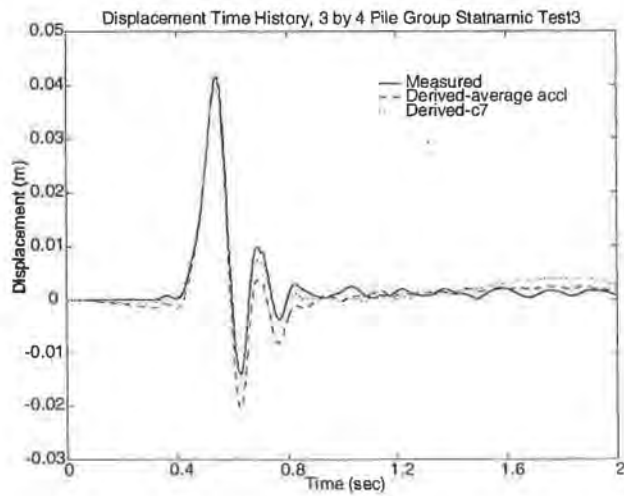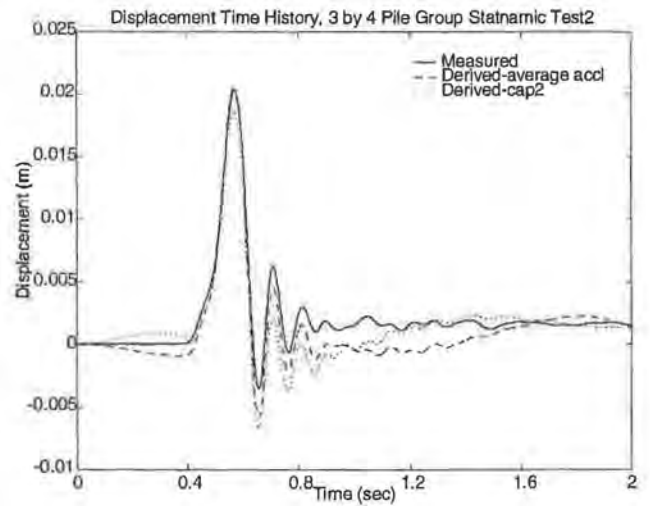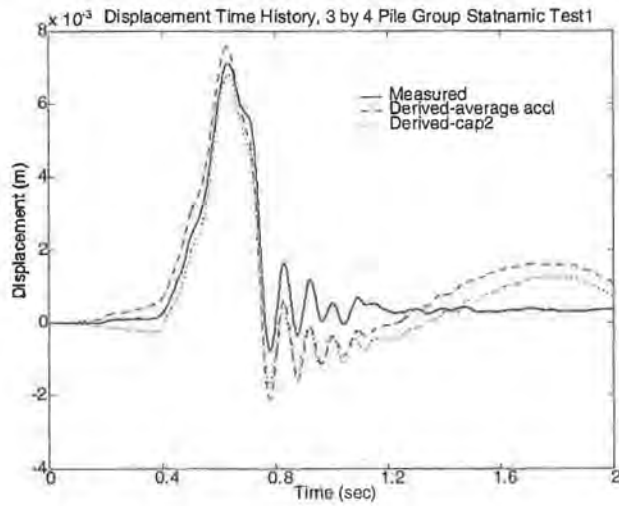
*Figure 37. Computed and Measured Dynamic Response, 3 by 4 Pile Group at Spring Villa Test Site*

162
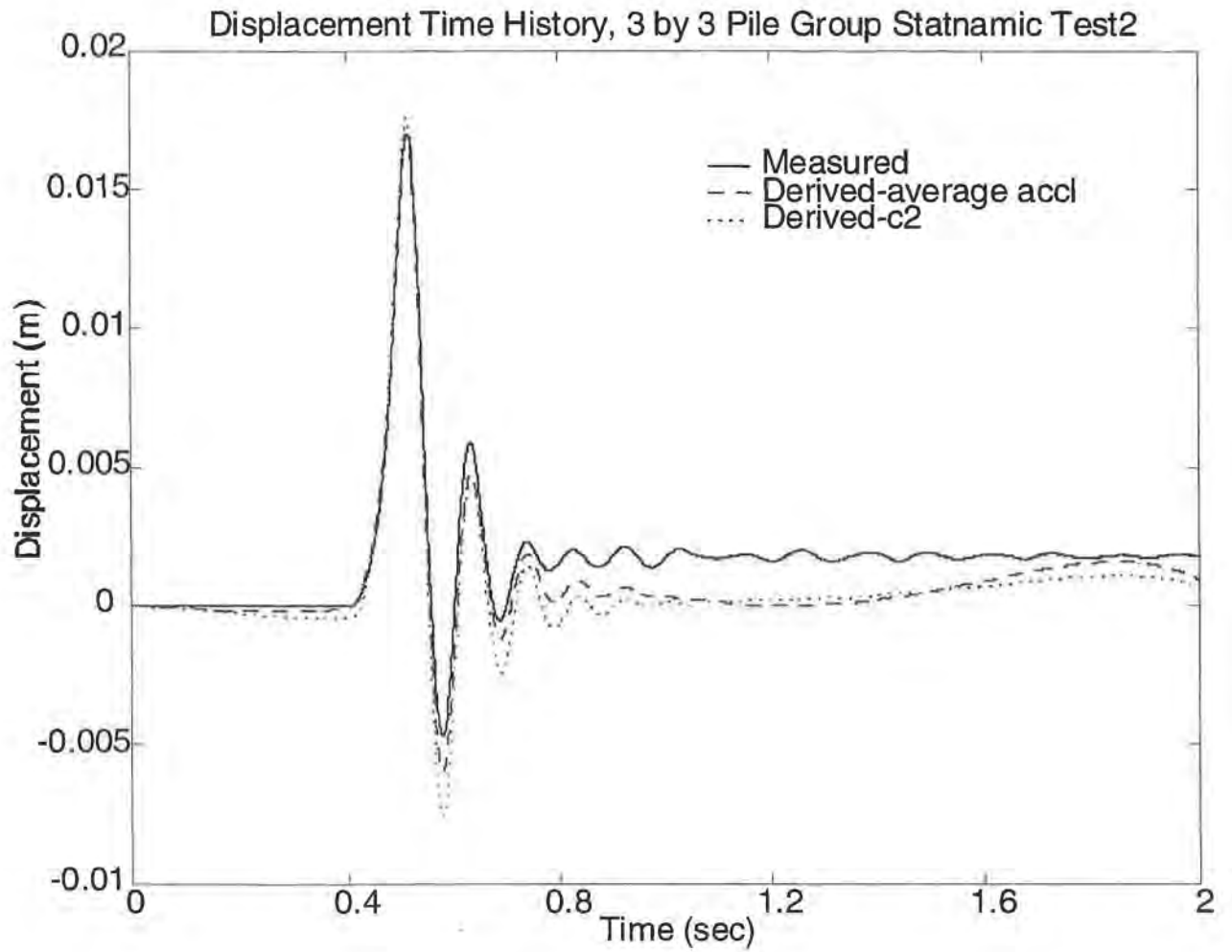
Figure 38. *Computed and Measured Dynamic Response, 3 by 3 Pile Group at Spring Villa Test Site*
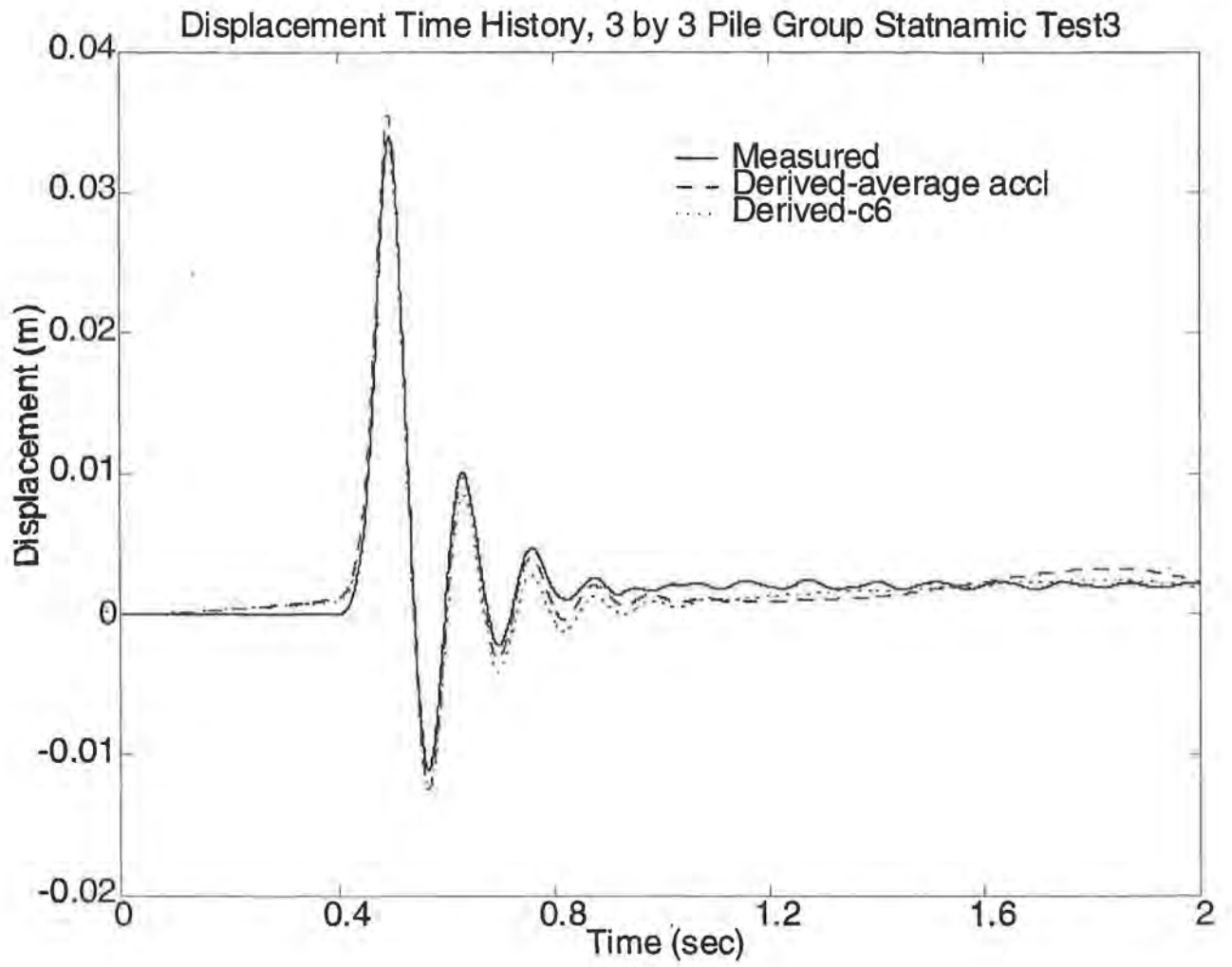
Figure 39. Computed and Measured Dynamic Response, 3 by 3 Pile Group
at Spring Villa Test Site